NTNU

Norwegian University of
Science and Technology

Relationship between environmental conditions and magnetic properties of Norwegian black shales

Emil Smedåsgjelten Qvam

Natural Resources Management
Submission date: May 2018
Supervisor: Maarten Felix, IGP

Norwegian University of Science and Technology
Department of Geoscience and Petroleum

Abstract

As part of a project to describe organic rich black shales from the Upper Jurassic from the Hekkingen Formation on the Norwegian shelf, cores 7430/10-U-01 North from the Nordkapp Basin (NE Barents Sea) and 7018/05-U-01 offshore Tromsø were investigated. The investigation was done by detailed sedimentological description, where the cores were investigated by facies description, and measurement of high resolution magnetic bulk susceptibility. The latter was done by measuring at intervals of 2 cm for core 7430/10-U-01 and 10 cm for core 7018/05-U-01. This small sampling interval is used to detect small variations. These two results are then combined to determine the relationship between the sedimentological characteristics and any variation or trend in the bulk magnetic susceptibility readings.

The results show that the Hekkingen Formation shows cyclicity of 28-30 kyr, 34-35 kyr and possibly 59-71 kyr in core 7018/05-U-01, 21.1-24.2 kyr, 28.9 kyr, 43.2 kyr and 66.3-99.9 kyr in core 7430/10-U-01. The connections between depositional environment and the magnetic properties can be seen in the amplitude spectrum, as they are created at intervals with similar lithology, and at the boundary between the different intervals, there is a change in composition of the core. In core 7018/05-U-01, the first spectrum is created for a shell-dominated interval, the second for an interval with few to no shell fragments, and the last for below the boundary between the upper Krill Member and lower Alge Member. For the 7430/10-U-01 core it is difficult to see the connection between the sedimentology and the magnetic signal.

Sammendrag

Som en del av prosjektet med å beskrive de organisk rike leirsteinene fra Øvre Juras i Hekkingen Formasjonen fra den norske sokkelen, er kjernene 7430/10-U-01 fra Bjarmeland platformen nord-øst i Barents havet, og 7018/05-U-01 fra nord i Harstad bassenget i Troms III området undersøkt.

Undersøkelsen ble gjort med detaljert sedimentologisk beskrivelse, hvor kjernene er undersøkt med hensyn til facies beskrivelse, og målinger av magnetisk susceptibilitet med høy oppløsning. De magnetiske målingene ble gjort ved å måle prøver med et intervall på 2 cm for 7430/10-U-01 og 10 cm for 7018/05-U-01. Det er for å fange opp små variasjoner at intervallene er så små. Disse to resultatene er så sammenlignet for å finne sammenhengen mellom den sedimentologiske karakteren og variasjonen eller trenden i det magnetiske signalet.

Resultatet viser at Hekkingen Formasjonen viser sykluser på 28-30 kyr, 34-35 kyr og muligens 59-71 kyr for 7018/05-U-01, og 21.1-24.2 kyr, 28.9 kyr, 43.2 kyr og 66.3-99.9 kyr for 7430/10-U-01.

Sammenhengen mellom avsetningsmiljøet og de magnetiske egenskapene kan vises i amplitude spektraene, da de er laget for dybdeintervall med lik litologi, og ved grensene mellom de forskjellige intervallene er det en endring i komposisjon av kjernene.

I 7018/05-U-01 viser det første spektret intervallet som er dominert av skjell og skjell-fragmenter, det andre intervallet har ingen eller minimalt med skjell, og det siste intervallet ligger nedenfor grensen mellom den øvre enheten Krill og nedre enheten Alge i Hekkingen Formasjonen.

For 7430/10-U-01 er det vanskelig å se en direkte sammenheng mellom sedimentologien og det magnetiske signalet.

Acknowledgements

This thesis is a part of a master's degree in natural resource management with specialization in geology, at the Department of Geoscience and Petroleum at the Norwegian University of Science and Technology (NTNU). The supervisor for this project is Professor Maarten Felix, with help from PhD candidate Justin Olabode Fadipe

First of all, I would like to thank Maarten Felix for great help and guidance through this project.

I would also thank the people in the geophysics group at the department, especially Suzanne McEnroe, Geertruida Wilhelmina ter Maat and Nathan Church for a lot of help with the magnetic measurements and access to the lab.

Finally, I would thank all my friends and family for help and support through this process of finishing my degree.

Table of content

Abstract 1
Sammendrag 2
Acknowledgements 3
Introduction 6
Geological background 7
Description of cores 9
Core 7430/10-U-01 10
Core 7018/05-U-01 11
Magnetic chronostratigraphy and time-series analysis of the Kimmeridge Clay Formation 14
Methods 16
Sampling 16
Magnetic susceptibility measurements 17
Sources of error 17
Logging 19
Sources of error 19
Data processing 20
Fourier Transform 20
Magnetic data from Weedon et al. (1999 and 2004) 21
Wavelet analysis 24
Results 25
Features in mudstone facies 25
Facies 31
Planar parallel laminated mudstone 31
Wavy laminated mudstone 35
Discontinuous laminated mudstone 38
Silty sandstone 40
Sandy mudstone 42
Massive mudstone 46
Siderite cemented mudstone 48
Slumps 49
Bulk susceptibility measurements 53
Core 7018/05-U-01 53
Core 7430/10-U-01 57
Filtering of slumped sections 60
Wavelet analysis 63

Core 7018/05-U-01 63
Core 7430/10-U-01 65
Discussion 67
Environmental influence on magnetic signal 67
Environmental influence on the magnetic signal 68
Cyclicity in the Hekkingen Formation 69
Conclusions 72
Further work 73
References: 74
Appendix 1-Legend 77
Appendix 2 – Logs 78
7430/10-U-01 79
7018/05-U-01 82

Introduction

The Hekkingen Formation was deposited during the late Oxfordian/early Kimmeridgian to Ryazanian, and consists of organic carbon rich mudstones interpreted to have been deposited under anoxic conditions in a calm, deep marine setting (Dalland et al., 1988; Smelror et al., 2001; Langrock et al., 2003; Georgiev et al., 2017). The Hekkingen Formation is equivalent to the extensively studied Kimmeridge Clay Formation from the U.K. in terms of time of deposition, lithology, and inferred depositional setting. Several studies of the Kimmeridge Clay Formation have linked variation in the deposits to orbital cyclicity (Dunn, 1974; Weedon et al., 1999, 2004). They identified the 38 ka obliquity cycle, and, to a lesser extent, the 28 ka precession cycle, in magnetic susceptibility data, photo electric effect and gamma-ray values. Orbital cyclicity has been suggested for the Hekkingen Formation by Langrock et al. (2003), who suggested that the 100-kyr orbital Milankovitch cycle might be reflected in core 7430/10-U-01 in variations in total organic carbon, hydrogen index values, and the Mo/Al ratio. This core is from the Bjarmeland Platform in the western central Barents Sea. These studies worked on different types of data, which might explain why different cycles were found.
To see whether the same orbital cycles can be found in Kimmeridge Clay Formation and the Hekkingen Formation from the Barents Sea, two cores have been investigated in this study: core 7018/05-U-01 offshore Tromsø, and core 7430/10-U-01 from the Bjarmeland platform, NE Barents Sea. The analysis used magnetic susceptibility data measured for these two cores, and the cyclicity was investigated using Fourier analysis and wavelet analysis. To catch the small-scale variation in the magnetic signal, the cores are sampled at an interval of every 2 cm for the shallow part and every 10 cm for the deeper part of core 7430/10-U-01, and every 10 cm for core 7018/05-U-01. Some changes in magnetic susceptibility do not reflect the overall long-term changes in depositional conditions, and they need to be removed from the data. For this reason, sedimentary descriptions of the cores were made in order to determine the depositional conditions, the depositional processes of different parts of the cores (slow deposition or particulate gravity current deposition), and to determine any lithology variations which would change magnetic susceptibility values (e.g. siderite cement, nodules, etc.). This description indicated which intervals should be excluded from the analysis in order to avoid artefacts.

The questions answered in this study are if the Hekkingen Formation shows cyclicity, does the two cores show the same durations of cycles and can they be compared to the cyclicity of the Kimmeridge Clay Formation, what effect does the environmental conditions have on the magnetic properties.

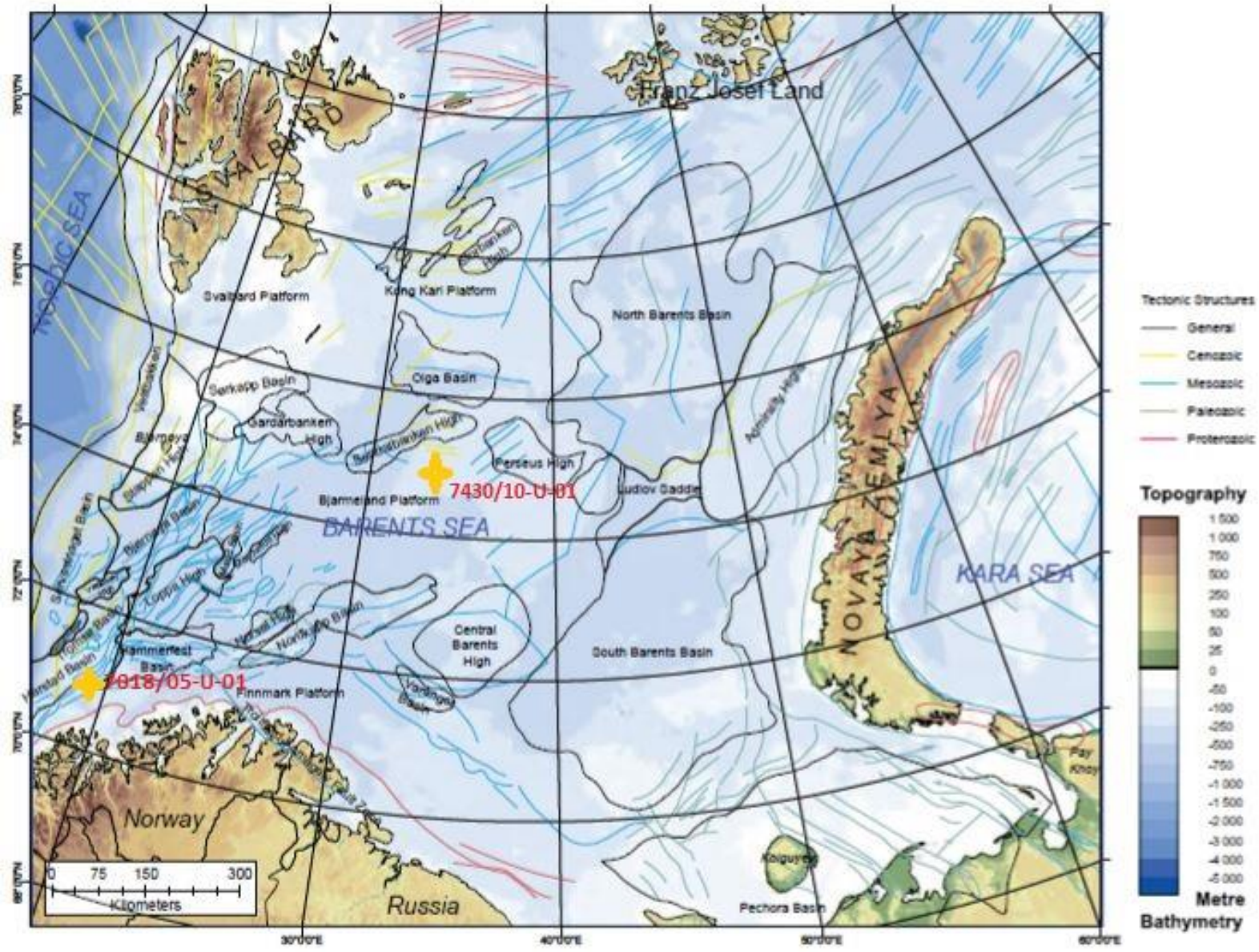

Figure 1: Overview of the Barents Shelf. Cores in this study are marked with a yellow star. From Smelror et al. 2009.

The Barents Shelf consists of a series of basins and highs, formed mostly as a result of continental collisions between the Silurian-Devonian Scandian phase of the Caledonian orogeny in the west, and the Carboniferous-Triassic Uralian orogeny in the east (McKerrow et al. 2000; Gee et al. 2006). The Neo-Proterozoic Timanian orogeny, the proto-Atlantic rifting in the western part, the opening of the Euramerican Basin in the North and the break-up and opening of the North Atlantic (northern part) along the western part of the shelf are also major events that lead to the development of the Barents Shelf (Smelror et al. 2009).

Following the Caledonian orogeny, exhumation and hinterland erosion deposited Old Red Sandstones in the Western Barents Sea, which characterised the Devonian to Early Carboniferous (Faleide et al. 1993; Smelror et al. 2009). The denudation was accompanied by rifting after the creation of the Caledonides, resulting in many early-rift basins along the Caledonian structural features (Smelror et al. 2009).

In the eastern part of the Barents Shelf, the progressive closure of the Uralian Ocean in the Carboniferous lead to the collision between Baltica and Kazakhstan which in turn lead to the creation of the Uralian mountains (Smelror et al. 2009). In the Early to Late Permian transition, seaways opened regionally around Baltica and the western shelf margins. In the central and western parts of the Barents Shelf, the Uralide orogeny and the opening of the connection with the Tethys Ocean changed the depositional environment drastically, turning from warm-water platform carbonates to cold and deep-water fine clastic sediments (Smelror et al. 2009).

In the Early Triassic, a major rift episode occurred in the western part of the Barents Sea, and Lower to Middle Triassic records show transgressive-regressive cycles of marine, deltaic, and continental clastic sediments with some minor tectonic events (Smelror et al. 2009).

A significant change in palaeogeography occurred during the Middle to Late Triassic, which coincided with the start of the uplift of the northern, southern, and eastern parts of the Barents Sea region, and by late Carnian time much of the western Barents Shelf was covered by alluvial plains and coastal and shelf-break environments. Tectonic activity started towards the end of the Late Triassic and continued into the Early Jurassic (Smelror et al. 2009).

During the Late Jurassic-Early Cretaceous, Atlantic rifting extended into the southern Barents Sea, opening the Norwegian-Greenland Sea, and later the Arctic Ocean (Cenozoic), developing many deep basins which subsided rapidly and split into sub-basins and highs. The rifting also started the development of marine connections across the Barents Shelf (Faleide 1984; Smelror et al. 2009). The rifting thinned the crust significantly and submerged the rift below sea-level (Anell et al., 2014).

This rift-related subsidence and major transgressions during the early Late Jurassic and at the very end of the Jurassic period flooded the entire Barents Shelf, and resulted in a deep-marine depositional setting (Smelror et al. 2009).

Description of cores

The cores used for this study are 7018/05-U-01 from the Troms III area, drilled in 1990 and 7430/10-U-01 from the NE Barents Sea on the Bjarmeland Platform, drilled in 1988. Both cores contain deposits from the Hekkingen Formation.

Work done by Georgiev et al. (2017) on Re-Os isochron measurements dates the start of deposition of the Hekkingen Formation at 157.7 Ma and the end at 138.8 Ma, thus lasting 18.9 Myr. The Hekkingen Formation consists of 10-20 % algal matter and 10-20 % amorphous matter, with the remaining portion made up of terrigenous material of variable composition (Smelror et al. 2001). The base of the formation is described by Smelror et al. (2001) to be observable by the grey silty mudstones of the underlying Fuglen Formation, and at the top of the formation there is a sharp contact to the overlying carbonates of the Knurr Formation.

Smelror et al. (2001) state that lack of evidence of any current activity and high organic content suggest a deep shelf depositional environment, potentially in a restricted basin, and that it was deposited under anoxic to dysoxic condition.

The Hekkingen Formation is divided into the upper Krilll Member and the lower Alge member. Smelror et al. (2001) state that the boundary between these members is found at 210 metre in core 7018/05-U-01, but in core 7430/10-U-01 it is hard to find any information about this boundary.

The two members are differentiated by a significantly lower gamma ray reading in the Alge Member than in the Krill Member (Smelror et al. 2001).

The cores worked on in this study were sawed in half before being put in storage, and the two halves will be referred to as the varnished half or the display core, which is treated with a varnish before being put into metal boxes with epoxy to keep them in place, and the unvarnished half, which is untreated and put in plastic boxes without any epoxy to keep them in place.

Core 7430/10-U-01

The core was taken on the Bjarmeland platform, NE Barents Sea, which was situated between the Sentralbanken High and Gardabanken High to the north, and the Loppa High and the Nordkapp Basin to the south (seen in Figure 1).

Work done by Langrock et al. (2003) on core 7430/10-U01 shows that it has a total organic carbon (TOC) content that varies from 3 to 36 wt.% throughout the core. The relationship between TOC content and sedimentation rate, and high Mo/Al ratio indicate anoxic bottom-water conditions during deposition, and that the anoxic condition is the reason for the high preservation of organic carbon. They also obtained high hydrogen index values and state that the organic matter is characterised by type II kerogen, but that the occurrence of spores, freshwater algae, coal fragments and charred land-plant remains suggests deposition with a proximity to terrestrial areas.

Several sedimentation rates have been suggested for this core, and for this study, three different sedimentation rates will be compared. Langrock et al. (2003) estimates the sedimentation rate for core this core to be as low as 0.2cm/Kyr, while Mutterlose et al. (2003) suggest a biostatigraphic sedimentation rate at 19.0 m/Myr and an astronomical sedimentation rate at 16.2 m/Myr.

In general, the core is in quite poor condition (see Figure 2) where a lot of varnish has been used for the display core, making it shiny and black. This makes the structures in the core hard to see, but by using the unvarnished half of the core it is possible to examine the structures and facies.

Core 7018/05-U-01

The core is taken from the Troms III area, near the NE margin of the Harstad Basin between the Barents and Norwegian Seas (see Figure 1). It consists of mostly planar parallel and wavy parallel laminated mudstone, with occasional massive mudstone. It shows an abundance of siderite concretions and cement, and veins filled with sideritic material (referred to here as siderite veins). The lower part of the core is dominated by siderite veins, cement, and concretions, while the upper part (~50 - ~90 m) is dominated by shell fragments. Smelror et al. (2001) state that the upper 50 metres of the Krill Member in this core have a relatively high fossil content, consisting of ammonites and benthic bivalves, while the lower part of the core has a sparse fossil content. There is also evidence of slumping and mudflows through the core these are further explained in the results section and noted down in the sedimentary logs found in appendix 1.

This core is, like core 7430/10-U-01, in relatively poor condition (at some depths it is broken up into small fragments, as seen in Figure 3), but is not as heavily varnished as the 7430/10-U-01 core, making the structures easy to see in the display core). The unvarnished half of the core is in poor condition as well, being almost completely broken up by either the sawing of the core, the drilling or from when it is pulled up, so there is little help in comparing depths in the display core to the unvarnished half to better see the structures.

Georgiev et al. (2006) used dating from Re-Os isochrones to estimate a compacted sedimentation rate for the Hekkingen Formation in this core, which is given at 16.8 m/Myr for the Alge member and 13.1 m/Myr for the Krill member.

Figure 2: Example of the broken up parts of core 7430/10-U-01 at depth 54.90 m

Figure 3: Example of broken parts of core 7018/05-U-01 at depth 65.40 m

Magnetic chronostratigraphy and time-series analysis of the Kimmeridge Clay Formation

This formation is an equivalent to the Hekkingen Formation, deposited at the same time and in roughly the same sedimentary environment, and can be used for a comparison with the Hekkingen Formation; potentially the shales of the Kimmeridge Clay Formation could have stored the same kind of magnetic response as those of the Hekking Formation.

Dunn (1974) did a time-series analysis on a 20 m section of the Kimmeridge Clay Formation called the Blackstone unit, and reasoned that the cyclicity he found could be linked to Milankovitch cycles.

Weedon et al. (1999) and Weedon et al. (2004) used magnetic susceptibility data for time-series analysis of the Kimmeridge Clay Formation. The data are available online at http://kimmeridge.earth.ox.ac.uk. In these studies, Weedon et al. (1999, 2004) demonstrate that magnetic susceptibility is useful for the generation of a high-resolution time-series analysis in mudstones, but they also state that within the same lithological unit, such as the Kimmeridge Clay Formation, the character and the origin of the magnetic susceptibility signal can change, which could reflect changes in the palaeoenvironment and diagenetic effects.

Weedon et al. (1999) split the data into smaller segments to be able to observe the bedding-scale cyclicity, and in some parts of the data they observe a (single) dominant peak (peaks at 1.16 metre and 1.23 metre in Figure 4 a), while in other parts they observe a secondary peak as well (peak at 0.62 metre in Figure 4 b). They conclude that the Kimmeridge Clay Formation records a relatively strong influence by a 38 ka obliquity cycle and a weaker influence by a 20 ka precession cycle.

Weedon et al. (2004) also investigated the cyclicity in the Kimmeridge Clay Formation with three independent variables, magnetic susceptibility, photoelectric factor, and total gamma ray. They identified regular metre-scale sedimentary cycles of both large wavelength and shorter wavelength, and state that the longer-wavelength cycles represent orbital obliquity with a period of 38 ka, and the shorter cycles represent precession with periods of 22 ka and 18 ka. It is also stated that both obliquity and precession forcing affected the terrestrial environment, and that obliquity cycles dominate the marine environment.

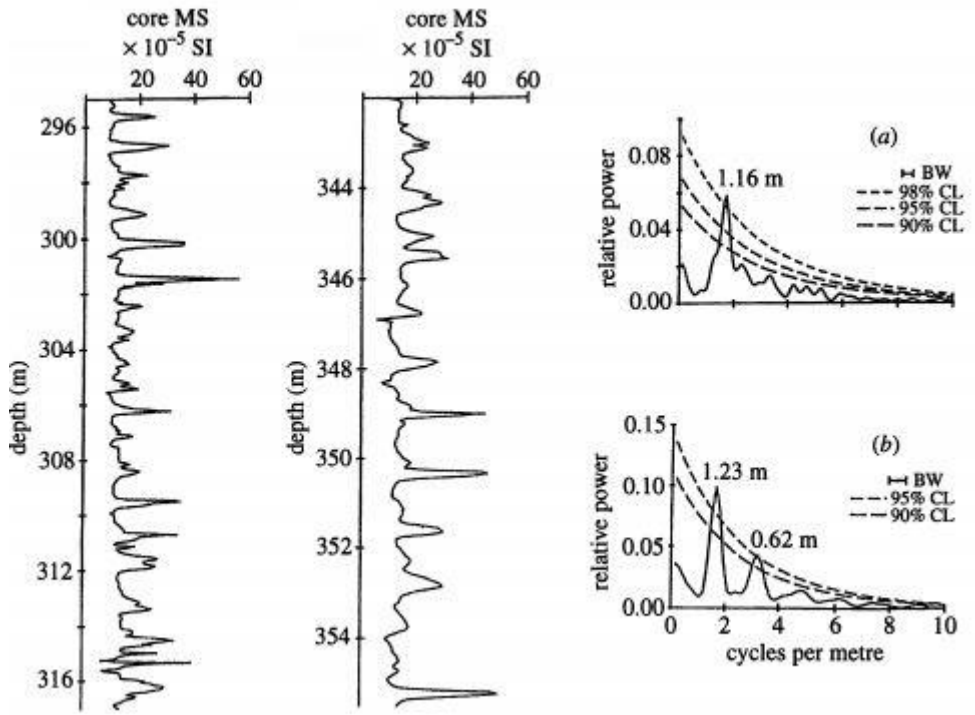

Figure 4: Results from Weedon et al. (1999). Amplitude spectrum shown on the right, with dominant peaks at 1.16m for the upper part and 1.23m and 0.62m for the lower part

Methods

Sampling

The sampling of the cores for magnetic susceptibility-measurements was done by taking a small amount from the unvarnished half of the core, either by sawing, chipping, handpicking core-bits, or by drilling. The cores are quite brittle in general, so the easiest method was to use a tapestry-knife (or another thin blade) and chip off a small sample or use forceps to pick out a piece. Where the core is completely broken up, a representative sample is just picked out at the correct depth, though the sample might have moved a bit in the box itself.

Determining the exact depth when taking a single sample out from the unvarnished core can sometimes be difficult, as the core itself can have moved a few cm inside this box. It is also important to be careful when taking out the samples not to break up the core more than it already is and to get as solid as possible a sample taken out (see sources of error below).

The sampling interval for core 7430/10-U-01 was at every 10 cm from depth 42.9m to 55.0m and every 2 cm from 55.0 to 67.0. The change in sample depth in this core was due to the realisation that every 10 cm was close enough to catch the variations in the core. Core 7018/05-U-01 was sampled at every 10 cm throughout the whole core.

The samples were then put in plastic bags marked with core name, depth, and sample number.

Magnetic susceptibility measurements

The core samples were put through a multifunctional Kappabridge, agico MFK1, which measures the bulk magnetic susceptibility. When starting, the machine needs 10 minutes to stabilize, and then it needs to be calibrated. The calibration is done by first putting a standard measuring sample in the machine, of a known susceptibility, which is measured three times, and the manual for the MFK1 indicates that it will show an error for this calibration if the measured value is less than 65% or more than 135% of the nominal value. Then the machine needs to be corrected for the holder used for the samples. This is done by putting in the empty holder and taking three measurements and then calculating the average. If the three measurements have too great variation, the holder correction will be marked suspicious, and the holder needs more cleaning before the process can be repeated. The manual for the machine does not state at what variation between the three measurements it will return the correction as suspicious, but in examples they show in the manual of different types of holders, it works with +/- 1% of the average.

When the machine is ready for use, the samples are taken out of the bag, weighed, put in the holder, and then put into the machine to measure bulk susceptibility. The samples need to be normalized by weight before they are used in the data analysis, done by dividing the magnetic susceptibility reading of the sample by its weight.

Some of the samples from the 7430/10-U-01 core were quite brittle and became crushed to powder when they were put in the plastic bags, and therefore the measurements on these samples were done by putting the powdered sample into a small plastic container. The measurements needed to be corrected for this plastic container. The containers were weighed, and the magnetic susceptibility was tested without the powder in them to compensate for the signal they would contribute when the samples were tested in the machine.

Sources of error

One important thing that was discovered during some repeating of some samples, was that the time between sample measurements cannot be too short. Some repeating was done without any time in between, so as soon as the sample came out of the machine, it was put back in almost immediately, giving only about 10-20 seconds between testing. This caused the reading to be affected by the previous one, so the resulting reading was higher than what it should be. This can be shown by comparing the result from the repeated measurements to the repeated measurements where there was sufficient time between the readings, about 1 minute. This is the normal time used between the samples, where the readings are not affected by this effect.

There also seems to be a problem with using the small plastic containers for the powdered samples, as they in general have a slightly higher reading than the samples from 2-4 cm above or below, without having any clear reason to why, but it could be that a change in the depositional processes makes the core more brittle and this could have resulted in the slightly higher susceptibility. The plastic containers were only used for the 7430/10-U-01 core, so more effort was put into taking more solid samples from the other core so that the containers were not necessary. The values with the plastic container are still used for core 7430/10-U-01 for the analysis.

Logging

The sedimentary graphical logging was done at NTNU's facilities at Dora, on a scale of 1:20 with a focus on sedimentary structures, textures, colour variations and other visible aspects of the core. Both a handheld lens and a microscope were used to help with the identification of the different structures and facies. The description of the core was used to define the different facies occurring throughout the core, described in detail in the results chapter. The term facies is used to divide a sedimentary succession into smaller blocks or units and should be based on a good description of the succession. The facies are given descriptive names based on what constitutes and characterises them.

Sources of error

Some parts of the cores are layered with a thick glossy varnish which makes it hard to see what is in the core itself, but also to distinguish sedimentary features from features caused by the varnishing. At some places the varnish is peeling from the core, which creates holes in the apparent core surface, and makes it "spotty", but this is distinguishable from actual textures and structures since it is possible to rub the spots off the core. It is also possible to spot this artefact by using the hand lens.

Some of the classification of lamination can be difficult, as the boundary between the different types is not easily visible in the core itself. The heavy use of varnish on especially the 7430/10-U-01 core makes this even harder. The lamination types in the facies can be quite similar at some depths in the cores, so it is therefore important to use enough time to investigate the lamination type, and to compare it with similar laminae at other depths in the core.

Data processing

To be able to get the magnetic susceptibility data displayed in a Discrete Fourier transform power spectrum to show possible cyclicity, the signal needs to be processed in several ways. Very high values, generally caused by iron rich siderite or siderite cement, need to be filtered out and this is done by setting a max value at $8 \cdot 10^{-8}$ so that any values above this are removed from the data set, chosen based on the values for the siderite as cement, concretions and veins. Also, the abnormal small values below $3 \cdot 10^{-8}$, are removed, as these low values are a result of too small a sample, resulting in the machine reading the magnetic susceptibility in the holder instead of the sample. These values are easily seen when comparing the weight of the sample and the resulting magnetic susceptibility of that depth.

Fourier Transform

The data is first detrended to remove any end-effects where the start and end values of the time-series are not zero. If this were not done, the power spectrum would only show a peak close to zero cycles per metre, as these trends tend to be much longer than the magnetic cyclicity.

A Hanning window was applied to the amplitude spectrum to avoid end effects, and it does not produce side-lobes and suppresses side-lobes resulting from tapering (Weedon, 2003).

The amplitude spectrum is then made by plotting power (squared average amplitude) versus the frequency (cycles per metre).

More specifically, the Fast Fourier Transform is used to make the amplitude spectrum in this study, and it works best (best sampling frequency) and faster with data sets with a length that is a power of two, and to adjust for this, zeroes were added to the data (zero-padding).

Only a selected interval of the core is processed at a time, as the cyclicity might change throughout the core, dependent on sedimentation rate and the depositional environment. This interval of depth is found by looking both at the original data and detrended data, to see if there are any abrupt changes or trends that could make a “boundary” for the chosen interval. The processing does not work well with gaps in the data, and the interval should not be chosen for parts that show changes in appearance like suddenly jumping to higher values over a few data-points or in other ways drastically change over a short distance.

To not lose too much information, there is little filtering applied to the data, but what is done is to remove data points at depths that include the high magnetic susceptibility from siderite and remove the depths that show evidence of slumping. Some sections of core

7018/05-U-01 also show evidence of other types of disturbance, like mud-flow or turbidite flow, and these are also removed, and extra amplitude spectrums are produced to see if they become clearer than the spectrums with the disturbed sections not removed. This is done because the slumping (especially in core 7018/05-U-01) causes a thick package of sediment to be deposited at a short interval of time, compared to the thickness that would be present if only "normal" deposition at normal sedimentation rate had happened. The slumped sediments are also transported from some other area (possibly a slope) and possibly deposited at another time, and so disrupt the magnetic signal at the depth in the core of interest. There are also a couple of short intervals from turbidity currents in core 7430/10-U-01 that are removed for the same reason.

Magnetic data from Weedon et al. (1999 and 2004)

The data collected from the Swanworth Quarry 1 core and used by Weedon et al. (1999 and 2004) was available on the internet, so the same signal processing used on the data from cores 7430/05-U-01 and 7018/05-U-01 was used on the Kimmeridge Clay Formation data, to see if the amplitude spectrum created by this is comparable to what they found originally. The findings of Weedon et al. (2004) are presented in Figure 5.

By using the same processing method as used on the data collected from the Hekkingen Formation in this study and comparing the results, the validity of the method chosen here can be assessed, and the resulting graph and amplitude spectrum are shown in Figure 6.

As can be seen in Figure 5 and Figure 6 the dominant peaks of the recreated figure correspond well with the dominant peaks found originally by Weedon et al. (1999). Some of the differences can be found in the filtering of the data. Weedon et al. (1999) have used more filtering on their data, as can be seen from the smoother amplitude spectrums they created.

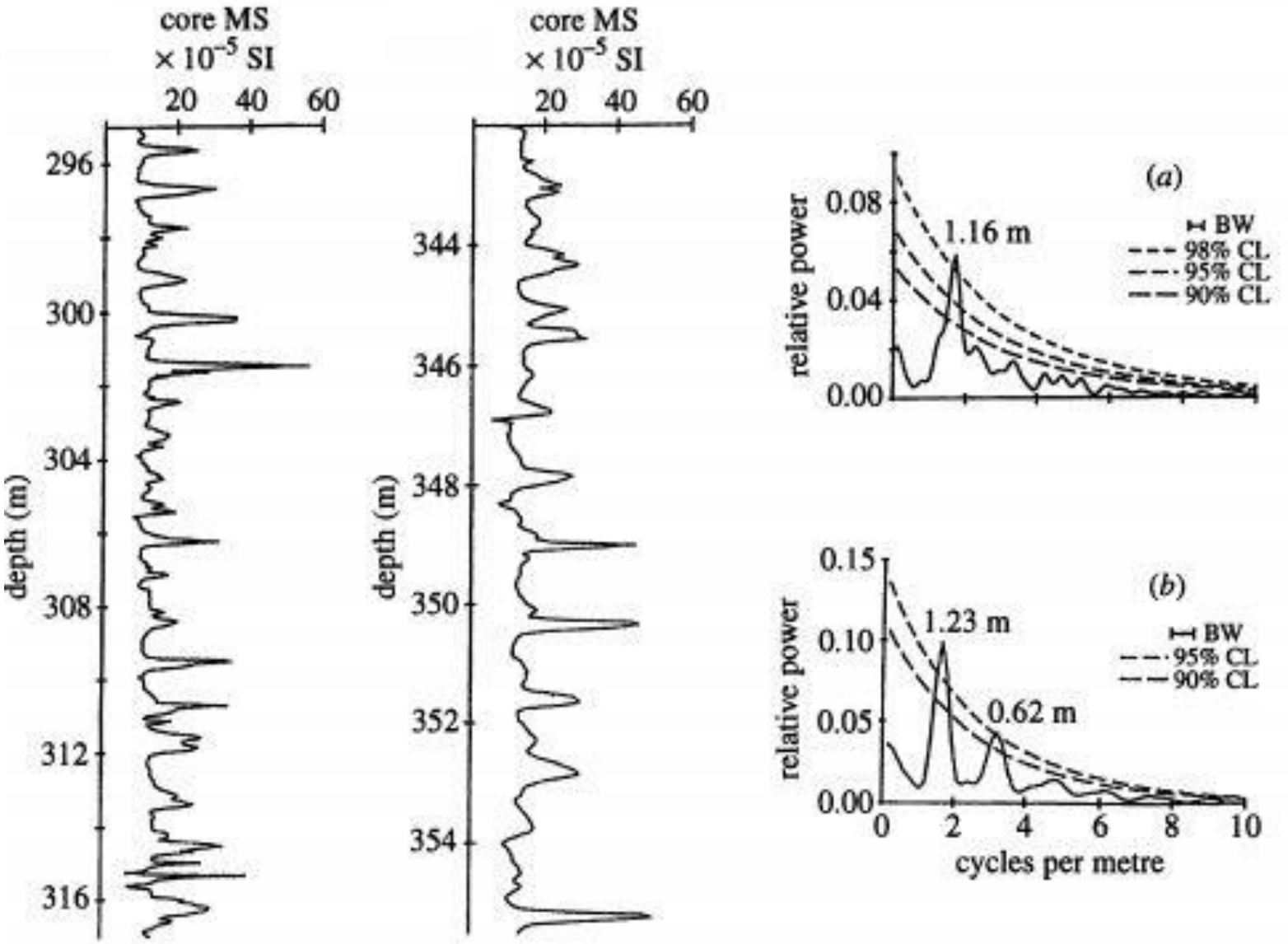

Figure 5: Results from Weedon et al. (1999). Original signal of two chosen depth intervals on the left, and the corresponding amplitude spectrum is shown on the right.

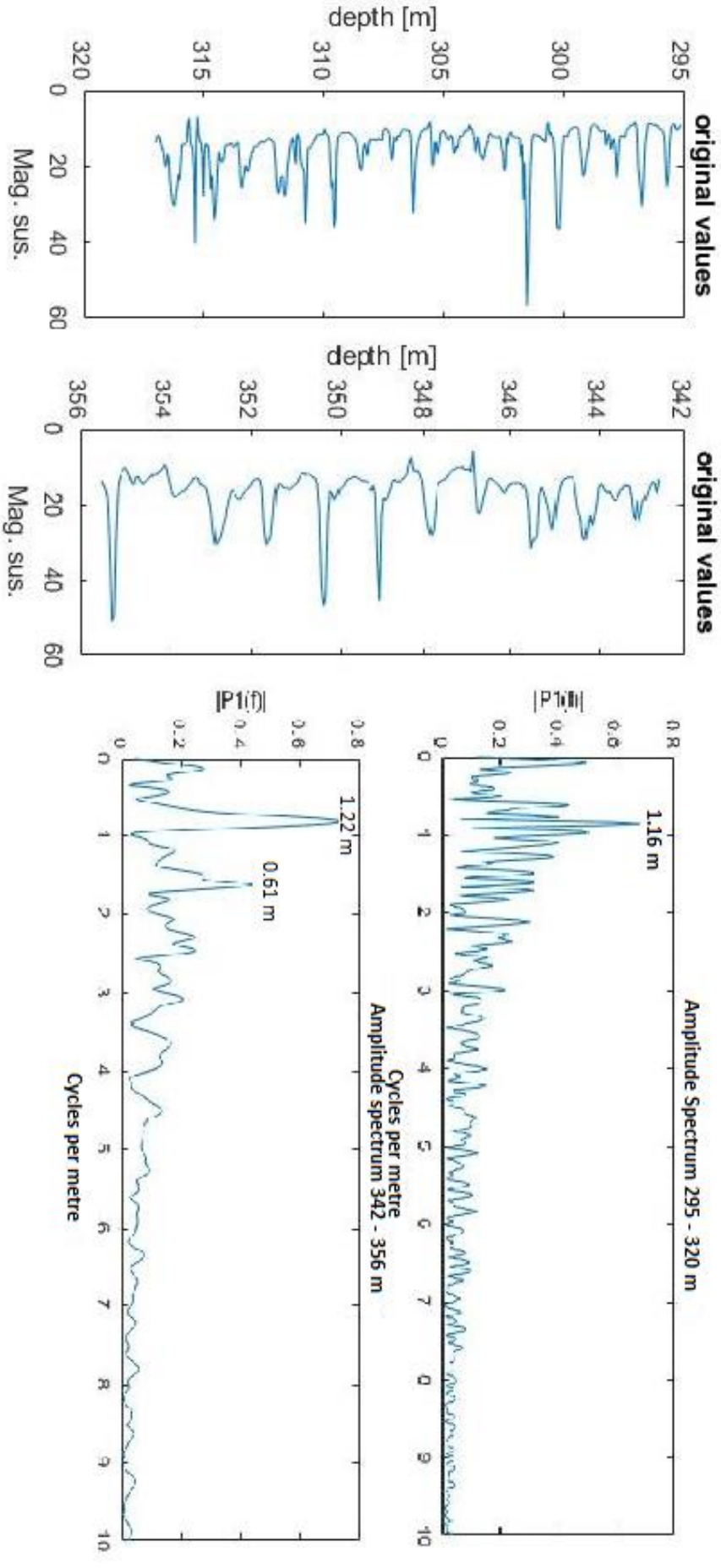

Figure 6: recreation of the spectrum of Weedon et al. (1999). Original data shown on the left, and the amplitude spectrums are shown on the right.

Wavelet analysis

The Fourier analysis works well for stationary time-series, but as the cyclicity changes over time, a wavelet analysis can be useful to further investigate the dominant cycles in the magnetic susceptibility data.

Due to the fact that the wavelet analysis algorithm used in this analysis does not work with gaps in the data, the best result from this analysis come when the data consist of a long section without any datapoint missing, so the whole dataset has been tested, but only the longest and clearest results are shown. No values are removed from the data, so the high siderite values are present, but avoided where possible.

A wavelet transform used on time-series expands the data into time frequency space, and is helpful in analysing intermittent oscillations in a time-series, and shows it in an intuitive way, where depth is plotted against cycles per metre, and the relative power grading from blue to yellow. The 5% confidence interval is drawn in as a black line (Grinsted et al. 2004). In this analysis, the Continuous Wavelet Transform (CWT) was applied using a Morlet wavelet, using the software package of Grinsted et al. (2004). This package is available online at http://www.pol.ac.uk/home/research/waveletcoherence/.

Results

This chapter shows the results from the core logging, magnetic susceptibility measurements, and the amplitude spectrums. An interpretation of the facies is presented together with pictures of the cores to show examples of facies and other interesting features found during logging. The logs with a legend are found in the appendix.

Features in mudstone facies

Some features appear in several or all different mudstone facies and are discussed here.

Lamination

Lamination is one of the most dominant structures of mudstones, but it varies in appearance, so the table shown in Figure 7 created by Collinson et al. (2006) is used to differentiate facies based on lamination type. Generally, individual laminae are separated by a sharp contact resulting from an abrupt change in grainsize from mud to silt, or possibly by concentrations of coarse micas or heavy minerals (Potter et al., 2005, p. 43). This is what is seen in both cores here, where the laminae consist of alternating dark black mud and lighter grey silt.

In both cores 7018/05-U-01 and 7430/10-U-01 the lamination types grade into each other at some points, and this makes it hard to assign deposition type to one or the other, especially to differentiate between the planar parallel laminated mudstone, the discontinuous planar parallel laminated mudstone and the wavy parallel or discontinuous wavy parallel laminated mudstone.

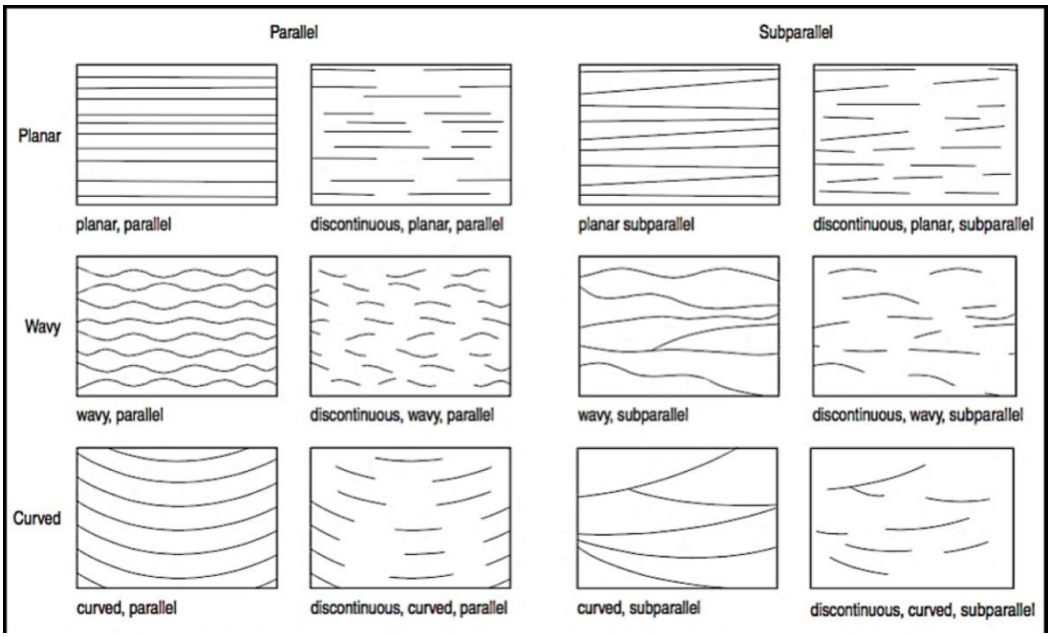

Figure 7: Overview over different lamination types. From Collinson et al. (2006).

Pyrite

In the cores studied here, the pyrite either appears as small nodules of a few mm with sharp edges to surrounding mudstone distributed randomly across different facies, or as bigger grains up to a few cm in both length and thickness lying parallel to underlying lamination and with overlying lamination draping the grain as shown in Figure 8 and Figure 9. In core 7430/10-U-01 pyrite is most common as bigger grains or concretions, while in core 7018/05-U-01 it appears mostly as small mm sized grains spread out through the facies.

The pyrite does not have any clear effect on the magnetic signal, most likely because the grains are too small and widespread to be part of the samples for measurement.

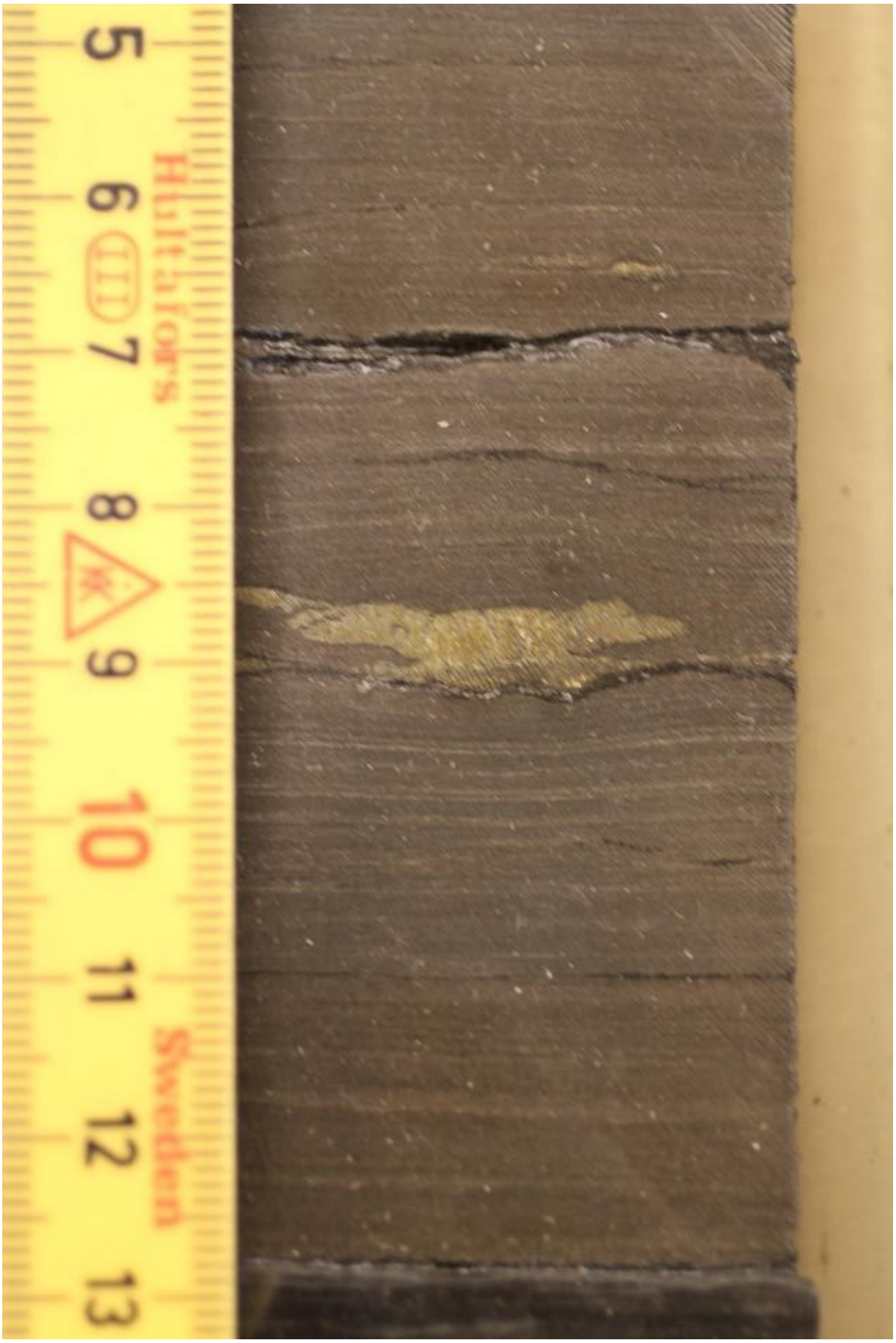

Figure 8: Pyrite in core 7430/10-U-01 at depth 60.26 m.

Figure 9: Pyrite in core 7430/10-U-01 at depth 61.16 m.

Colour

The colour of mudstones studied here varies mostly between dark black and lighter grey but can also have a brown colour at some depths.

The dark black shales indicate reducing conditions with a high content of organic material preserved (Boggs, 2009. p. 527) and the greyer mudstone might indicate a more dysoxic condition (Potter et al., 2005, p.66). Potter et al. (1980) state that the colour is dependent on the organic content and the oxidation of the iron present in the organic rich mudstone. According to Boggs (2009. p.214) the colour of the mudstone should not be used as a reliable indicator in determining the depositional environment, due to changes caused by diagenetic effects that can change the colour at a later stage than deposition.

Most of the colour changes observed in cores 7430/10-U-01 and 7018/05-U-01 are caused either by the varnish turning the core either to a darker colour than the core actually is, or siderite cementation turning the mudstone brown and yellow, and where a higher portion of silt is present the colour turns grey.

Siderite

In the two cores studied here, siderite is present in the form of nodules/grains, concretions, cement, and veins, of different size and thickness. The siderite cement, when thicker than 1-2 cm, is put in its own facies, as it is quite dominant in parts of the cores, especially core 7018/05-U-01.

In core 7018/05-U-01 the siderite veins are quite abundant, and usually show an appearance like that in Figure 10. They tend to appear where some sort of soft-sediment deformation or disturbance has created cracks or fractures that then became filled in by the sideritic material. Siderite is an iron sulphide, which means it has a great effect on the magnetic signal, and thus it needs to be filtered out, as mentioned in the methodology section. By checking the magnetic data, it is clear that these depths need to be filtered out for time series analysis, but they do not seem to affect the immediate surrounding material, so the high reading is only present when there is a part of the vein in the sample.

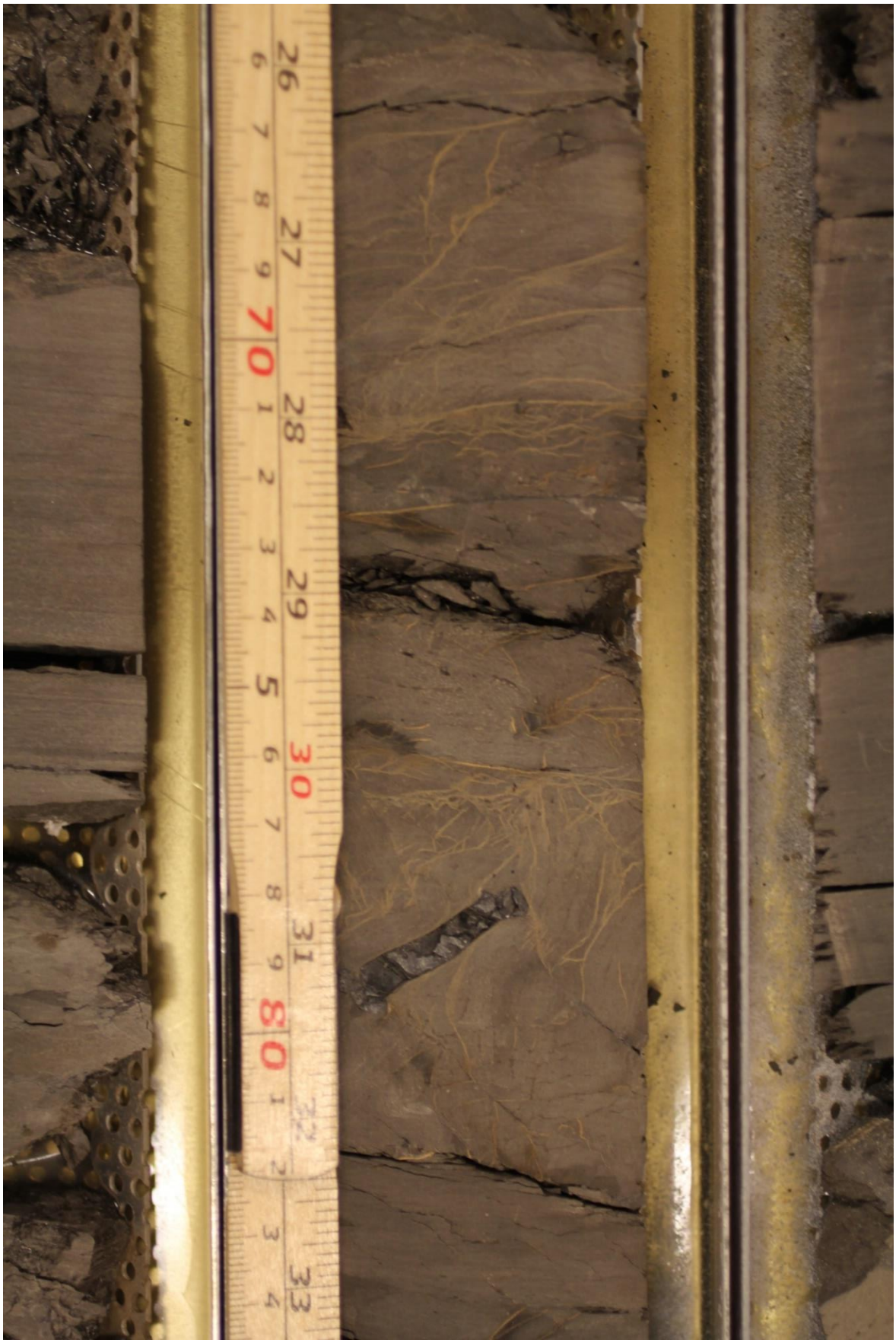

Figure 10: Siderite veins at depth 76.70 m from core 7018/05-U-01. A 2 cm coal fragment is present just above the 80 cm mark in the figure.

Facies

Seven different facies have been identified based on the core descriptions and are described here. The facies are:

1. Facies planar parallel laminated mudstone
2. Facies wavy parallel laminated mudstone
3. Facies discontinuous parallel laminated mudstone
4. Facies silty sandstone
5. Facies sandy mudstone
6. Faces massive mudstone
7. Facies siderite cemented mudstone

Planar parallel laminated mudstone

The lamination is generally indistinct and generally no thicker than 1 mm but varies between 0.5 mm and 2 mm, alternating between dark and light laminae, and is sometimes not easily observed due to the heavy use of varnish on some parts of the cores. This makes it hard to distinguish from the discontinuous parallel laminated mudstone at some points. Pyrite nodules of various sizes are present spread out through the facies, varying from 1-2 mm (especially in core 7018/05-U-01) to 1-2 cm (in core 7430/10-U-01).

The facies varies somewhat in appearance between the cores, as shown in Figure 11 and Figure 12, with the lamination being clearer and just a bit thicker in core 7018/05-U-01 than in 7430/05-U-01. The colour of the facies stays the same dark grey in core 7430/10-U-01, but in 7018/05-U-01 it changes appearance through the core, from a dark grey/black, to a lighter grey, and back to a blacker colour towards the top.

Interpretation

The lamination of mudstones is often a result of slight differences in grain-size between silt and mud, but in these cores, it can be hard to spot the laminae at some depths, and the effect from the varnish hides some of the laminae in the core.

Potter et al. (2005. P 43-44) state that millimetre scale weak to moderately strong colour banded lamination can have several origins, and is poorly understood, but it is in general deposited from suspension by different processes such as a suspension settling mechanism, and it suggests slow deposition in a low-energy water environment where bioturbation is not intense enough to disrupt the lamination, but could also be a result of a traction transport

mechanism in some shales, such as a dilute, low-velocity turbidity current (Schieber, 1978; Boggs, 2009. p. 68-70).

This lamination might be created by processes such as a pulsed hemipelagic deposition, by suspension from the tail of a turbidity current, or a dilute pelagic suspension (Potter et al. 2005. P 43; Boggs. 2009. p. 68-70).

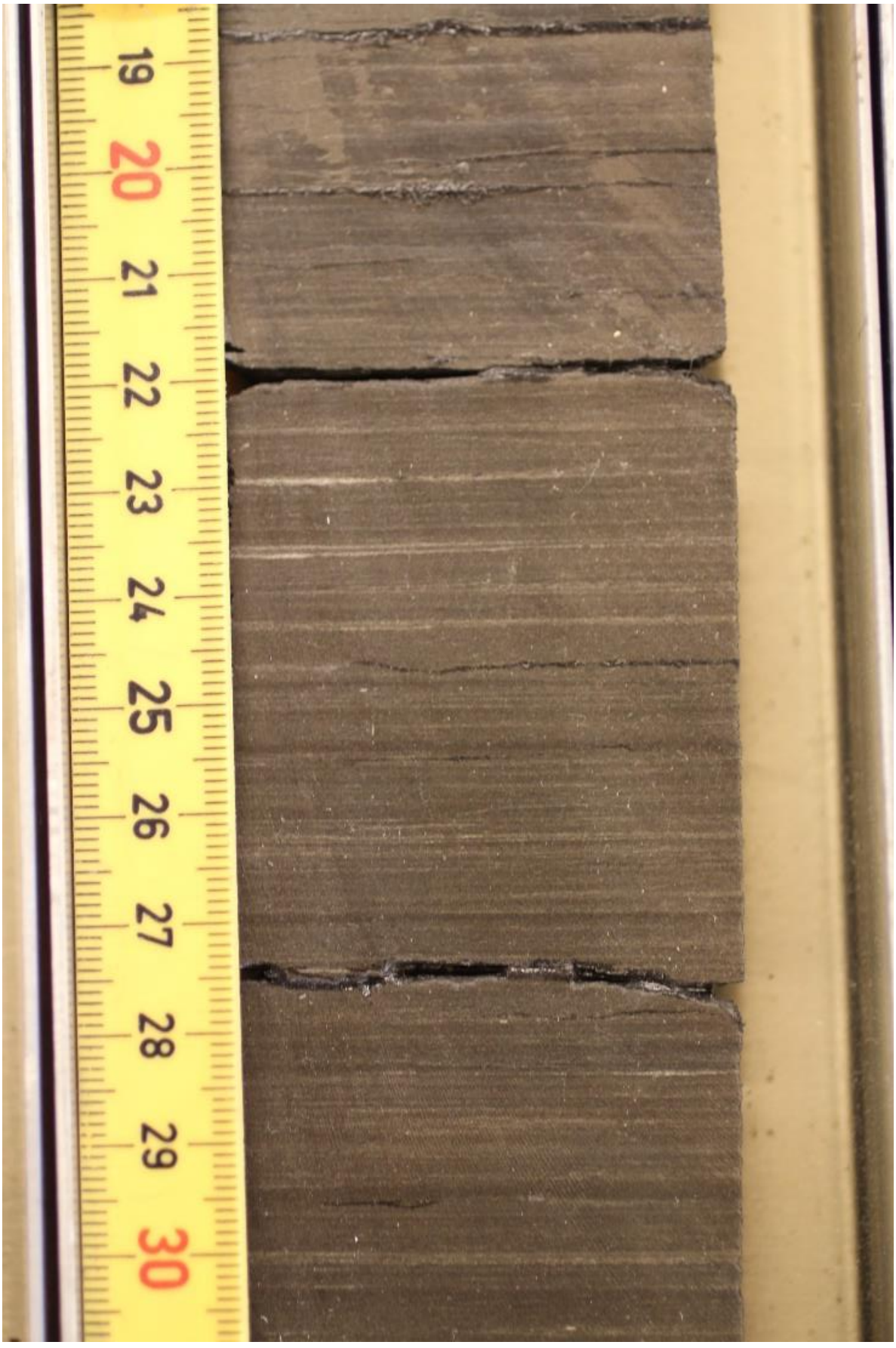

Figure 11: Planar parallel lamination in core 7430/10-U-01 at depth 60.40m.

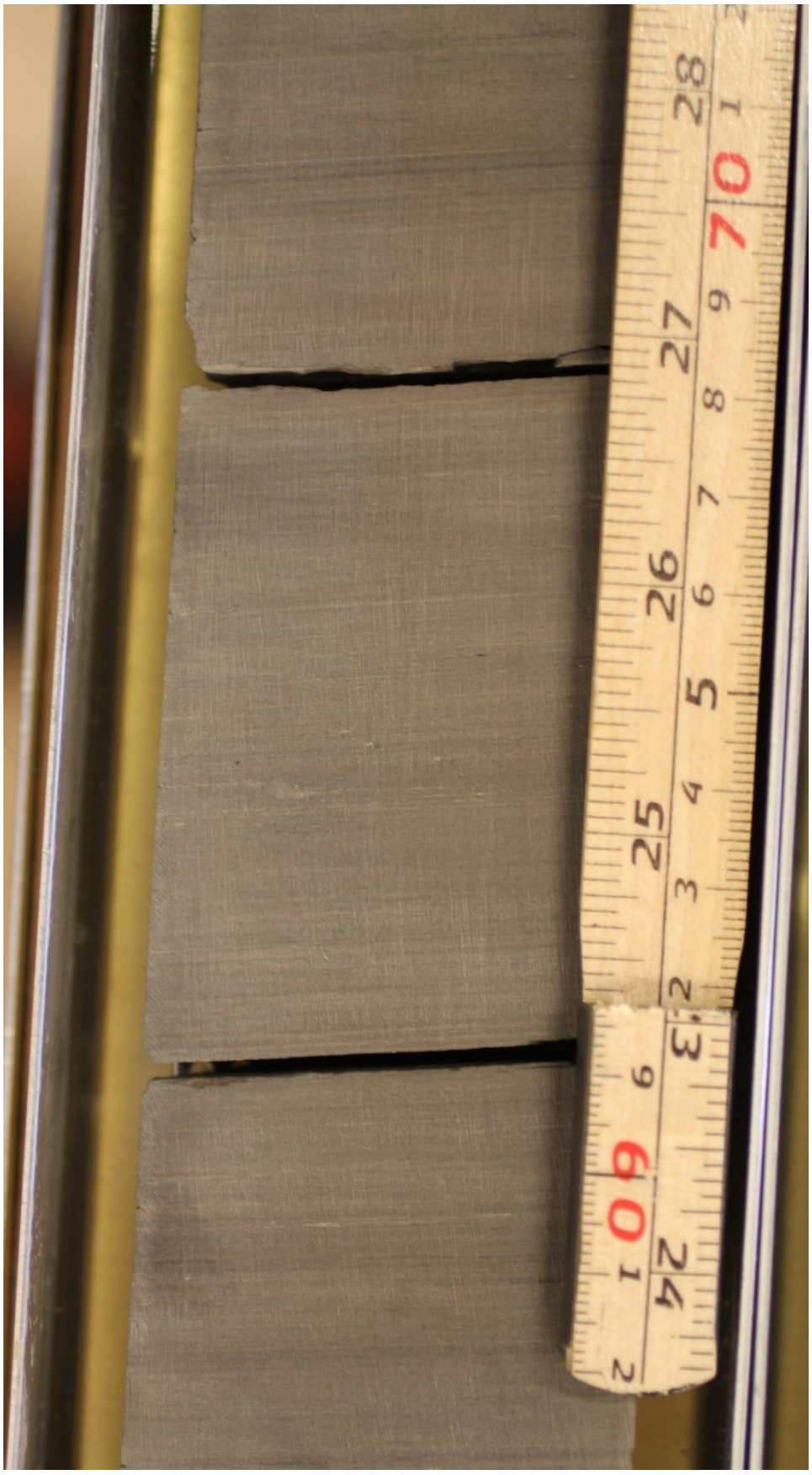

Figure 12: Planar parallel laminated mudstone from core 7018/05-U-01 at depth 198.70 m.

Wavy laminated mudstone

This facies is similar to the parallel laminated mudstone, and still shows continuous lamination, but the laminae are wavier and not planar laminated, as shown in Figure 13.
In the 7430/10-U-01 core the facies is present as short intervals of 10-20 cm (Figure 13), but in core 7018/05-U-01 it appears as longer sections of 1-2 metres (Figure 14). The waviness is clearer in core 7018/05-U01 than in core 7430/10-U-01, and easier to distinguish from the planar laminated mudstone.

Interpretation

Wavy lamination has many of the same characteristics as the planar lamination, but in general there is more energy involved in deposition, such as an interaction from a bottom current (Schieber 1978).

Figure 13: Wavy lamination in core 7430/10-U-01 at depth 65.96m.

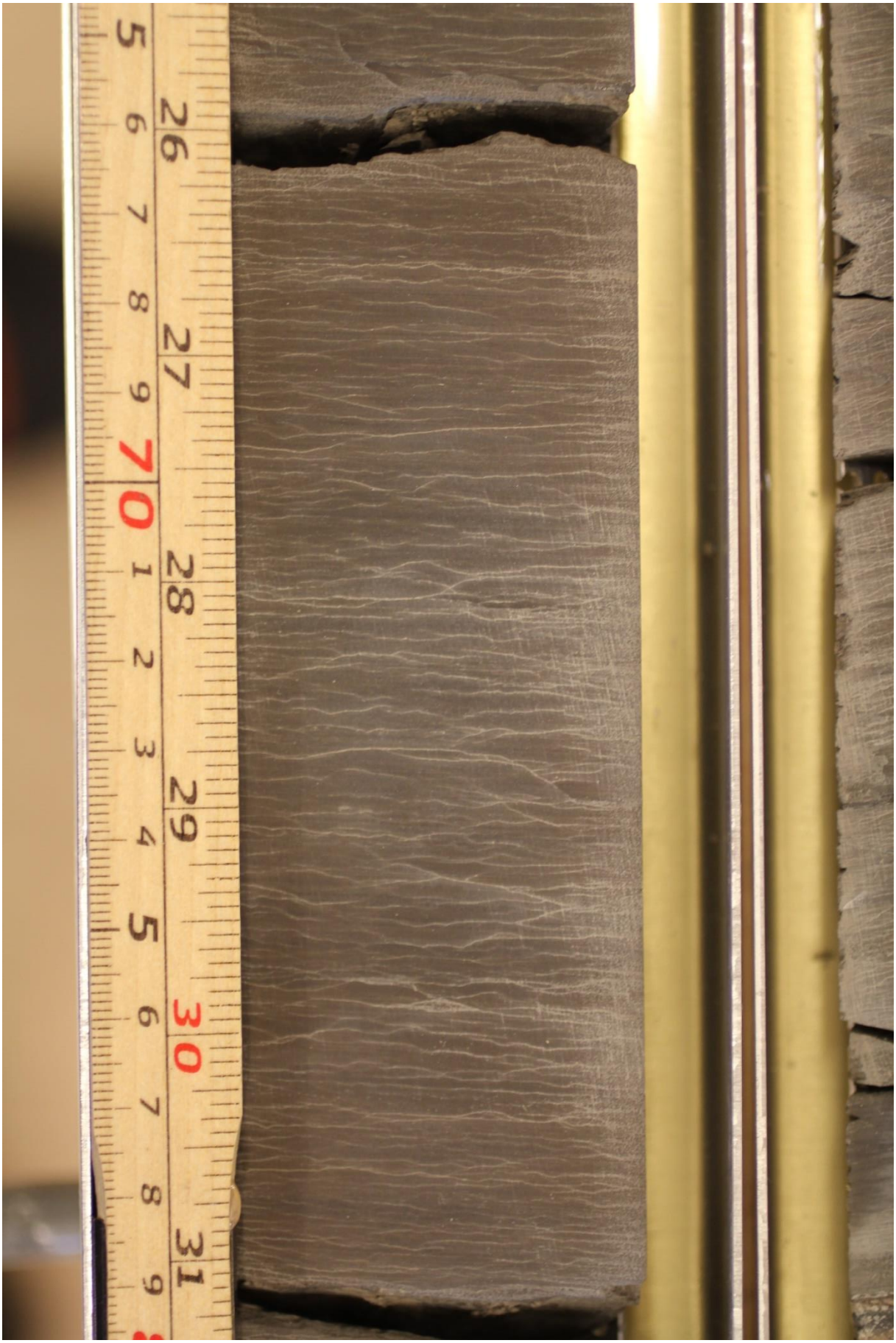

Figure 14: Wavy laminated mudstone from core 7018/05-U-01 at depth 209.60 m.

Discontinuous laminated mudstone

The facies consists of a dark mudstone, with planar parallel lamination that is no longer than a couple of cm at most, and in general thinner (from 0.5 to 1 mm) than in the planar parallel laminated mudstone. It is only present in core 7430/10-U-01, but here it is quite clear and easy to spot, as shown in Figure 15. Also present are silt lenses that are a bit thicker than the laminae (shown in Figure 15 inside red circles) and clearly containing silty material. Several sections of this facies are in poor condition in the display core, but still recognisable in the unvarnished half of the core. Shell fragments can be found both as a single fragment and as "clusters" throughout the facies. Silty material appears as single lenses throughout the facies, varying in thickness from 0.5 to 1.5 mm in thickness and in length from a few mm to a couple of cm.

Interpretation

The discontinuous lamination can be caused by starved ripples moving across the bed, creating both thin short laminae, and the thicker ones called silt lenses. The silt lenses have different length and widths, but mostly show a thin oval shape. Yawar and Schieber (2017) show that as the bedload transports silty grains, both flocculated mud and silt migrate over the bed simultaneously, and these migrating ripples leave behind a thin layer of silty material that over time turns into a laminated deposit. The discontinuous laminae and silt lenses seen in this facies might be a result of this process not proceeding long enough to create continuous laminae, or that the input of silty material is not great enough to create continuous laminae and so resulting in discontinuous laminae. The coarser silt grains (~60 μm~20 μm) end up in ripples (silt lenses) and thicker laminae, and the finer grains (20 μm or less) stay mixed and suspended in the clay matrix (Yawar and Schieber 2017).

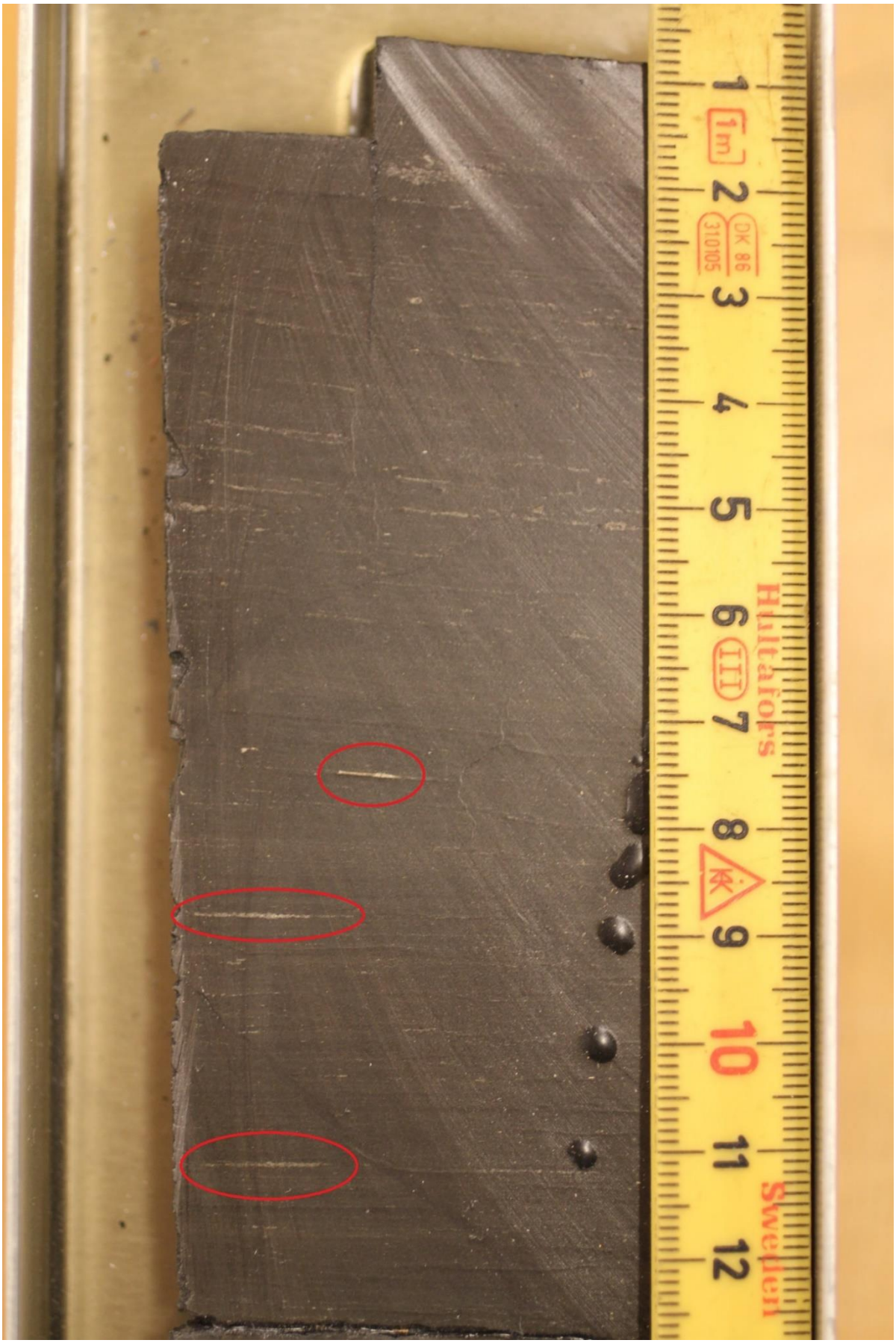

Figure 15: Discontinuous parallel lamination in core 7430/10-U-01 at depth 57.05m. Silt lenses are visible inside the red circles.

Silty sandstone

This facies only occurs in core 7018/05-U-01 as massive layers of 10s of cm, and shows planar parallel lamination as shown in Figure 16. The grainsize is visible under the microscope and is easily observable in the core as the colour is light grey, compared to the black mudstones, and the cored sediments are much harder, leaving the facies in a better condition than the mudstones.

Interpretation

As in the laminated mudstone, changing and short fluctuations of environmental conditions at deposition produce laminae that are separated due to grain size variations, mineral content (organic or other), and clay material (Potter et al. 1980; Boggs, 2006. p. 203-205). The lamination in this facies consists of coarser material than the mudstone facies, and hence giving the light grey colour as no mud is present. Collinson et al. (2006. P71-72) state that the change from darker to lighter laminae might indicate a sudden event that covers the background sedimentation of mud. As the lamination is quite thin, a weak, short-lived density current might be the reason for this deposit (Potter et al. 2005. P 37-40; Collinson et al. 2006. P 70-72).

Figure 16: Siltstone at depth 217.74 from core 7018/05-U-01. The colour change towards the bottom might be a result of siderite cement, as there is a more massive layer of siderite cement just below this facies, also represented in the magnetic susceptibility data.

Sandy mudstone

This facies occurs in a short interval from 55.90 to 56.06 m depth in the 7430/10-U-01 core (Figure 18) and consists of visible fine sand grains in a dark mudstone matrix, without visible structures. The silt/fine sand grains are 0.2 mm in diameter and evenly distributed throughout the section, and the light yellow-white colour makes it easy to spot the grains on the dark mudstone background.

In core 7018/05-U-01 there are some layers that show similarities to the one in 7430/10-U-01, but in this core, when looking under the microscope, the layers are made up by many small shells or shell fragments deposited in a massive mudstone matrix. There are some thin layers throughout the core of roughly 0.5-1.0 cm (see Figure 17) which contain the same kind of shell or shell fragments, but the concentration of shell is higher, and is more compacted in core 7018/05-U-01 than in 7430/10-U-01.

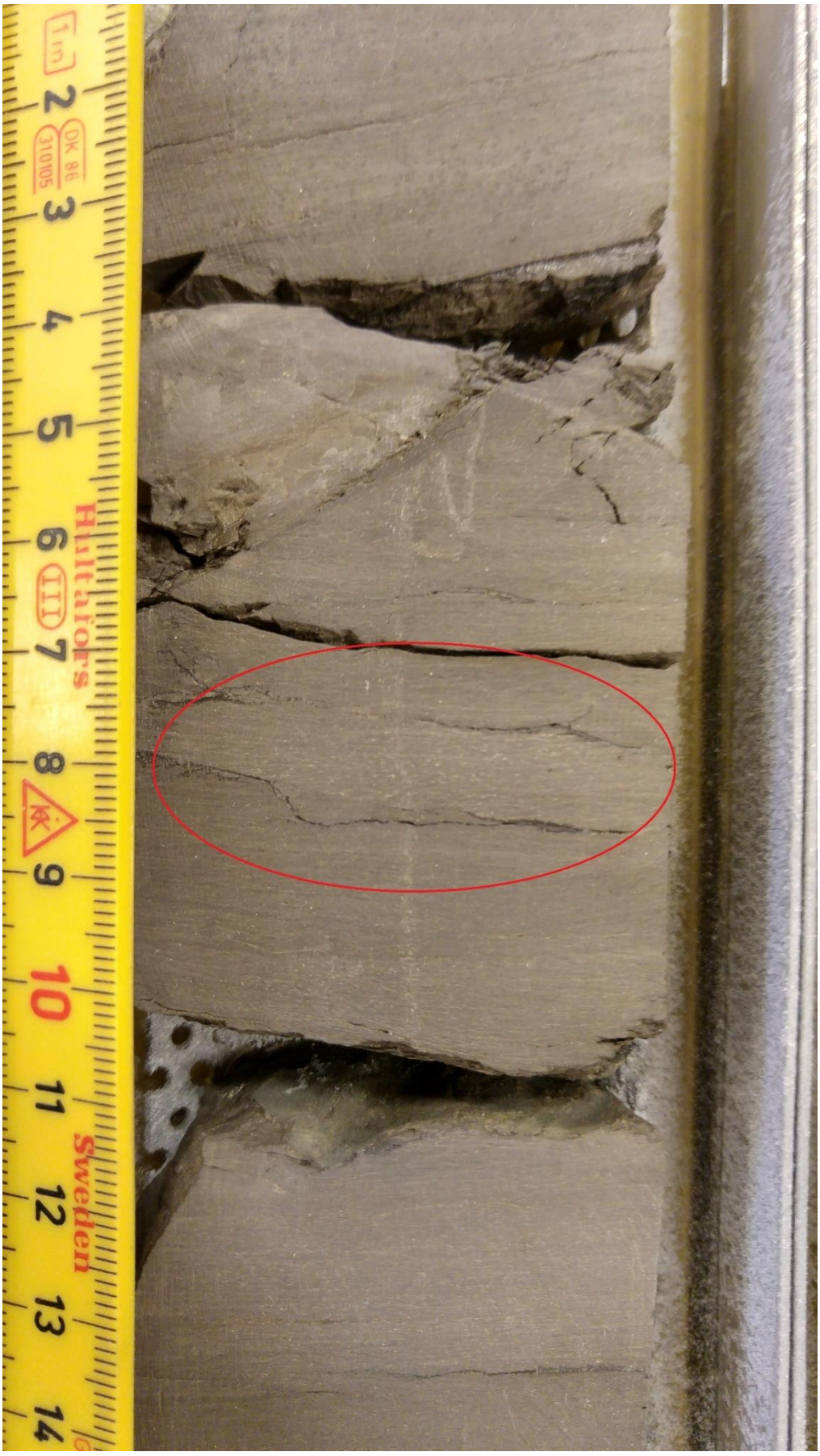

Figure 17: Shell-layer shown in red circle. From core 7018/05-U-01 at depth 76.10.

Interpretation

The presence of coarser visible grains in the mudstone matrix suggests an increase of the flow velocity during the time of deposition. The sand grains usually become deposited by suspension after moving as bedload transport, after reducing flow velocity (Collinson et al. 2006. P29-31).

The layers in 7018/01-U-01 with shell fragments, could indicate that the grains are shell fragments in the comparable layers of core 7430/10-U-01 as well, even where these cannot be easily identified. This could be interpreted as an event where a high number of shell-producing organisms died, was then broken up and transported (possibly broken by the transport) and deposited by suspension in a muddy matrix.

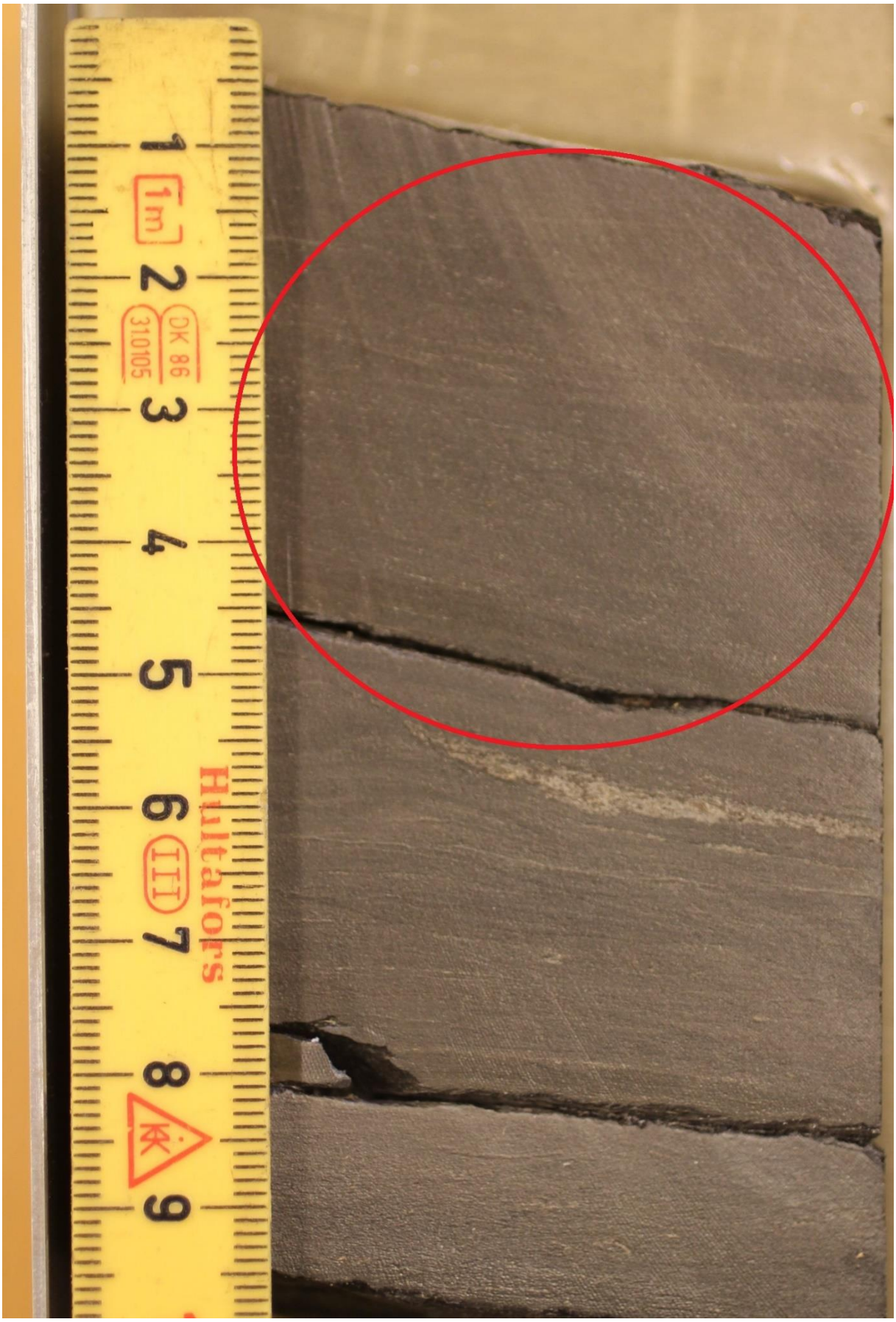

Figure 18: Sandy mudstone in core 7430/10-U-01 at depth 56.05. The sandy grains are the light-coloured spots in the red circle.

Massive mudstone

The facies consist of a dark mud, without visible textures or lamination. In the varnished half of the core, the facies is often broken up in pieces too small to distinguish features (Figure 19), but when looking in the unvarnished half of the core, where it is not completely broken up, it is easily observable. It is almost black in colour and with occasional shell fragments in core 7430/10-U-01 and with siderite veins and concretions in core 7018/05-U-01.

Interpretation

The lack of lamination and structureless appearance can be caused by continuous steady deposition or by destruction of original laminae (Collinson et al., 2006. P 133), and can appear massive due to no platy grains being present, or by fast sedimentation processes. Destruction of original laminae is not very likely here, as there are no signs of bioturbation present, and therefore continuous steady deposition is the most likely process that formed this facies.

Collinson et al. (2006. P72) state that the high sedimentation rate needed for creating a massive structureless mudstone is not unusual, but rather rare.

Figure 19: Massive mudstone at depth 152.20, from core 7018/05-U-01. This also shows how broken up the core is in some places.

Siderite cemented mudstone

The facies looks like both the planar parallel laminated mudstone and the discontinuous parallel laminated mudstone, except for the colour being brighter brown for the siderite cemented mudstone. It is much harder than PLM and DLM and does not break easily along lamination or bedding.

It is most prevalent in the 7018/05-U-01 core, spread out through the core at different thicknesses, where it varies from 1-2 cm to several 10s of cm, and has quartz or calcite veins present within the cement, usually cutting across the lamination. The cement is easy to see due to the bright brown/yellow colour, and it is also easily recognizable from the magnetic susceptibility data, as it has a significantly higher reading than surrounding mudstone.
In core 7430/10-U-01 it is only present at depth 57.54 to 57.68 m, but here it is hard to distinguish it from the laminated mudstone, as the varnish makes the brown colour hard to see. This interval still looks like it has some siderite cement but a lack of increase in the magnetic signal suggest that this might just be a varnish effect, or cementation to a lesser degree than in core 7018/05-U-01.

Interpretation

Siderite concretions and cement are a common feature to be observed in organic rich mudstones and are usually formed post-deposition. They contain iron-carbonate and are created within the sediment as a result of early diagenetic processes on organic matter (Potter et al., 1980, Nichols, 2009). Siderite is an indicator for a reducing depositional environment, as an alkaline environment must be present, and the precipitation of siderite is favoured by reducing conditions (Collins et al., 2006).

Slumps

In core 7018/05-U-01 there are several sections that show textures and characteristics that look like slumped beds. This is defined as irregular stratification caused by unconsolidated sediments moving due to gravity, and they are often bound on top and below by strata without evidence of deformation (Boggs, 2009. p.84-89).

This is clearly seen where the sections of the core show syn-sedimentary folding, and laminations turn and bend from horizontal to vertical, while the layers just above or below these layers show no indications of folding. The lower and upper boundaries are often sharp. Boggs (2009. p. 84-89) states that the slumps typically occur in environments where sedimentation rate is high and steep slopes lead to instability, such as at heads of submarine canyons, on continental slopes, and at the walls of deep-sea trenches, which could potentially be the case for these cores, as the deposition of the Hekkingen Formation occurred when the area moved to deep-marine setting, and so might be influenced by the continental slopes.

Figure 20: Slumping from depth 104.25-109.25m in core 7018/05-U-01.

Figure 21: Close-up of slumping at depth 104.70 m in core 7018/05-U-01. Lamination can clearly be seen bending without being broken up.

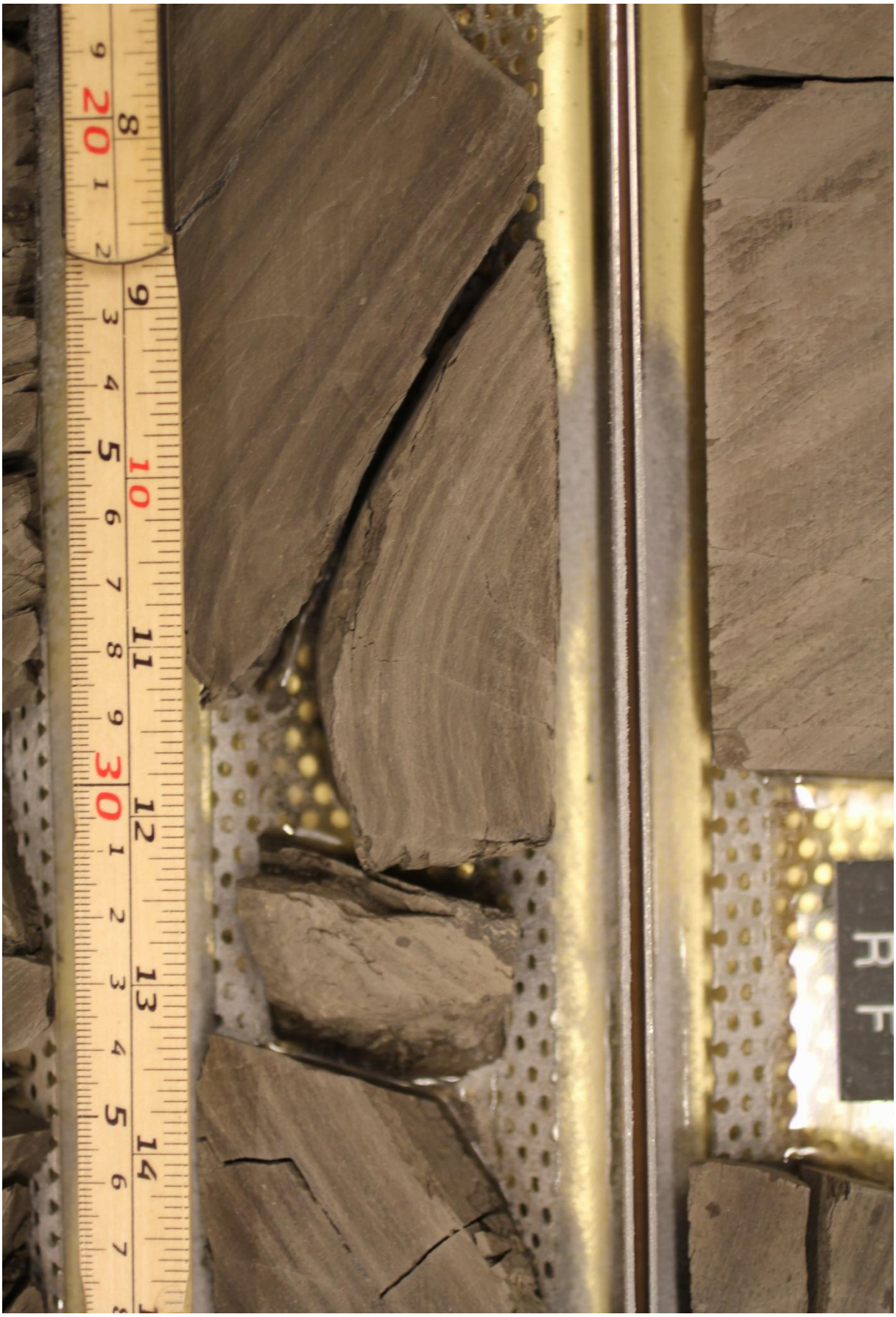

Figure 22: Close-up of slumping at depth 106.25m in core 7018/05-U-01. Lamination can be seen turning and going vertically down the core and bending within the layer.

Bulk susceptibility measurements

Core 7018/05-U-01

The non-processed bulk magnetic susceptibility data, normalized by weight, and with the relatively high siderite magnetic values removed, are shown in Figure 23.

The amplitude spectrums in Figure 24 were created for depths 51.6 m to 89.8 m, 95.3 m to 147.6 m and 211.0m to 246.5 m. The depths are found mostly by trial and error, to see what depths create the best amplitude spectrum, but the depths chosen here correlate to lithological changes in the core. The first interval, 48.6-125.2 m is roughly the depth that is dominated by shell fragments in the core, while the next interval, 136.4-211.0 m, represents a section with few or no shell-fragments in the core; the boundary at 211.0 m is approximately where the Hekkingen Formation goes from Krill member to Alge Member.

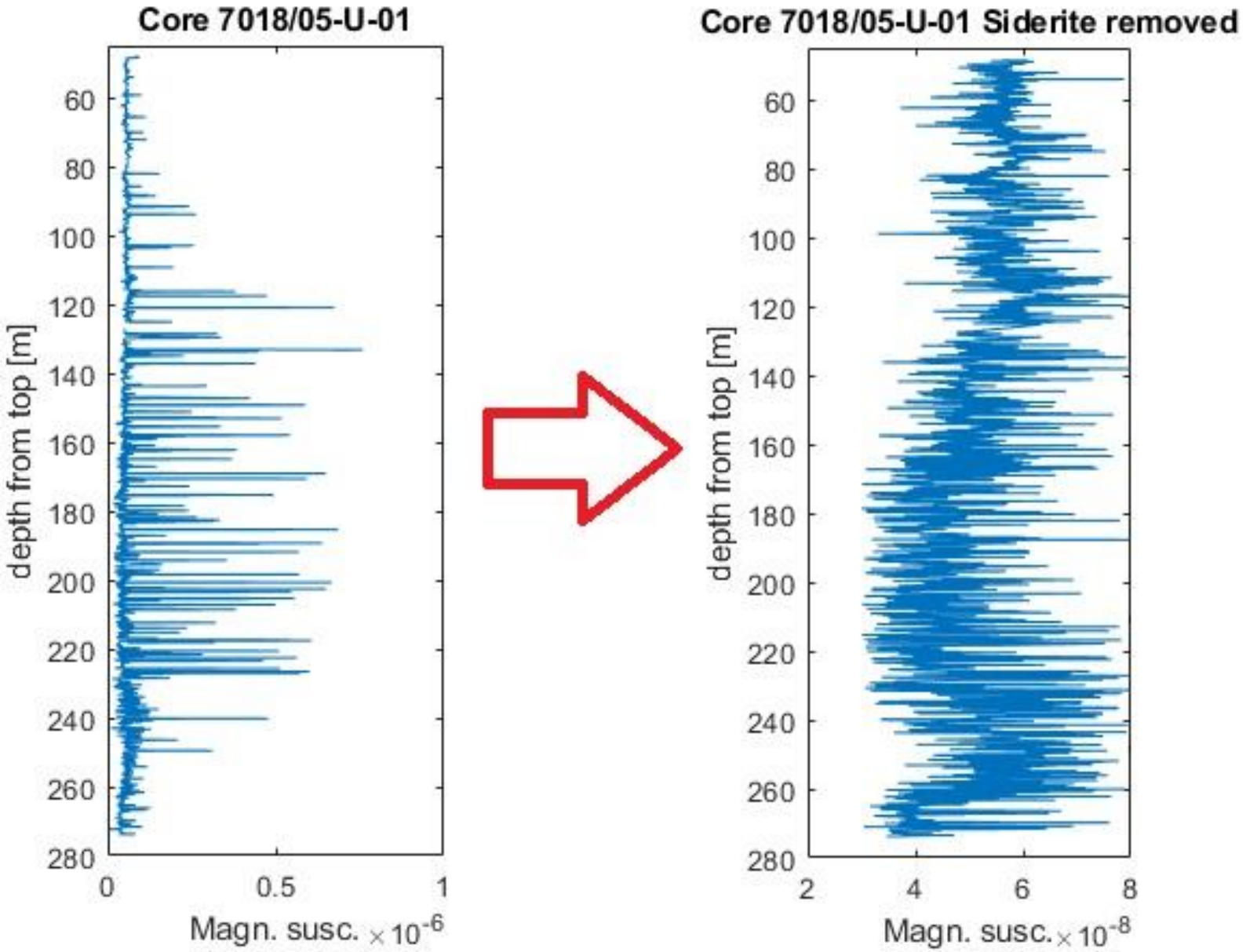

Figure 23: Magnetic susceptibility data from core 7018/05-U-01. Signal normalized by weight on the left, and with siderite values removed on the right.

By using the sedimentation rate, the time span for depositing 1 metre of sediment can be calculated, and then the duration for the cycles can be found, by multiplying the cycle length with the duration of depositing 1 metre.

For core 7018/05-U-01 the sedimentation rate is given as 16.9 m/Myr for the part above 211.0 m and 13.1 m/Myr for the part below 211.0 (Georgiev et al. 2006).
There is a lot of uncertainty to this sedimentation rate, as the value here is a compacted sedimentation rate, and the decompaction factor is not known.
The duration of each cycle is given in Figure 24 and the spectrums shows several peaks that could be the dominant ones,
For the first interval, 51.6-89.8 m, potential dominant peaks are the ones with a duration of 71 kyr, 35 kyr, 30 kyr and 22 kyr. In the second interval, 95.3-147.6 m, dominant peaks are the ones with a duration of 59 kyr, 28 kyr and 24 kyr, and for the last amplitude spectrums, 211.0-246.5 m, show peak at 34 kyr duration,

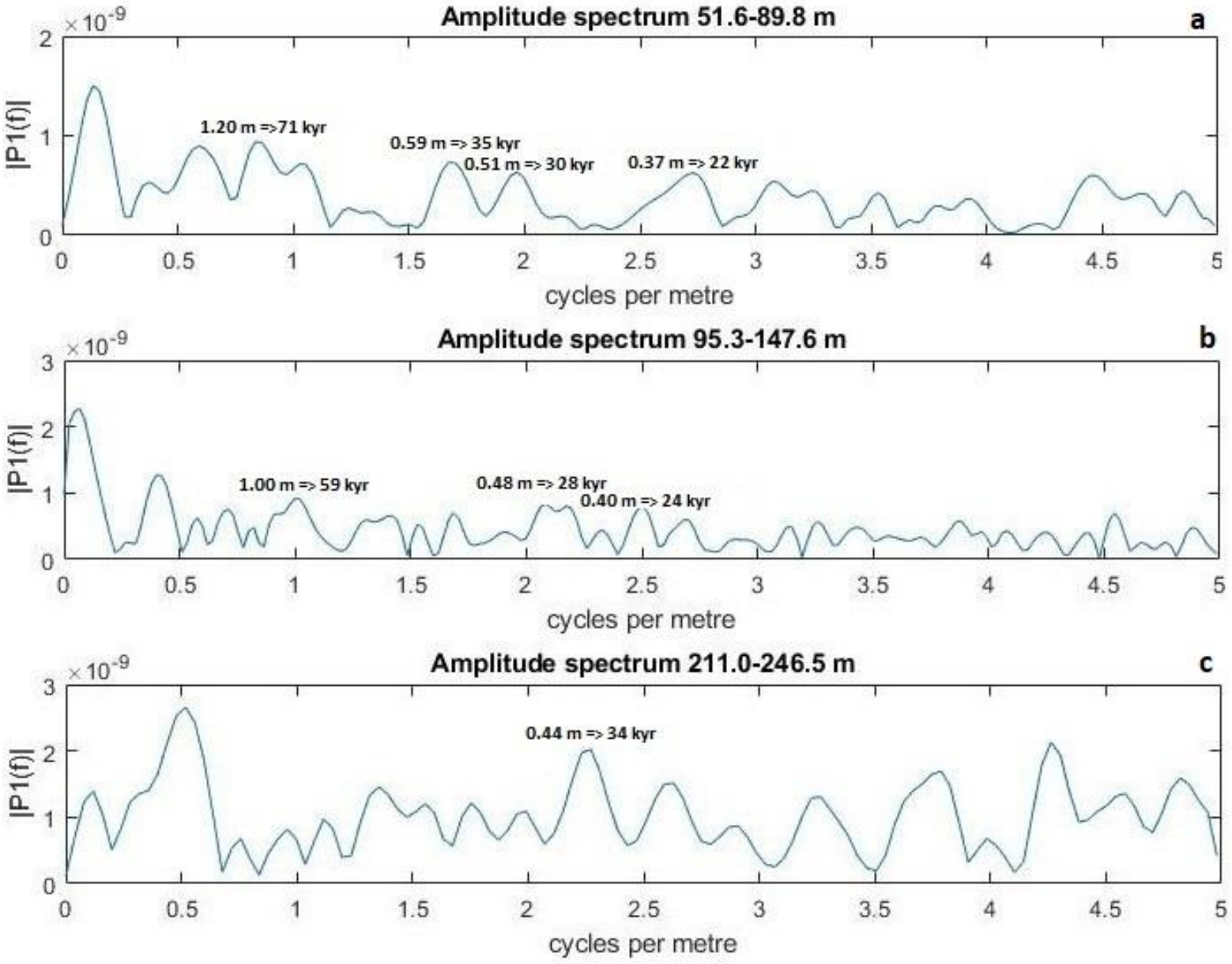

Figure 24: Amplitude spectrums created from core 7018/05-U-01. The number over the dominant peak gives the length and duration of the cycle. The different spectrums are labelled a, b, and c.

The unprocessed bulk magnetic susceptibility values normalized by weight, and with sideritic values removed are shown in Figure 25.

The resulting amplitude spectrums with cycle length and duration of dominant peaks are shown in Figure 26.

By using the sedimentation rate of 0.2 m/kyr, the cycles in this amplitude spectrum would be too long, so only the length of the cycles are mentioned in the spectrum. This is further mentioned in the discussion.

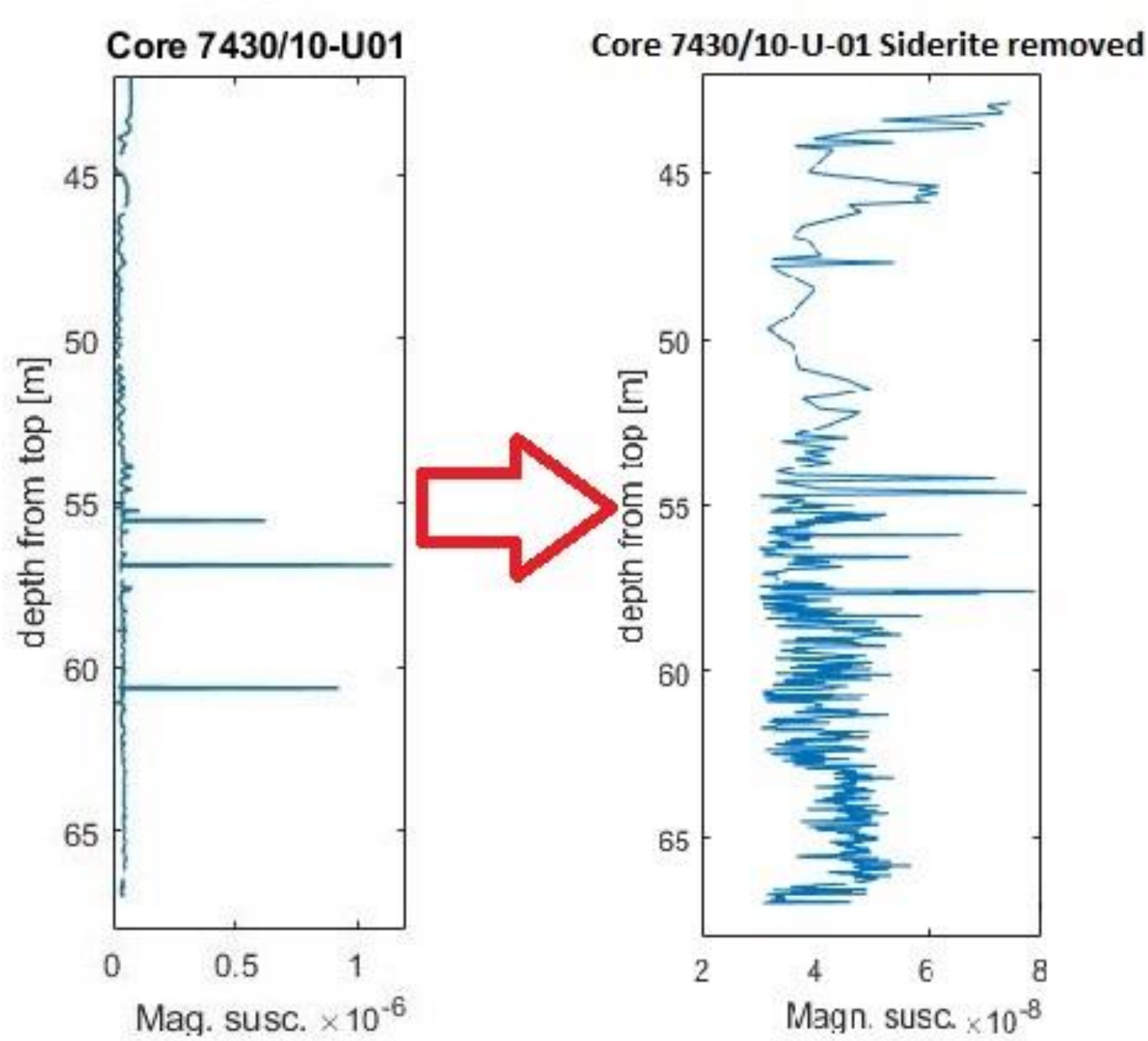

Figure 25: Magnetic susceptibility data from core 7430/10-U-01. Signal normalized by weight on the left, and with siderite values removed on the right. The pattern of the upper part is caused by a different sampling interval (10cm) than the lower part (2cm).

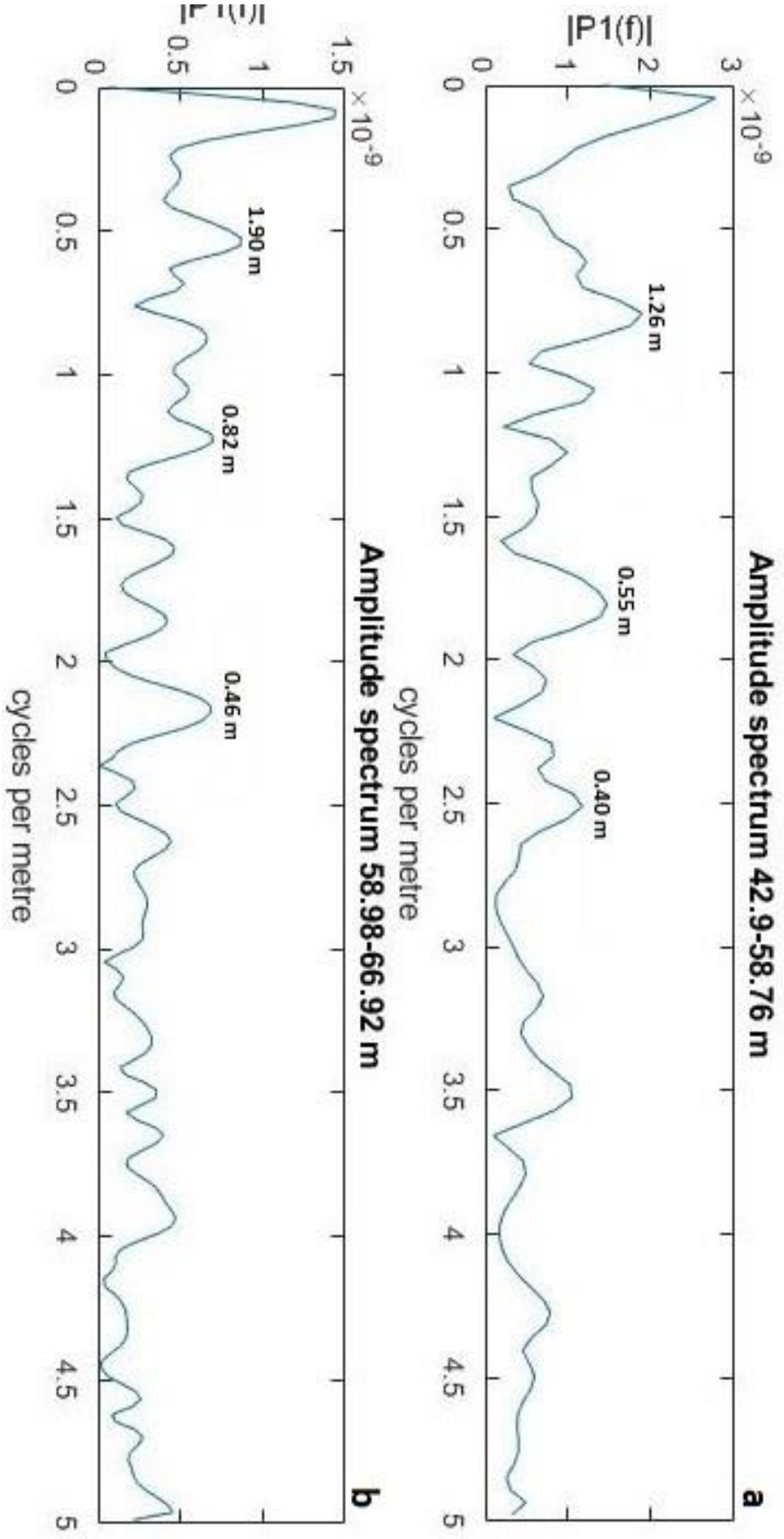

Figure 26: Amplitude spectrums created from core 7430/10-U-01. The number over the dominant peak gives the length of the cycle. The different spectrums are labelled a and b.

Filtering of slumped sections

After taking out the sections of the core which are slumped or are turbidites (see core descriptions in the appendix), a new thickness of the Hekkingen Formation in the cores is calculated. The new thickness of core 7018/05-U-01 becomes 213.2 m and core 7430/10-U-01 becomes 23.82 m.

The new amplitude spectrums can be seen in Figure 27 and Figure 28.

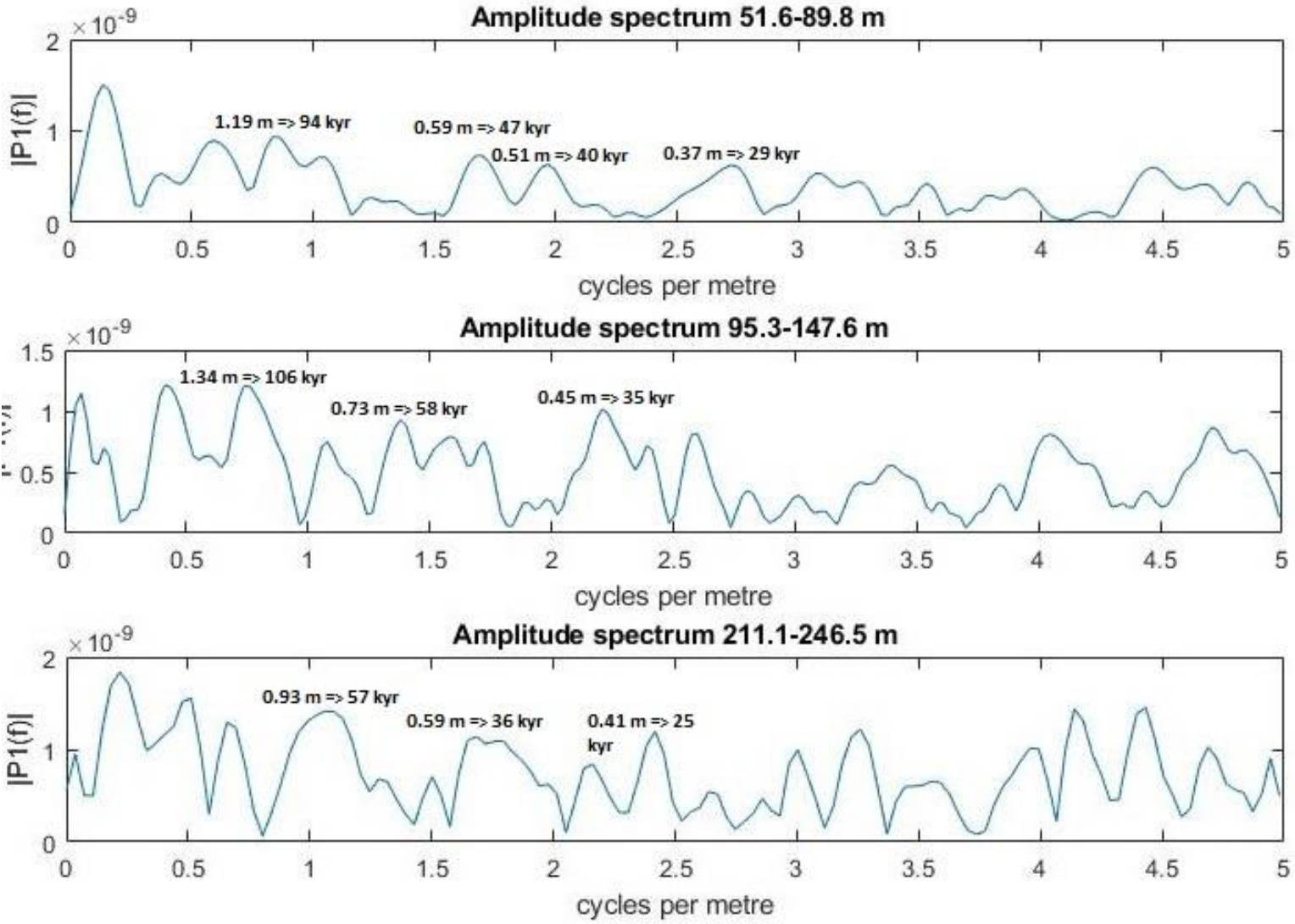

Figure 27: Amplitude spectrums created from core 7018/05-U-01 with the slumped sections removed. The number over the dominant peak gives the length and duration of the cycle.

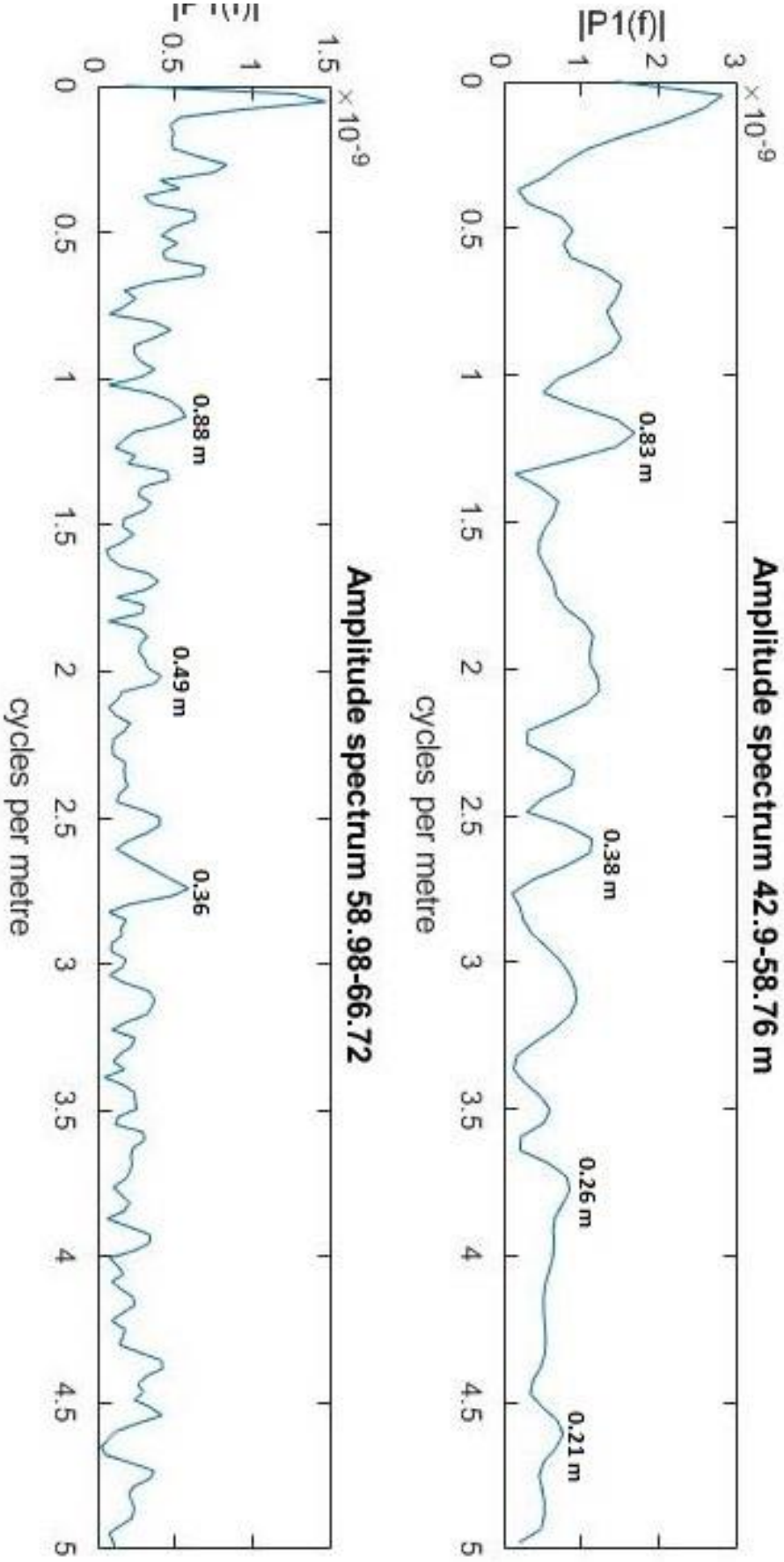

Figure 28: Amplitude spectrums created from core 7430/10-U-01 with the slumped sections removed. The number over the dominant peak gives the length of the cycle.

Wavelet analysis

Core 7018/05-U-01

The wavelet analysis was done on all depth intervals in the core, but only four different depth intervals had long enough sections without gaps, and these are shown below.

The first depth interval (Figure 29) is a bit unclear, but the dominant cycles lie around 2 and 4 cycles per metre.

The second interval (Figure 30) shows that dominant cycles are present at around 1 and 2 cycles per metre. The analysis also shows that there might be some dominant peaks from 0.3 – 0.7 cycles per metre, but it is also possible that this is an artefact.

The third analysis (Figure 31) shows that the dominant cycles are at around 1.1 cycles per metre and at 2.5-2.6 cycles per metre, and the analysis at the fourth depth interval (Figure 32) shows dominant cycles to be around 1 and 2 cycles per metre. These analyses are helpful in determining the dominant cycles from the amplitude spectrums and show that the dominant cycles change somewhat through the core.

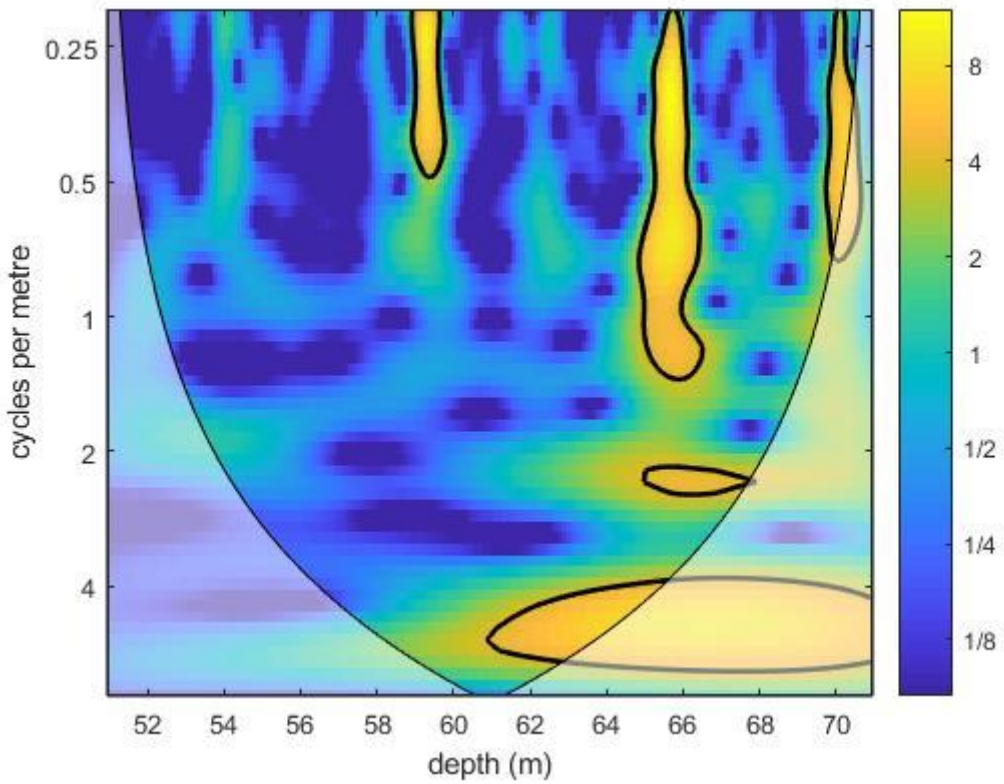

Figure 29: Wavelet analysis of core 7018/05-U-01 at depth 52-70 m.

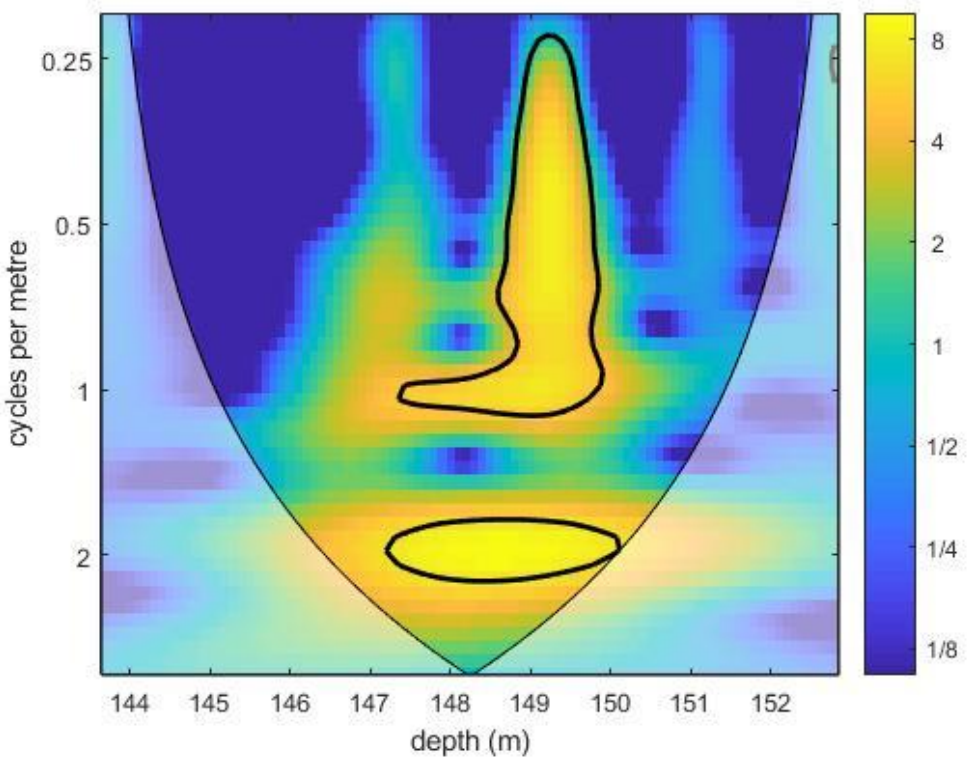

Figure 30: wavelet analysis of core 7018/05-U-01 from depth 144-152 m.

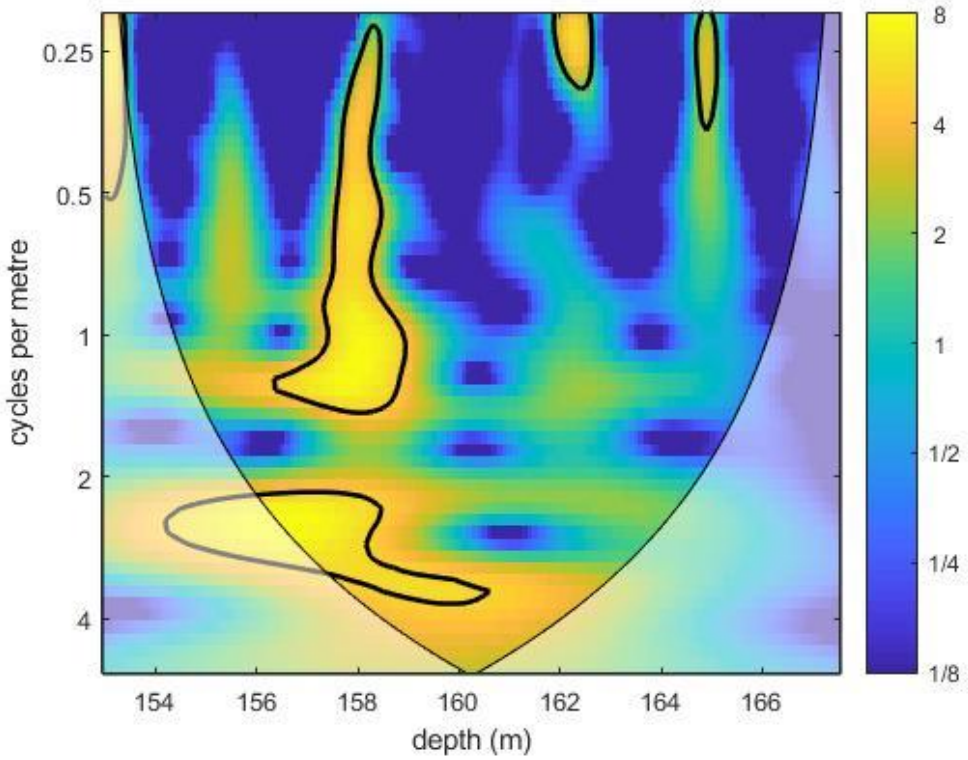

Figure 31: Wavelet analysis of core 7018/05-U-01 from depth 154-166 m.

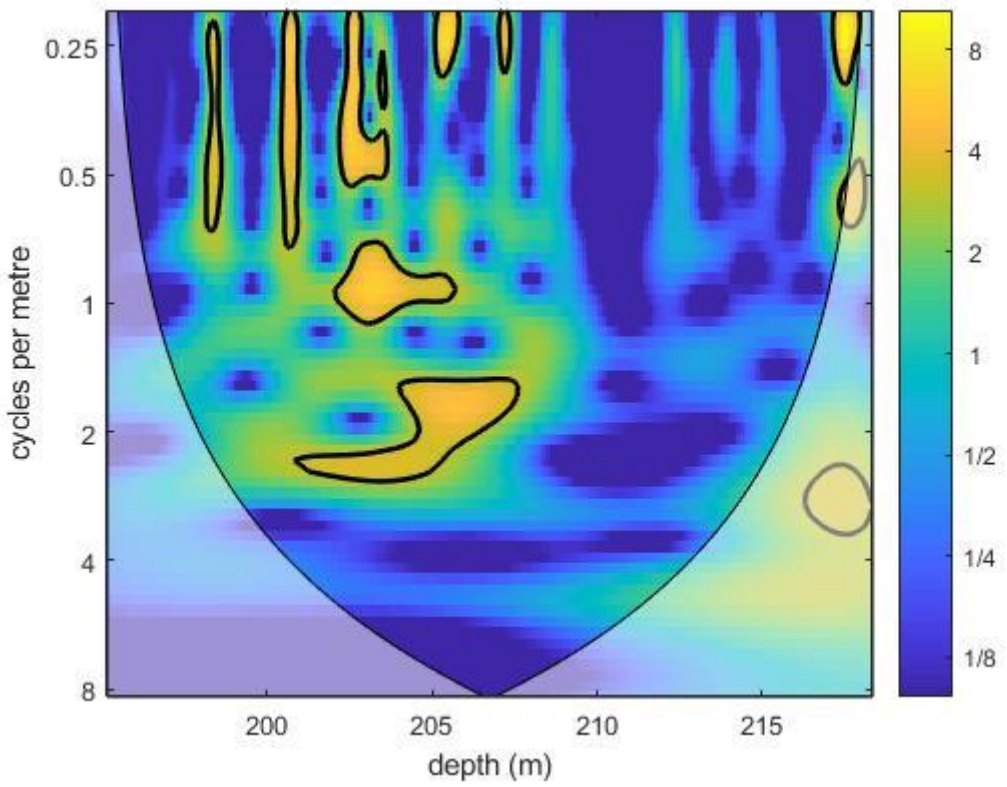

Figure 32: Wavelet analysis of core 7018/05-U-01 at depth 200-215 m.

Core 7430/10-U-01

The analysis for this core did not work as well as the analysis for core 7018/05-U-01, as there are a lot of gaps in the data, so that only very short sections of the core could be investigated. The first depth interval (Figure 33) shows that the dominant cycles lie around 0.3-0.4 cycles per metre, and the second one (Figure 34) also shows the dominant cycles to lie around 0.3-0.4 cycles per metre.

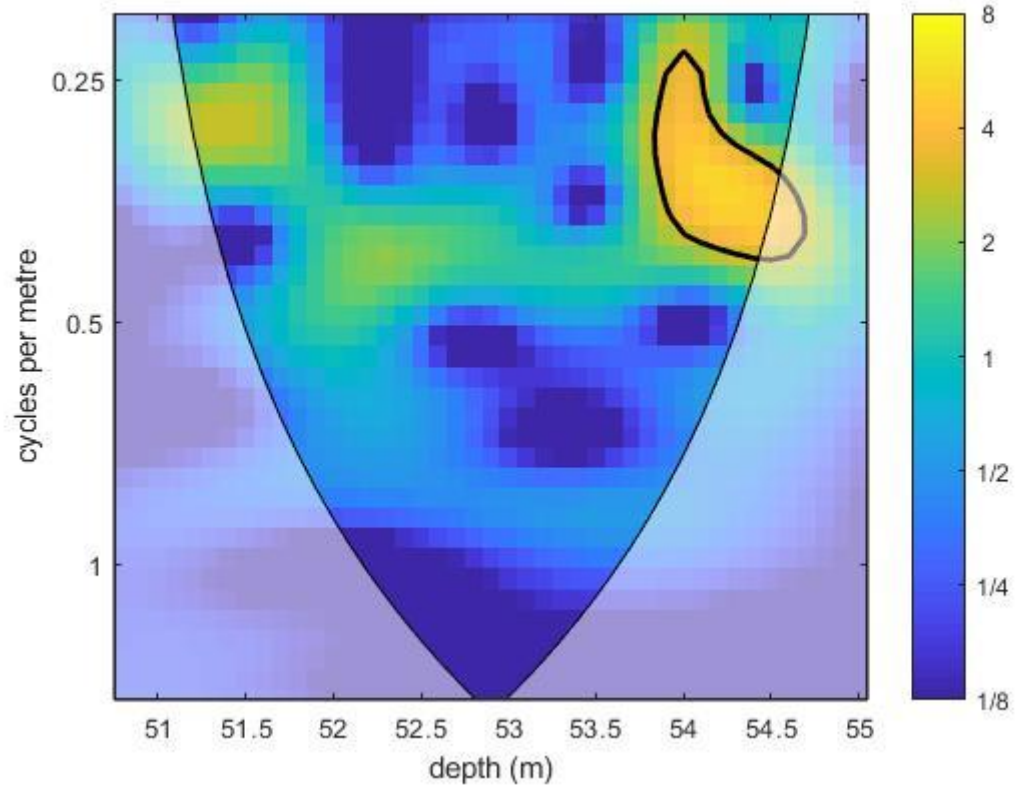

Figure 33: Wavelet analysis of core 7430/10-U-01 at depth 51-55 m.

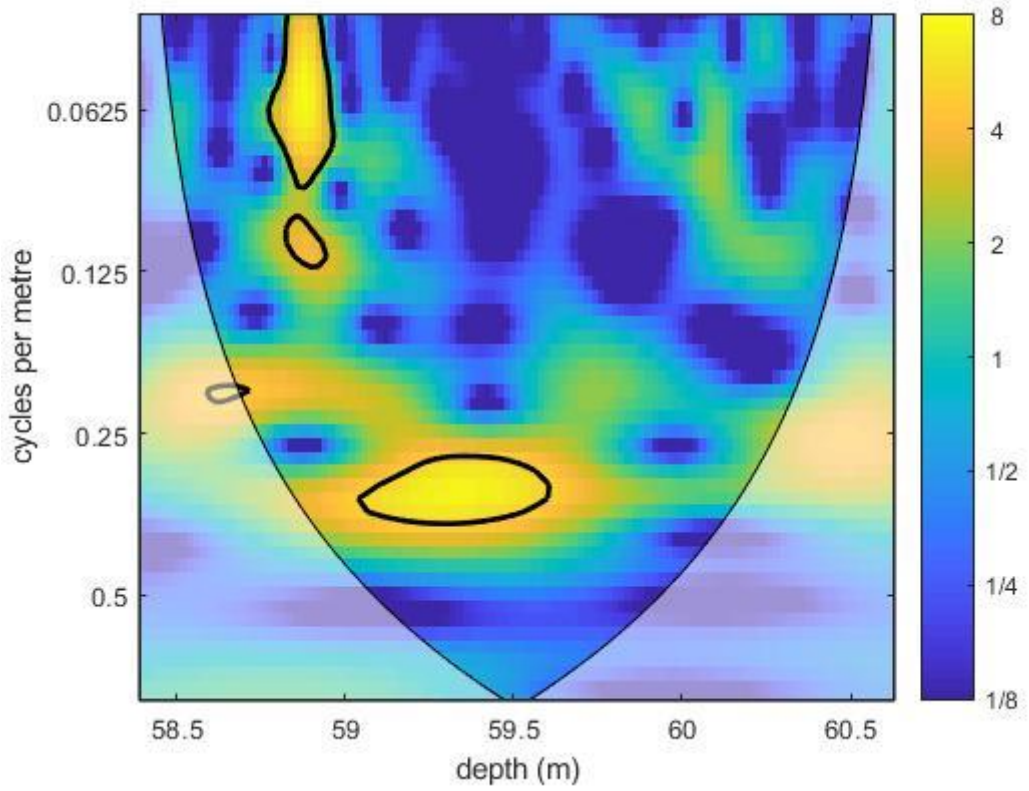

Figure 34: Wavelet analysis of core 7430/10-U-01 at depth 58.5-60.5 m.

Discussion

Environmental influence on magnetic signal

To best show how the depositional environment affects the magnetic susceptibility signal, a table is created as a comparison between facies and average magnetic susceptibility of the specific interval. The facies and signal are taken from core 7018/05-U-01 as this is the longest core, with thicker examples of each facies, and a clear separation between the different facies. The depths that are looked at are the ones that are not disturbed or have any siderite present either as veins or cement, and display the longest and most homogenous example of the specific facies. The values in the table are given as the average value of that depth interval.

Laminated mudstone		Wavy laminated mudstone		Massive mudstone	
Depth	**Average signal**	**Depth**	**Average signal**	**Depth**	**Average signal**
61.5-64.2	5.37240E-08				
70.5-71.7	6.20452E-08				
82.6-85.7	5.36033E-08				
121.1-122.0	5.49322E-08	113.9-115.5	5.86097E-08	118.4-119.2	6.00325E-08
131.8-132.5	5.33052E-08	130.2-130.9	4.87366E-08		
140.6-142.3	5.13708E-08	138.7-139.4	4.7454E-08	151.4-152.2	4.94591E-08
174.0-175.0	3.86115E-08	202.7-203.4	4.3055E-08		
214.3-214.7	4.51222E-08	211.4-212.2	4.60042E-08		
244.4-245.3	6.61212E-08	218.8-220.4	4.15419E-08	235.6-236.2	6.76843E-08
272.4-273.8	4.10458E-08	266.9-270.0	4.24848E-08		

There seem to be some small differences in the average signal in the different facies. The planar parallel laminated mudstone and massive mudstone has a slightly higher average magnetic susceptibility than the wavy laminated mudstone. They are not significantly higher, so they will not affect the amplitude spectrums directly, but rather be a part of the natural variation and cyclicity found.

The small differences might be due to a small difference in the magnetic mineral content, and the small changes in sedimentation might lead to this, as some of the heavy magnetic mineral such as iron can be transported and deposited by a slightly higher energy environment.

This could be the reason for the planar parallel laminated mudstone and massive mudstone to have slightly higher average magnetic susceptibilities, as the wavy laminated mudstone might be influenced by a higher velocity current than the other two facies, resulting in the magnetic minerals to be transported away, and not deposited.
The differences between the facies seen here are much smaller than the effects caused by the siderite cement, concretions, and veins.

Environmental influence on the magnetic signal

When looking at the sedimentary logs, there is evidence of more current activity than earlier stated by Smelror et al. (2001). The presence of slumping, turbidity currents and mudflows show that there was more activity during deposition than just being deposited at a calm deep marine setting. There is also presence of ripples, either as very small compacted ripples, or as starved ripples as can be seen in the discontinuous laminated mudstone facies. The variation in lamination type also indicates a change in energy-levels, as the wavy laminated mudstone would need more movement during deposition to be created, if not it would either be deposited as a planar parallel laminated mudstone or as a massive mudstone.

When looking at the depths at which the amplitude spectrums are created, especially for core 7018/05-U-01, there seems to be a connection between the environmental condition and the resulting magnetic signal and cyclicity. Spectrum a from core 7018/05-U-01 (Figure 24 shows) the section that is dominated by shell fragments, and when the depth of this spectrum is extended beyond this depth, no cycle can be seen to be dominant (Not shown in any figure).
Spectrum b (Figure 24), the section without shell fragments, and spectrum c (Figure 24), below the boundary between Krill Member and Alge Member, also show differences, and if the depth of the second spectrum is extended down, or the third spectrum is extended up, no clear dominant cycles can be observed.
This means that there is some change between the depths of the amplitude spectrums, reflecting a change in the depositional environment or a change in sedimentation rate. This change is not easily seen in the wavelet analysis, but might be clearer if the missing datapoints were fixed, and several longer sections could be analysed,
Weedon et al. (2004) state that in the Kimmeridge Clay Formation, the longer cycle (38 kyr) is an obliquity cycle that affects terrestrial and marine environments, and that the shorter cycle (18 and 22 kyr) are precession cycles that affect the terrestrial environment. If this is

compared to the Hekkingen Formation, it could be that the oldest part of the Hekkingen Formation is dominated by precession cycles, as it is closer to the terrestrial environment, and as the subsidence and transgression in Late Jurassic prograded, and causing the depositional environment to move to deeper marine, the longer obliquity cycles influence the Hekkingen Formation.

Looking at the dominant cycles from Figure 24, going from the lowest depth interval (c) and upwards, it goes from being dominated by a 34 kyr cycle, while a and b show more influence by a 59 kyr and 71 kyr cycles. This reflects a change from a precession dominated environment, towards an obliquity dominated environment.

Cyclicity in the Hekkingen Formation

From the amplitude spectrums, both core 7018/05-U-01 and 7430/10-U-01 show cycles that are significant.

For core 7018/05-U-01, the two spectrums created (Figure 24) from the top part, 51.6-89.8 (a) and 95.3-147.6 (b) show some similarities based on the duration of the cycles, and they show the same cycles through both spectrums. This goes for the 22 kyr and 30 kyr cycles in spectrum a, corresponding to the 24 kyr and 28 kyr cycles in spectrum b. Spectrum b also shows a peak at 59 kyr , that correspond to the 71 kyr cycle in spectrum a.

The lower spectrum, c, shows at least one dominant peak, corresponding to a 34 kyr cycle. This reflect some of the change between the upper and lower member of the Hekkingen Formation, but spectrum a also shows a potential peak at 35 kyr duration. The change between spectrums a and b reflects the change between the upper shell-dominated part and the lower siderite vein dominated part, and can be seen as spectrum a looks more dominated by the 35 Kyr cycle, which is not seen in spectrum b.

The similarities between spectrum a and b, and the differences to spectrum c, reflects the changing sedimentation rate at this depth, where it goes from 16.8 m/Mye to 13.1 m/Myr.

Core 7430/10-U-01 shows several dominant cycles per metre as seen in Figure 26, although the sedimentation rate is too uncertain for this core to be certain about the duration of the cycles. The different sedimentation rates given by Langrock et al. (2003) and Mutterlose et al. (2003) will be tested, and the resulting durations of the different cycles are given in Table 1 below.

Spectrum a (42.9-58.76 m)			
Cycle length(m)	**Duration kyr (0.2cm/Kyr)**	**Duration Kyr (19.0 m/Myr)**	**Duration Kyr (16.2 m/Myr)**
1.26	630	66.3	77.8
0.55	275	28.9	33.9
0.4	200	21.1	24.7
Spectrum b (58.98-66.92 m)			
Cycle length (m)	**Duration kyr (0.2cm/Kyr)**	**Duration Kyr (19.0 m/Myr)**	**Duration Kyr (16.2 m/Myr)**
1.9	950	99.9	117.3
0.82	410	43.2	50.6
0.46	230	24.2	28.4

Table 1: : Duration of the different cycles for core 7430/10-U-01. The two spectrums are labelled a and b, and the duration of the cycles are calculated with the different sedimentation rates.

It is clear that by using the low sedimentation rate of 0.2 cm/My of Langrock et al. (2003), the cycles get unreasonably long durations, and the sedimentation rate that gives the cycle durations that is most comparable to core 7018/05-U-01 is the 19.0 m/Myr given by Mutterlose et al. (2003). Using the latter sedimentation rate, the durations of the cycles in core 7430/10-U-01 are 66.3 Kyr, 28.9 Kyr and 21.1 Kyr for spectrum a, and 99.9 Kyr, 43.2 Kyr and 24.2 Kyr for spectrum b. Thus the most likely sedimentation rate would be the one proposed by Mutterlose et al. (2003) at 19.0 m/Myr, but there is still a lot of uncertainty around this rate, as it is given as 19.0 +/- 7.6 m/Myr.

The amplitude spectrums created when the slumped sections were removed (Figure 27 and Figure 28), can be compared to the original spectrums to see if there is any improvement in clarity of the dominant peaks. For core 7018/05-U-01 (Figure 27), the first spectrum, 51.6-89.8 m, does not change, as there is no data removed from this interval. The second one does show a bit of improvement from the original amplitude spectrum, especially for the peak at 0.45 cycles per metre. The third one, depth 211.0-246.5 m, shows more dominant peaks than the original one, and indicates that there are several cycles present in the amplitude spectrum.

For core 7430/10-U-01 (Figure 28) does not show much improvement, but rather more peaks show up, and disturb the amplitude spectrum.

The cycles found in core 7018/05-U-01 and 7430/10-U-01 can be compared to the cycles Weedon et al. (1999, 2004) found in the Kimmeridge Clay Formation. They state that the dominant cycles have a duration of 20 kyr and 38 kyr, which corresponds to the cycles found in the amplitude spectrums for cores studied here. For core 7018/05-U-01 spectrum a shows cycle at 35 kyr, spectrum b shows cycle at 28 kyr, and spectrum c show cycle at 34 kyr. For core 7430/10-U-01, amplitude spectrum a shows a cycle at 21.1 Kyr, and spectrum b shows cycles at 24.2 Kyr and 43.2 Kyr.

The small differences between the Kimmeridge Clay Formation's cycles and the ones found in the Hekkingen Formation can be explained by the uncertainty in sedimentation rate for core 7018/05-U-01. If the sedimentation rate was better known, and possibly how it changes through the core, the cycles found might be closer to the ones found by Weedon et al. (1999, 2004). Future work could use the results from this work to tune the sedimentation rates to the orbital cyclicity in order to get a better handle on sedimentation rate variations in the Hekkingen Formation.

Conclusions

From the sedimentary logs, it can be seen that the cores mostly consist of laminated mudstones, with some intervals of silty material and massive mudstone. Core 7018/05-U-01 mostly consists of planar parallel laminated and wavy laminated mudstone, with a lot of siderite veins, cement and concretions for the lower part (87 -273.8) and a large amount of shell fragments in the upper part (49.6-87 m). Core 7430/10-U-01 consists of planar parallel laminated mudstone, with some wavy parallel laminated and discontinuous laminated mudstones. There is evidence of slumping in core 7018/05-U-01 and turbidity currents in both cores, and there is also presence of some small ripples, either compacted nearly flat or as starved ripples in both cores, so the depositional environment is not as quiet as stated by Smelror et al. (2009).

There seems to be a connection between the facies and the resulting magnetic susceptibility signal, where the facies deposited from a higher energy environment (wavy laminated mudstone) have a higher average magnetic susceptibility than the planar parallel laminated mudstone, which again has a higher average magnetic susceptibility reading than the massive mudstone.

When analysing the magnetic susceptibility data for the Hekkingen Formation, it is evident that there is some cyclicity. The cyclicity varies through the cores, and by analysing both Fourier amplitude spectrums and wavelet analysis for core 7018/05-U-01, the dominant cycles can be found at 71 kyr, 35 kyr and 30 kyr for the interval 51.6-89.8 m. For the second interval, 95.3-147.6 m, the dominant cycles have durations of 59 kyr and 28 kyr, while the third interval, 211.0-246.5 m, shows a cycle with duration of 34 kyr. For core 7430/10-U-01, the cycles have durations of 99.9 kyr, 43.2 kyr and 24.2 kyr for the interval 58.98-66.92 m, and 66.3 kyr, 28.9 kyr and 21.1 kyr for the interval 42.9-58.76 m.

Several of the cycles correlate, so the dominating cycles through the Hekkingen Formation in core 7018/05-U-01 consist of cycles with duration of 28-30 kyr, 34-35 kyr and possibly 59-71 kyr. The variation is most likely caused by a changing sedimentation rate. The Kimmeridge Clay Formation, which is an equivalent to the Hekkingen Formation, shows cycles with duration of 38 kyr and 20 kyr, which is comparable to the cycles with duration of 34-35 kyr in core 7018/05-U-01 and 43.2 kyr and 21.1 kyr in core 7430/10-U-01. Thus, the similar depositional conditions resulted in similar deposits, both showing similar cyclicity, even though the locations were far apart at the time of deposition.

Further work

- Other cores in the area, and potentially cores further south on the Norwegian Shelf, should be investigated for cyclicity in the same manner as is done here, to be able to link the Hekkingen Formation over a larger area. Correlation based on the cyclicity should also be done.
- The same cores as studied here, should also be investigated for cyclicity in other properties, such as an XRD analysis through the core, Gamma ray values or photo electric effect.
- Further work on more detailed sedimentation rates for both cores would be interesting, to be able to calculate the durations of the cycles with greater certainty. It would also be interesting to see how the sedimentation rates changes through the core, as is known for the Kimmeridge Clay Formation.

References:

ANELL, I., BRAATHEN, A. & OLAUSSEN, S. 2014: The Triassic – Early Jurassic of the northern Barents Shelf: a regional understanding of the Longyearbyen CO_2 reservoir. Norwegian Journal of Geology 94, pp. 83–98.

BOGGS, S.J. 2009. Petrology of sedimentary rocks, Cambridge University Press

COLLINSON, J., MOUNTNEY, N. & THOMPSON, D. 2006. Sedimentary Structures. Terra Publishing

DALLAND, A., WORSLEY, D. AND OFSTAD, K. (eds.) 1988: A lithostratigraphic scheme for the Mesozoic and Cenozoic succession offshore mid- and northern Norway. NPD-Bulletin No. 4, 65 pp.

DUNN, C.E. 1974. Identification of sedimentary cycles through Fourier analysis of geochemical data. Chemical Geology, 13, pp 217–232.

FALEIDE, J.I., GUDLAUGSSON, S.T. & JACQUART, G. 1984: Evolution of the western Barents Sea. Marine and Petroleum Geology 1, 123–128.

FALEIDE, J.I., VÅGNES, E. & GUDLAUGSSON, S.T. 1993: Late Mesozoic-Cenozoic evolution of the southwestern Barents Sea in a regional rift-shear tectonic setting. Marine and Petroleum Geology 10, pp. 186–214.

GEE, D.G., BOGOLEPOVA, O.K. & LORENZ, H. 2006: The Timanide, Caledonide and Uralide orogens in the Eurasian high arctic, and relationships to the Palaeo-continents Laurentia, Baltica and Sibera. In Gee, D.G. & Stephernson, R.A. (eds.): European Lithosphere Dynamics. The Geological Society of London Memoirs 32, pp. 507–520.

GEORGIEV, S.V., STEIN, H.J., HANNAH, J.L., XU, G., BINGEN, B., WEISS, H.M. 2017: Timing, duration, and causes for Late Jurassic–Early Cretaceous anoxia in the Barents Sea. Earth and Planetary Science Letters 461, pp. 151-162.

GRINSTED, A., MOORE, J.C., JEVREJEVA, S. 2004. Application of the cross wavelet transform and wavelet coherence to geophysical time series. Nonlinear Processes in Geophysics, 11, pp 561-544.

LANGROCK, U., STEIN, R., LIPINSKI, M., BRUMSACK, H.J. 2003: Paleoenvironmental and sea-level change in the early Cretaceous Barents Sea – Implications from near-shore marine sapropels. Geo-Marine Letter 23. pp. 34-42.

MCKERROW, W.S., MAC NIOCAILL, C. & DEWEY, J.F. 2000: The Caledonian Orogeny redefined. Journal of the Geological Society London 157, pp. 1149–1154.

NICHOLS ,G. 2009. Sedimentology and stratigraphy, John Wiley & Sons.

POTTER, P.E., MAYNARD, J.B. & PRYOR, W.A. 1980. Sedimentology of shale: Study guide and reference source, New York, Springer-Verlag

POTTER, P.E., MAYNARD, J. B & DEPETRIS, P.J. 2005. Mud and mudstone: Introduction and Overview, Springer-Verlag Berlin Heidelberg

SCHIEBER, J. 1978. Depositional fabric of mudstones. Sedimentology. Springer, pp 323-327

SMELROR, M., MØRK, A., MØRK, M. B. E., WEISS, H. M., LØSETH, H. 2001: Middle Jurassic-Lower Cretaceous transgressive-regressive sequences and facies distribution off northern Nordland and Troms, Norway. Norwegian Petroleum Society Special Publications, Vol.10, pp. 211-232.

SMELROR, M., PETROV, O.V., LARSEN, G.B, WERNER, S. (eds.) 2009: Geological History of the Barents Sea. Geological Survey of Norway, Trondheim pp 42-46.

YAWAR, Z. & SCHIEBER, J. 2017. On the origin of silt laminae in laminated shales. Sedimentary geology, 360, pp 22-34.

WEEDON, G.P., JENKYNS, H.C., COE, A.L., HESSELBO, S.P., 1999: Astronomic calibration of the Jurassic time-scale from cyclostratigraphy in British mudrock formations. Phil. Trans. R. Soc. Lond. A., vol 357, pp 1787-1813.

WEEDON, G. P. (2003). Time-Series Analysis and Cyclostratigraphy: Examining Stratigraphic Records of Environmental Cycles. Cambridge, U.K.: Cambridge University Press. Pp 64-67, 69

Appendix 1-Legend

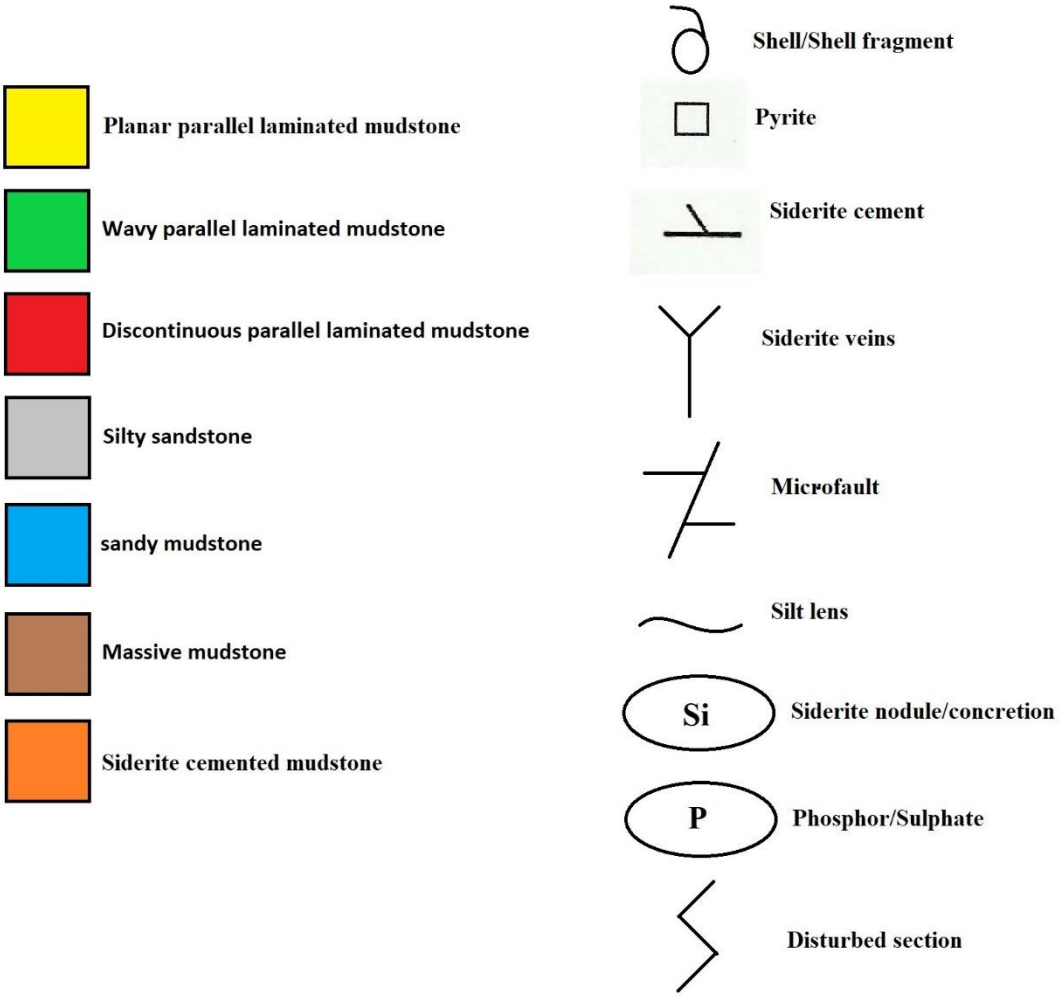

Appendix 2 – Logs

- 7430/10-U-01
- 7018/05-U-01

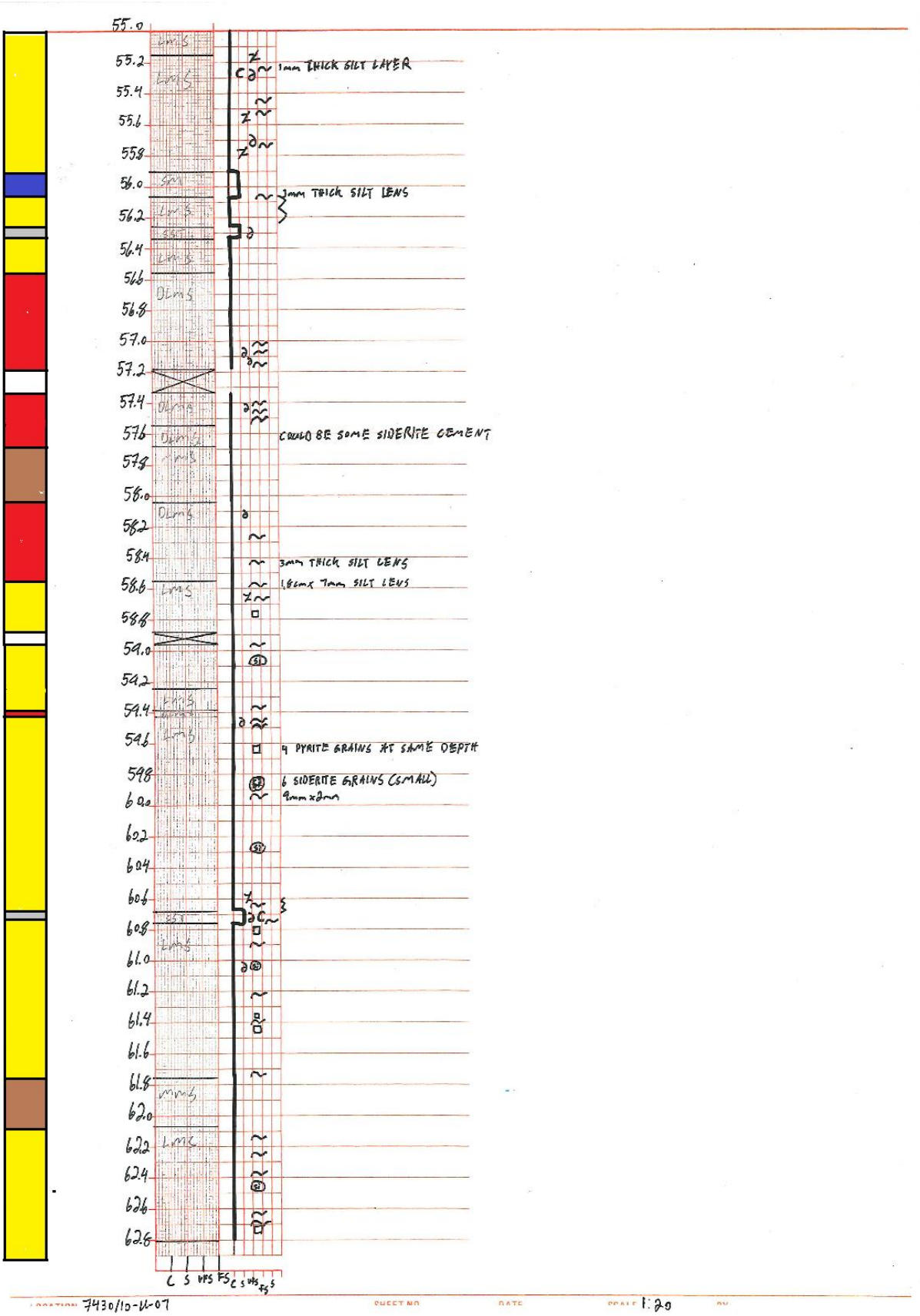
55.0
55.2
55.4
55.6
55.8
56.0
56.2
56.4
56.6
56.8
57.0
57.2
57.4
57.6
57.8
58.0
58.2
58.4
58.6
58.8
59.0
59.2
59.4
59.6
59.8
60.0
60.2
60.4
60.6
60.8
61.0
61.2
61.4
61.6
61.8
62.0
62.2
62.4
62.6
1mm THICK SILT LAYER
3mm THICK SILT LENS
COULD BE SOME SIDERITE CEMENT
3mm THICK SILT LENS
1.8cm x 7mm SILT LENS
4 PYRITE GRAINS AT SAME DEPTH
6 SIDERITE GRAINS (SMALL)
9mm x 2mm
C S VFS FS C S VFS FS
7430/10-U-07
1:20

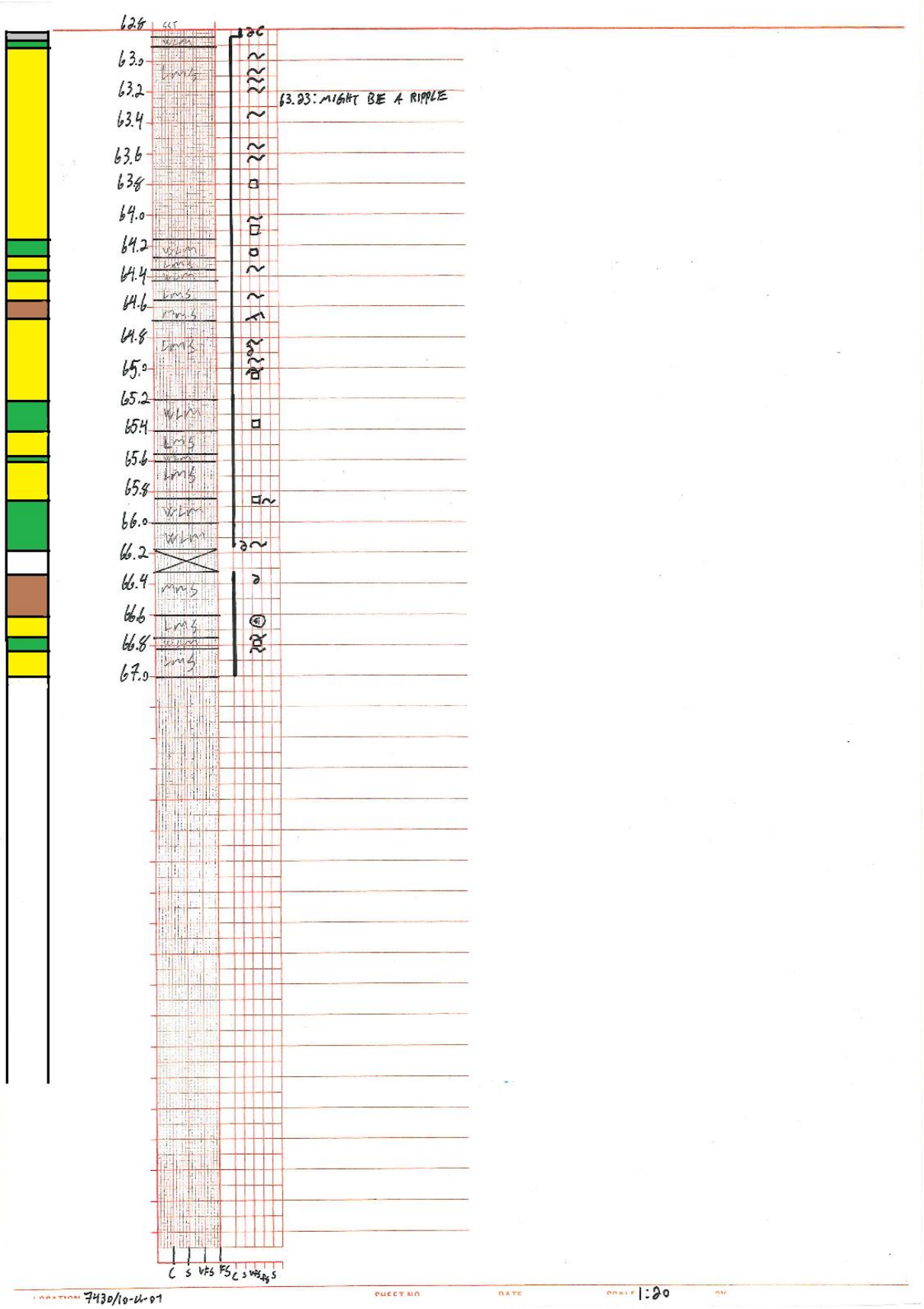
62.8
63.0
63.2
63.4
63.6
63.8
64.0
64.2
64.4
64.6
64.8
65.0
65.2
65.4
65.6
65.8
66.0
66.2
66.4
66.6
66.8
67.0
63.23: MIGHT BE A RIPPLE
C S VFS FS C S VFS FS S
LOCATION 7430/10-11-07
SHEET NO
DATE
SCALE 1:20

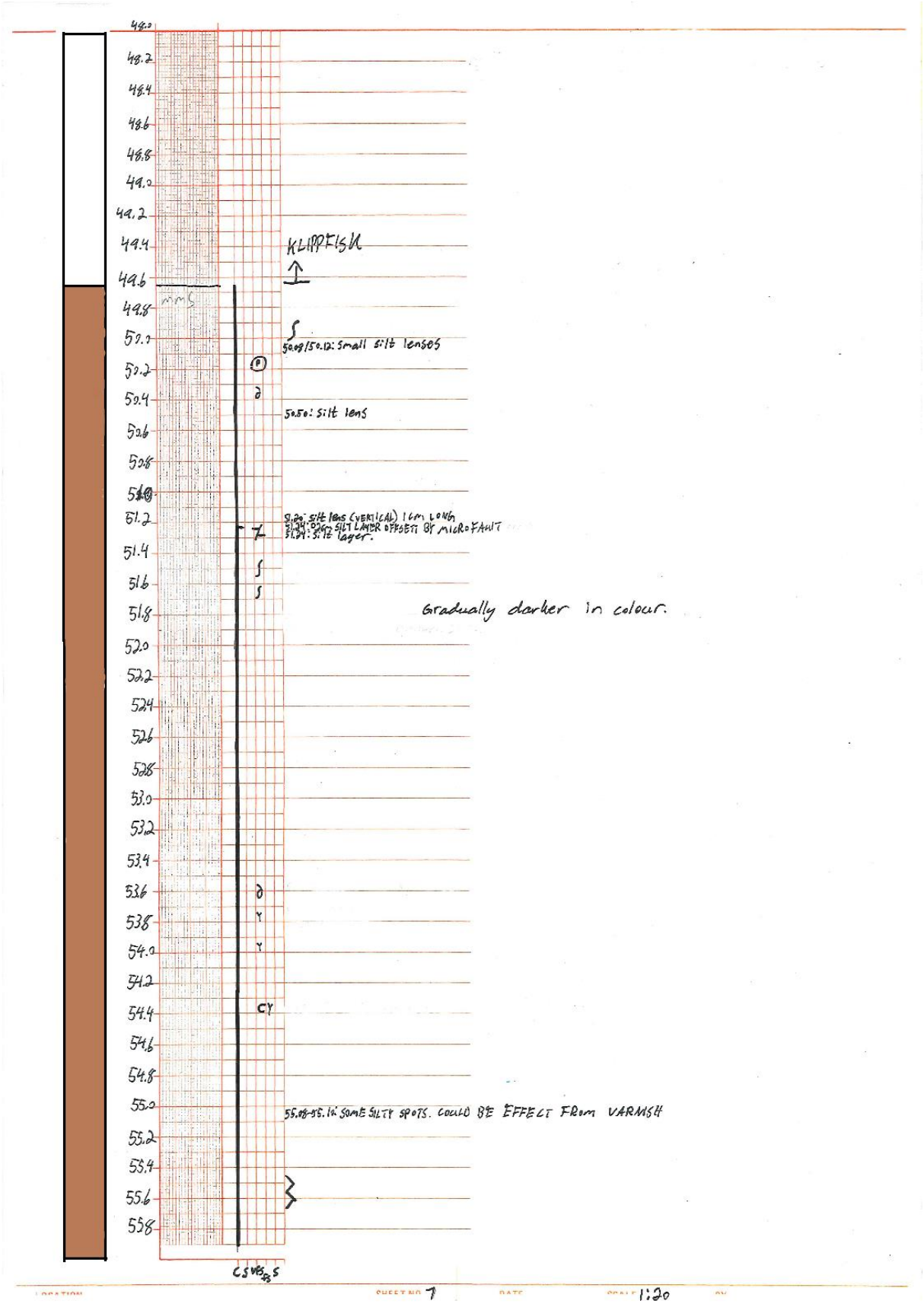
48.0
48.2
48.4
48.6
48.8
49.0
49.2
49.4
49.6
49.8
50.0
50.2
50.4
50.6
50.8
51.0
51.2
51.4
51.6
51.8
52.0
52.2
52.4
52.6
52.8
53.0
53.2
53.4
53.6
53.8
54.0
54.2
54.4
54.6
54.8
55.0
55.2
55.4
55.6
55.8
KLIPPFISK
50.08/50.12: small silt lenses
50.50: silt lens
51.20: silt lens (VERTICAL) 1cm LONG
51.24: 0.2cm SILT LAYER OFFSETT BY MICROFAULT
51.24: silt layer.
Gradually darker in colour.
55.08-55.10: SOME SILTY SPOTS. COULD BE EFFECT FROM VARNISH
CS VFS FS S
SHEET NO 7
DATE
SCALE 1:20
BY

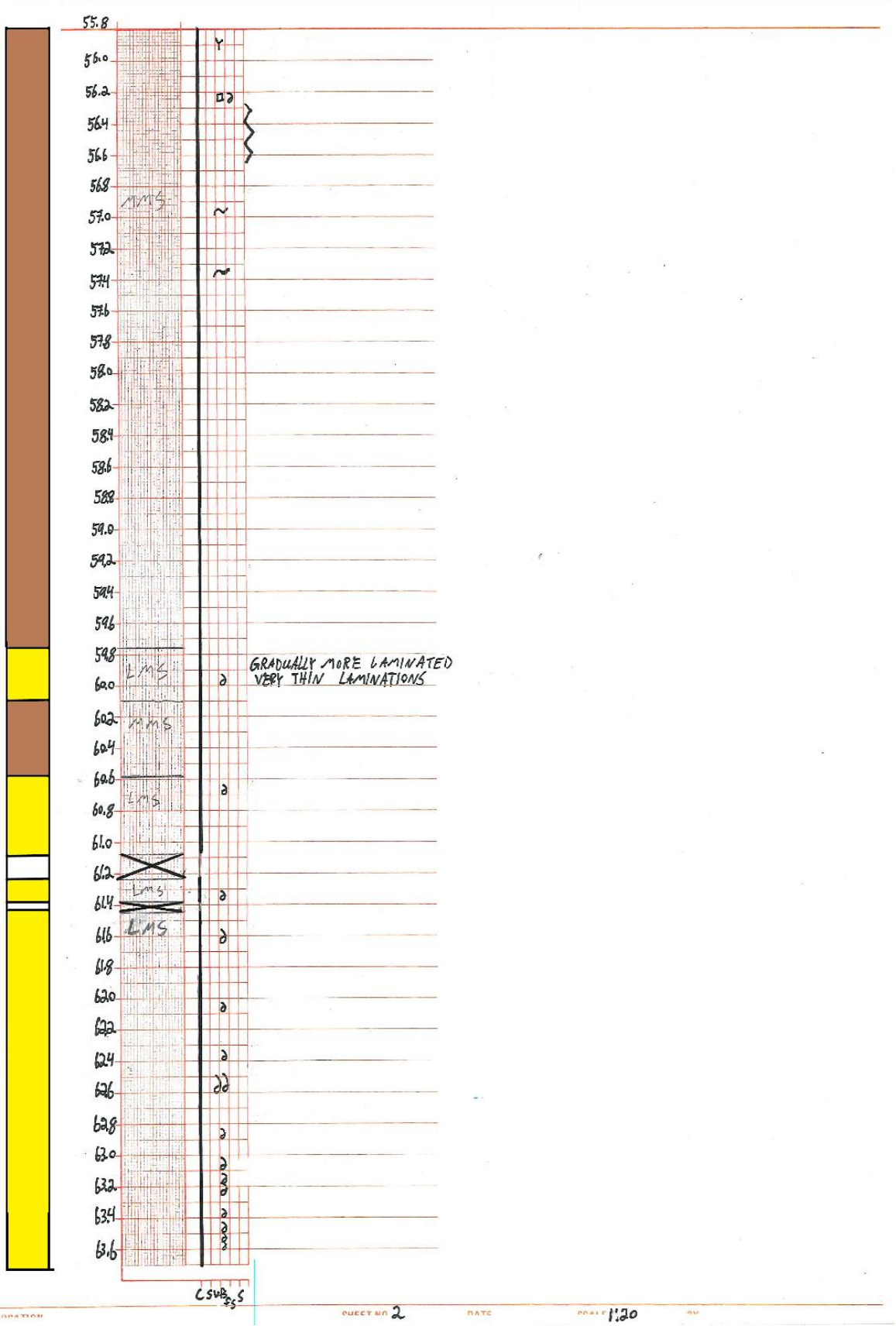
55.8
56.0
56.2
56.4
56.6
56.8
57.0
57.2
57.4
57.6
57.8
58.0
58.2
58.4
58.6
58.8
59.0
59.2
59.4
59.6
59.8
60.0
60.2
60.4
60.6
60.8
61.0
61.2
61.4
61.6
61.8
62.0
62.2
62.4
62.6
62.8
63.0
63.2
63.4
63.6
MMS
LMS
MMS
LMS
LMS
LMS
GRADUALLY MORE LAMINATED
VERY THIN LAMINATIONS
CSUB
SHEET NO 2
DATE
SCALE 1:20
BY

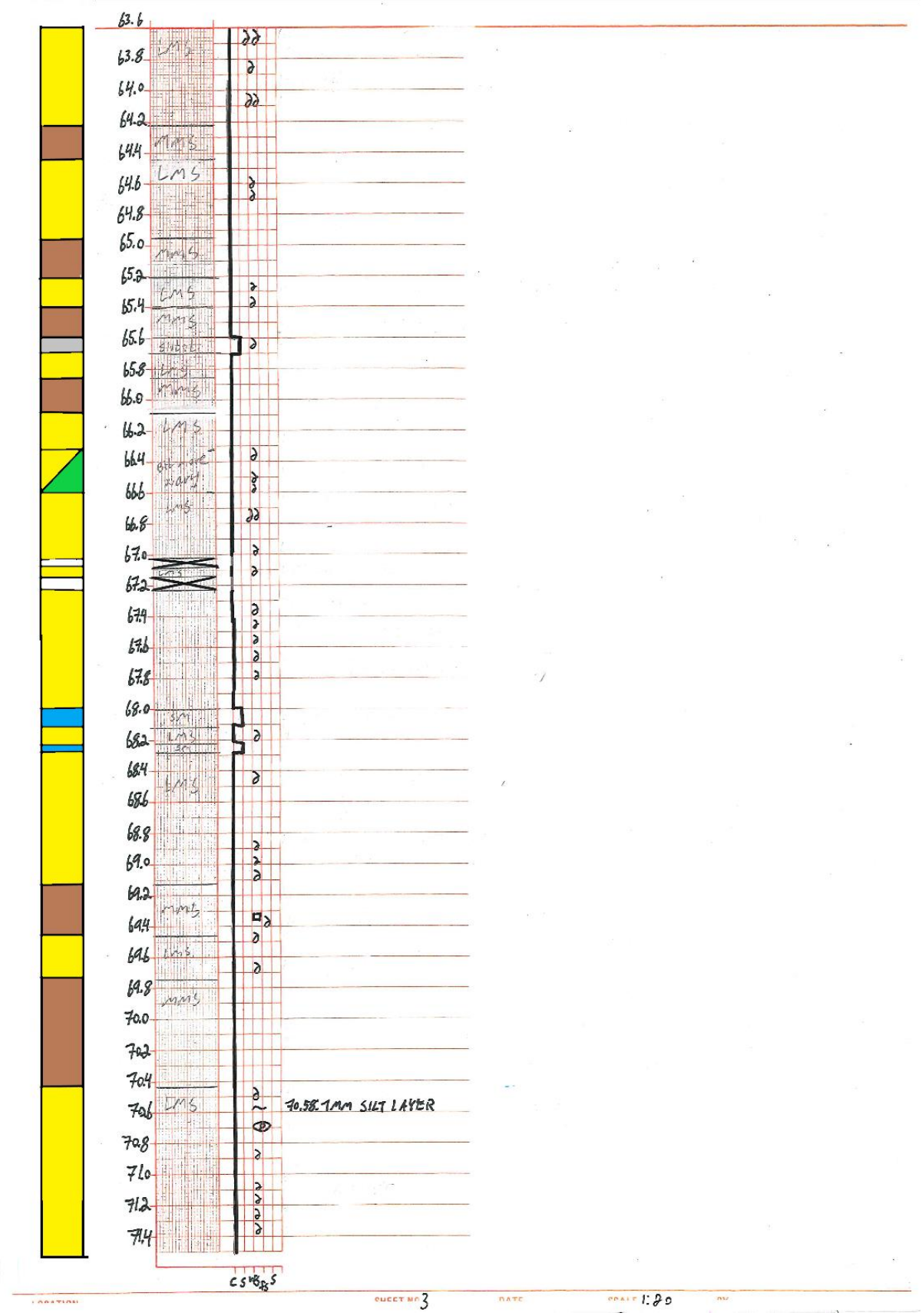
63.6
63.8
64.0
64.2
64.4
64.6
64.8
65.0
65.2
65.4
65.6
65.8
66.0
66.2
66.4
66.6
66.8
67.0
67.2
67.4
67.6
67.8
68.0
68.2
68.4
68.6
68.8
69.0
69.2
69.4
69.6
69.8
70.0
70.2
70.4
70.6
70.8
71.0
71.2
71.4
LMS
MMS
70.58.1MM SILT LAYER
C S VB FS S
SHEET NO 3
SCALE 1:20

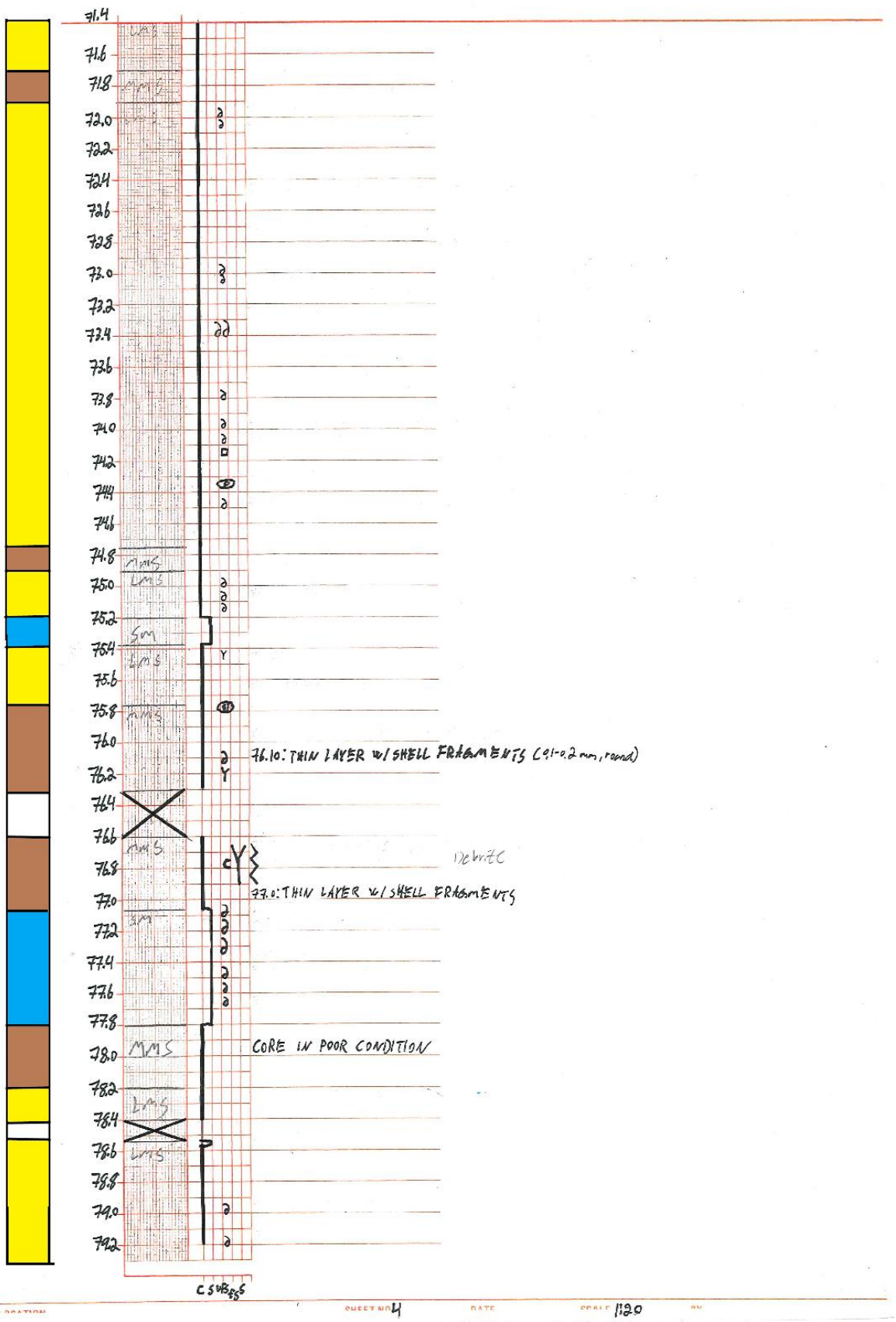
71.4
71.6
71.8
72.0
72.2
72.4
72.6
72.8
73.0
73.2
73.4
73.6
73.8
74.0
74.2
74.4
74.6
74.8
75.0
75.2
75.4
75.6
75.8
76.0
76.2
76.4
76.6
76.8
77.0
77.2
77.4
77.6
77.8
78.0
78.2
78.4
78.6
78.8
79.0
79.2
76.10: THIN LAYER w/ SHELL FRAGMENTS (0.1-0.2 mm, round)
Debris
77.0: THIN LAYER w/ SHELL FRAGMENTS
CORE IN POOR CONDITION
CSUBBSS
SHEET NO 4
SCALE 1:20

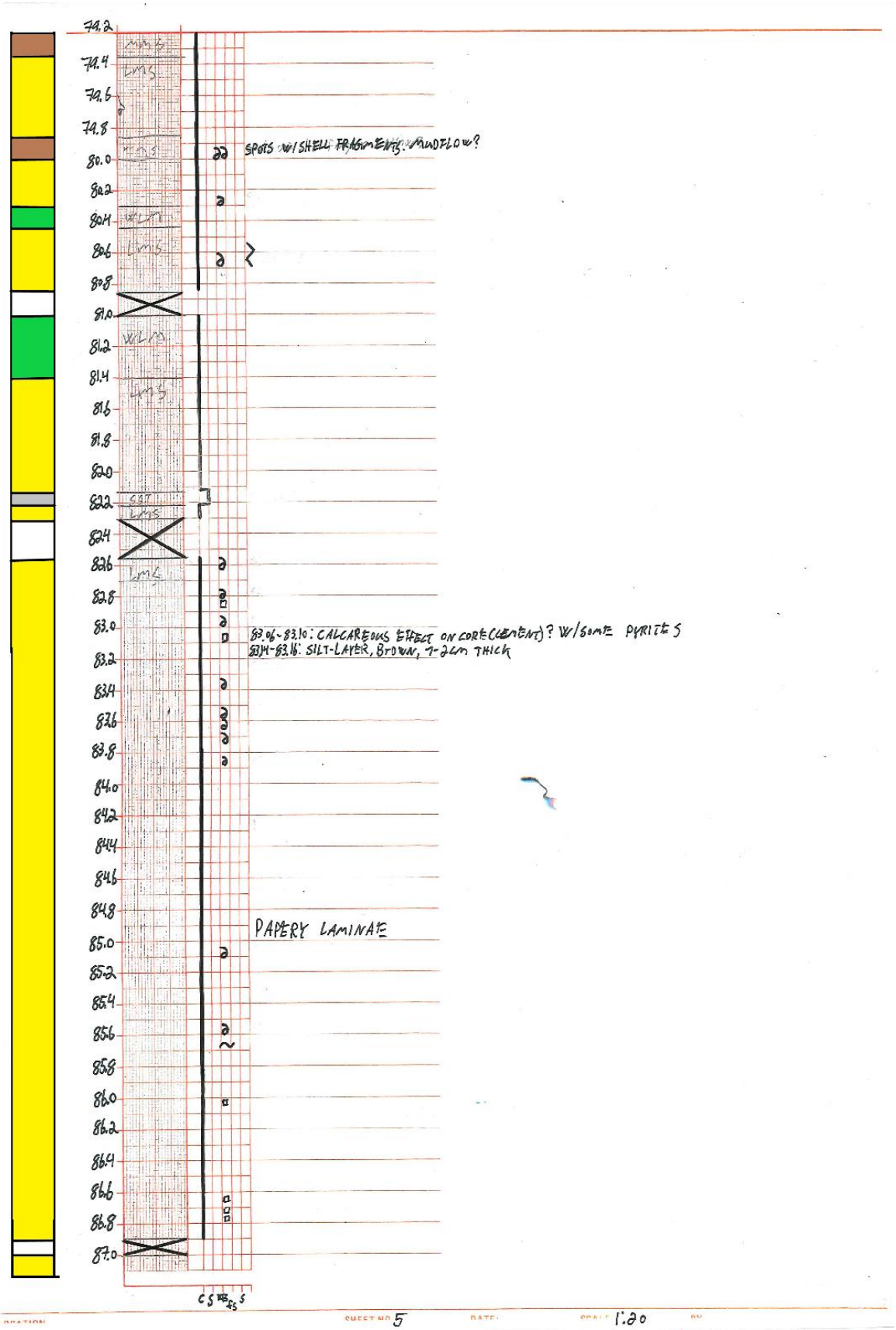
74.2
74.4
74.6
74.8
80.0
80.2
80.4
80.6
80.8
81.0
81.2
81.4
81.6
81.8
82.0
82.2
82.4
82.6
82.8
83.0
83.2
83.4
83.6
83.8
84.0
84.2
84.4
84.6
84.8
85.0
85.2
85.4
85.6
85.8
86.0
86.2
86.4
86.6
86.8
87.0
SPOTS W/ SHELL FRAGMENTS. MUDFLOW?
83.0'-83.10': CALCAREOUS EFFECT ON CORE(CEMENT)? W/SOME PYRITES
83.14-83.16': SILT-LAYER, BROWN, 1-2cm THICK
PAPERY LAMINATE
C S MS FS S
SHEET NO 5
SCALE 1:20

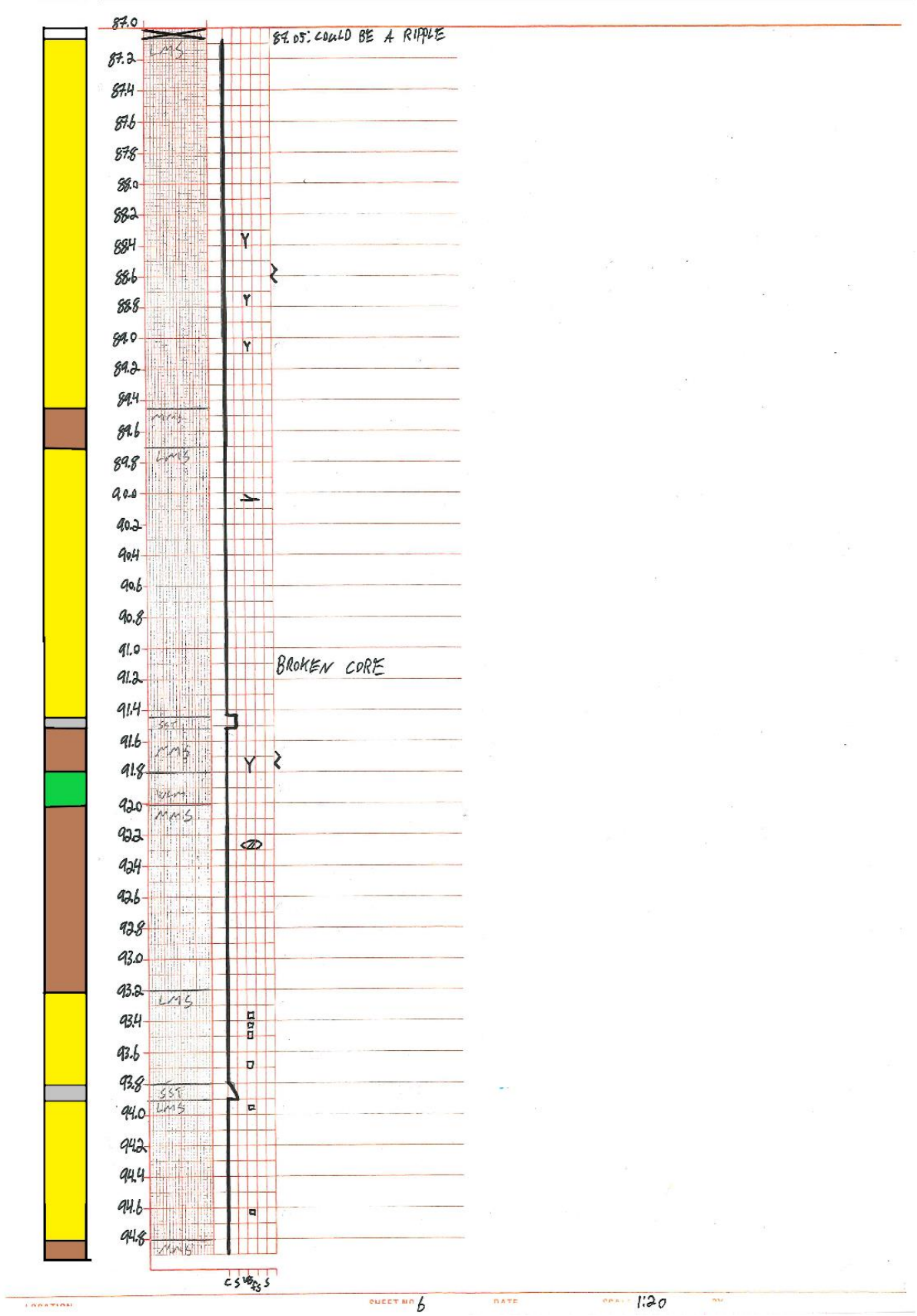
87.0
87.2
87.4
87.6
87.8
88.0
88.2
88.4
88.6
88.8
89.0
89.2
89.4
89.6
89.8
90.0
90.2
90.4
90.6
90.8
91.0
91.2
91.4
91.6
91.8
92.0
92.2
92.4
92.6
92.8
93.0
93.2
93.4
93.6
93.8
94.0
94.2
94.4
94.6
94.8
LMS
MMS
SST
87.05: COULD BE A RIPPLE
BROKEN CORE
SHEET NO 6
1:20

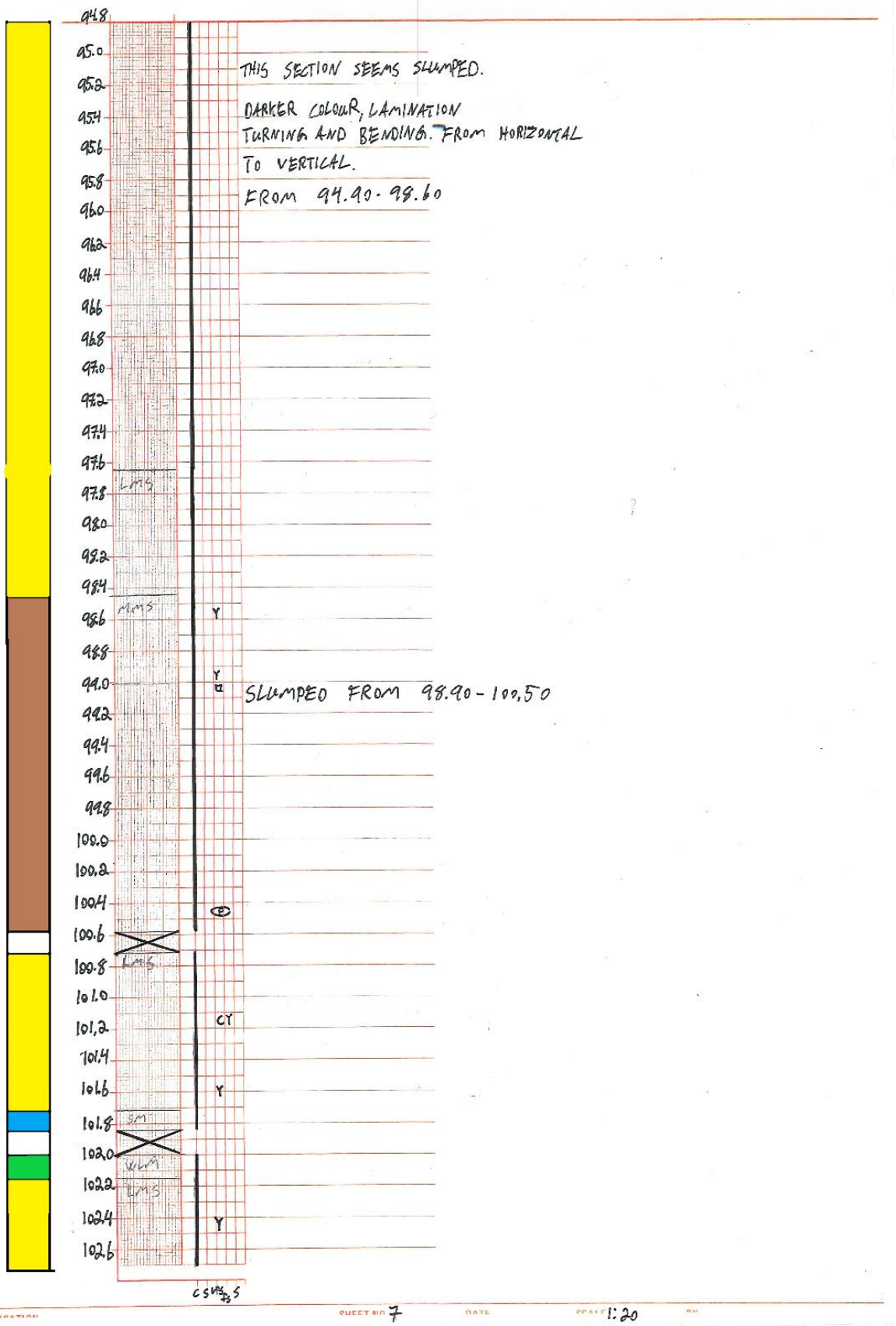
94.8
95.0
95.2
95.4
95.6
95.8
96.0
96.2
96.4
96.6
96.8
97.0
97.2
97.4
97.6
97.8
98.0
98.2
98.4
98.6
98.8
99.0
99.2
99.4
99.6
99.8
100.0
100.2
100.4
100.6
100.8
101.0
101,2
101.4
101.6
101.8
102.0
102.2
102.4
102.6
LMS
MMS
SM
VLM
Y
CT
THIS SECTION SEEMS SLUMPED.
DARKER COLOUR, LAMINATION
TURNING AND BENDING. FROM HORIZONTAL
TO VERTICAL.
FROM 94.90 - 98.60
SLUMPED FROM 98.90 - 100,50
SHEET NO 7
1:20

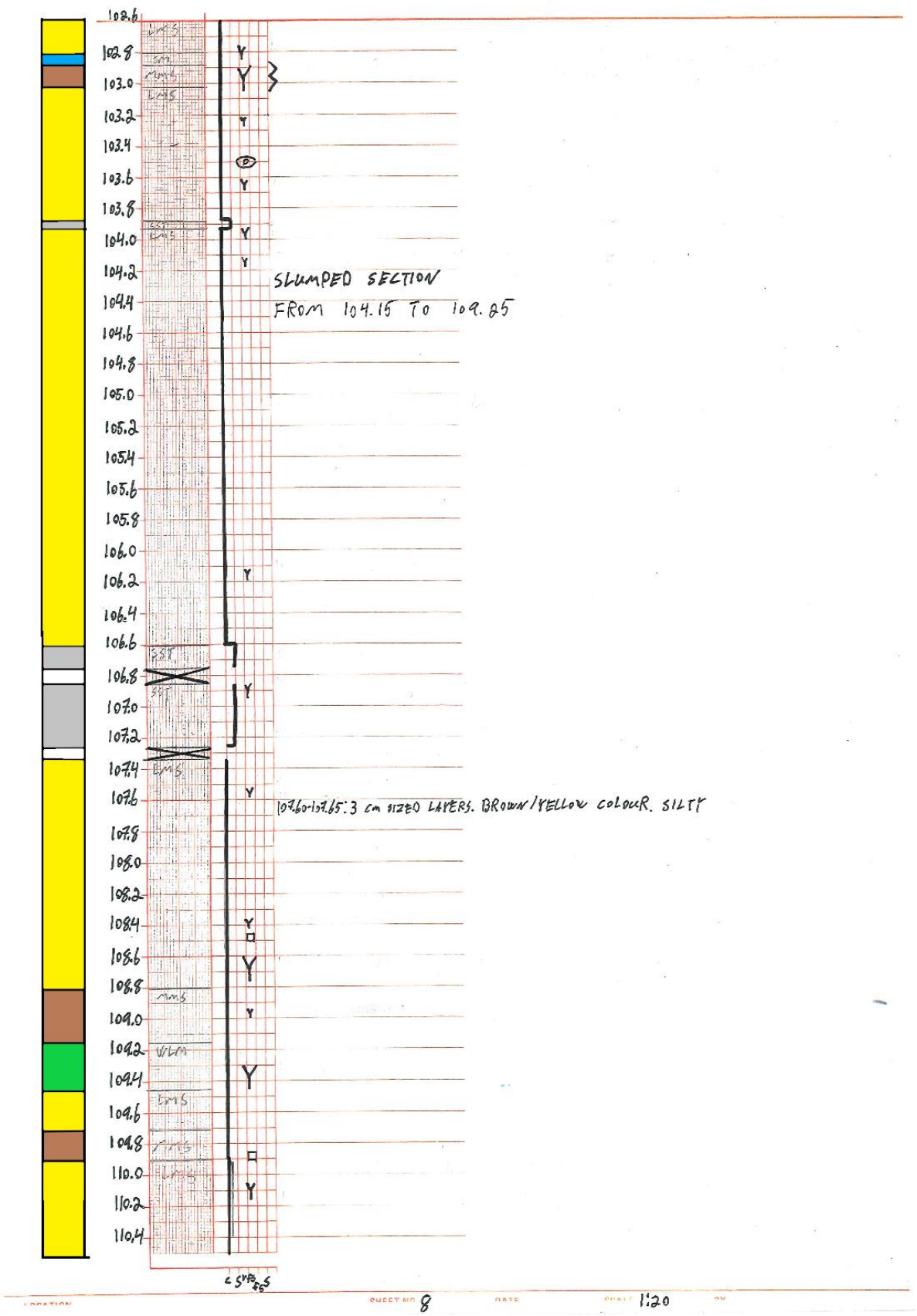
SLUMPED SECTION
FROM 104.15 TO 109.25
107.60-107.65: 3 cm SIZED LAYERS. BROWN/YELLOW COLOUR. SILTY
SHEET NO. 8
DATE
SCALE 1:20

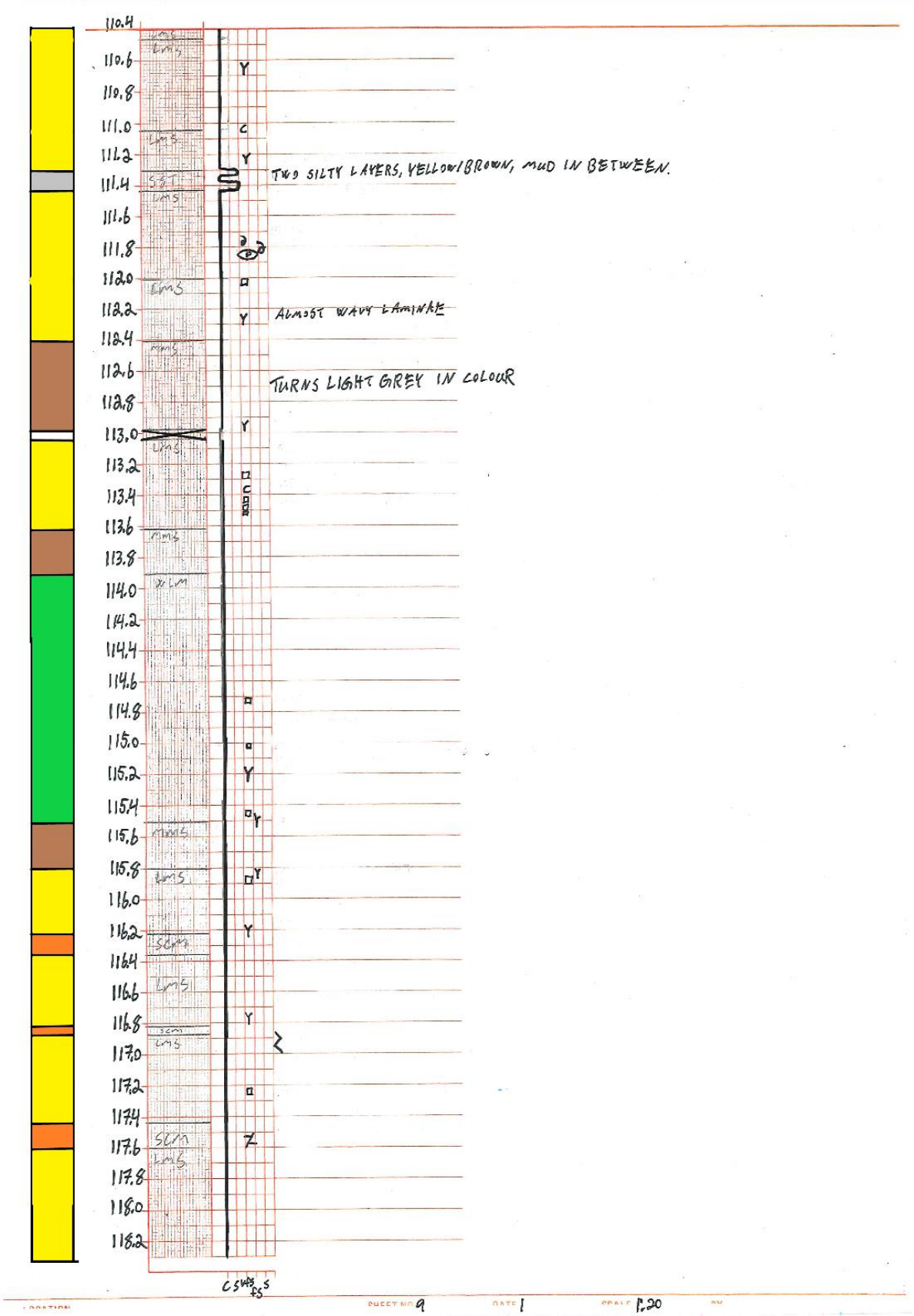
110.4
110.6
110.8
111.0
111.2
111.4
111.6
111.8
112.0
112.2
112.4
112.6
112.8
113.0
113.2
113.4
113.6
113.8
114.0
114.2
114.4
114.6
114.8
115.0
115.2
115.4
115.6
115.8
116.0
116.2
116.4
116.6
116.8
117.0
117.2
117.4
117.6
117.8
118.0
118.2
TWO SILTY LAYERS, YELLOW/BROWN, MUD IN BETWEEN.
ALMOST WAVY LAMINAE
TURNS LIGHT GREY IN COLOUR

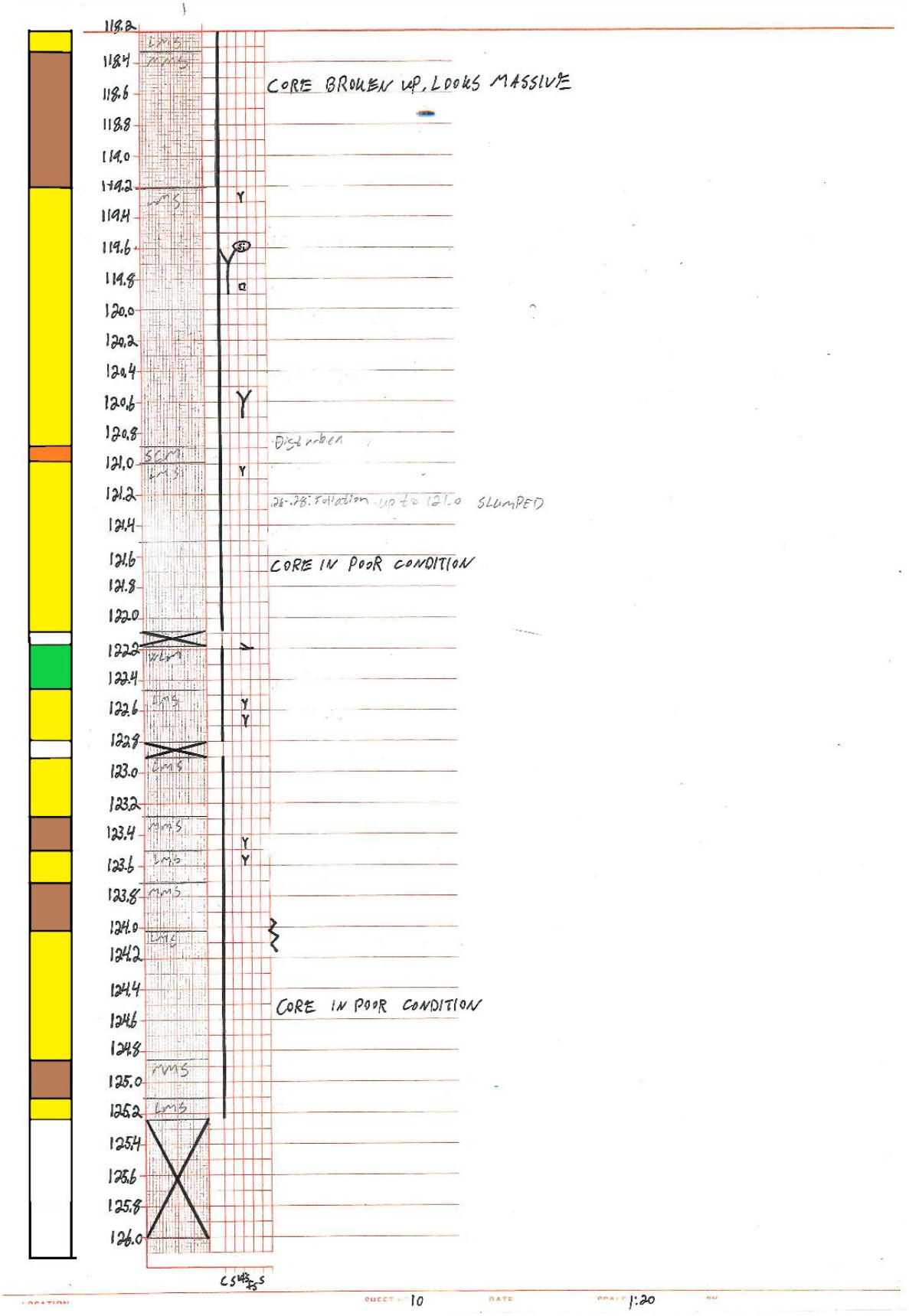
CORE BROKEN UP, LOOKS MASSIVE
Disturben
26-28: Foliation up to 121.0 SLUMPED
CORE IN POOR CONDITION
CORE IN POOR CONDITION
LOCATION
SHEET 10
DATE
SCALE 1:20
BY

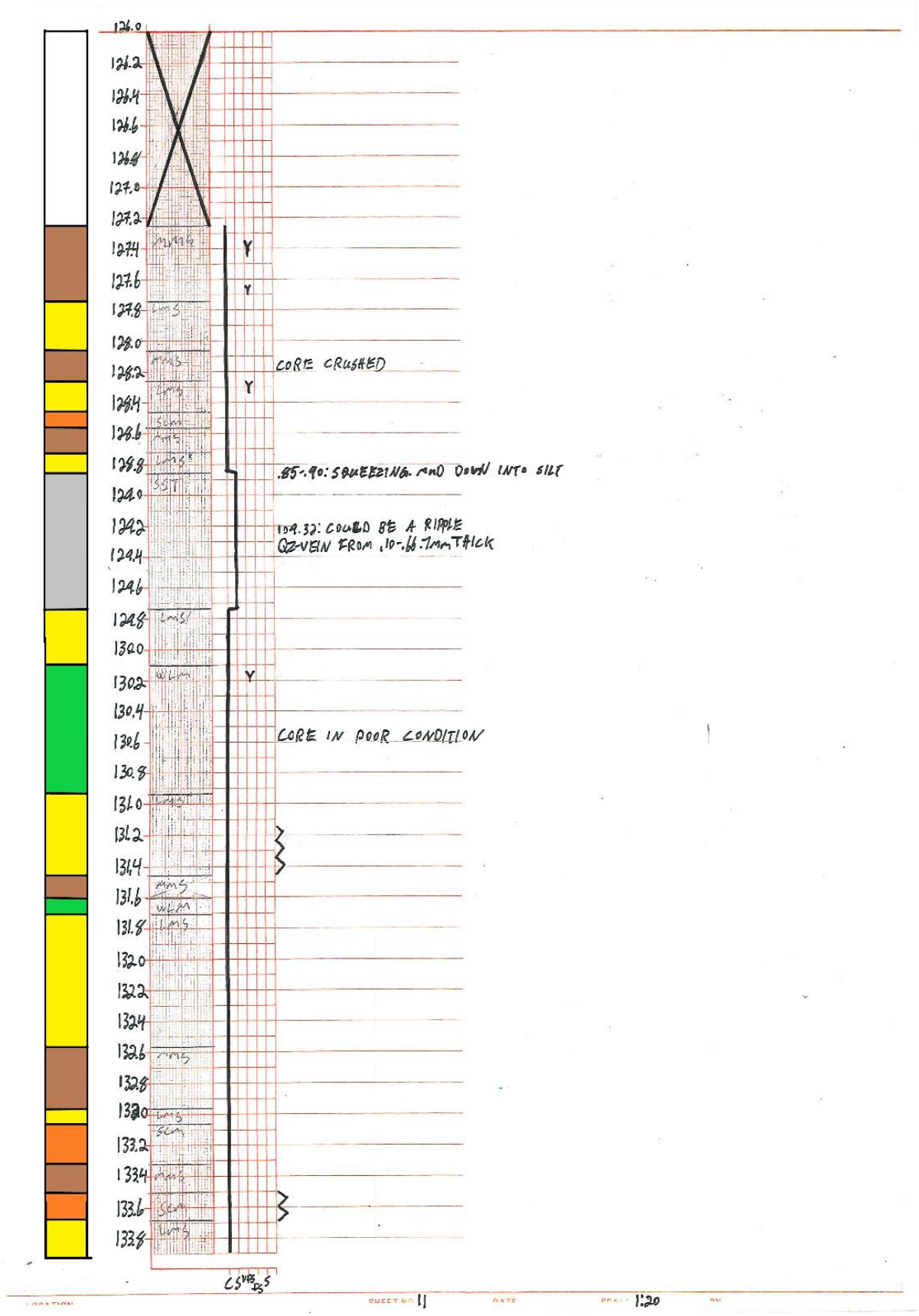
126.0
126.2
126.4
126.6
126.8
127.0
127.2
127.4
127.6
127.8
128.0
128.2
128.4
128.6
128.8
129.0
129.2
129.4
129.6
129.8
130.0
130.2
130.4
130.6
130.8
131.0
131.2
131.4
131.6
131.8
132.0
132.2
132.4
132.6
132.8
133.0
133.2
133.4
133.6
133.8
CORE CRUSHED
.85-.90: SQUEEZING MUD DOWN INTO SILT
129.32: COULD BE A RIPPLE
QZ-VEIN FROM .10-.66: 7mm THICK
CORE IN POOR CONDITION
SHEET NO 11
DATE
SCALE 1:20
BY

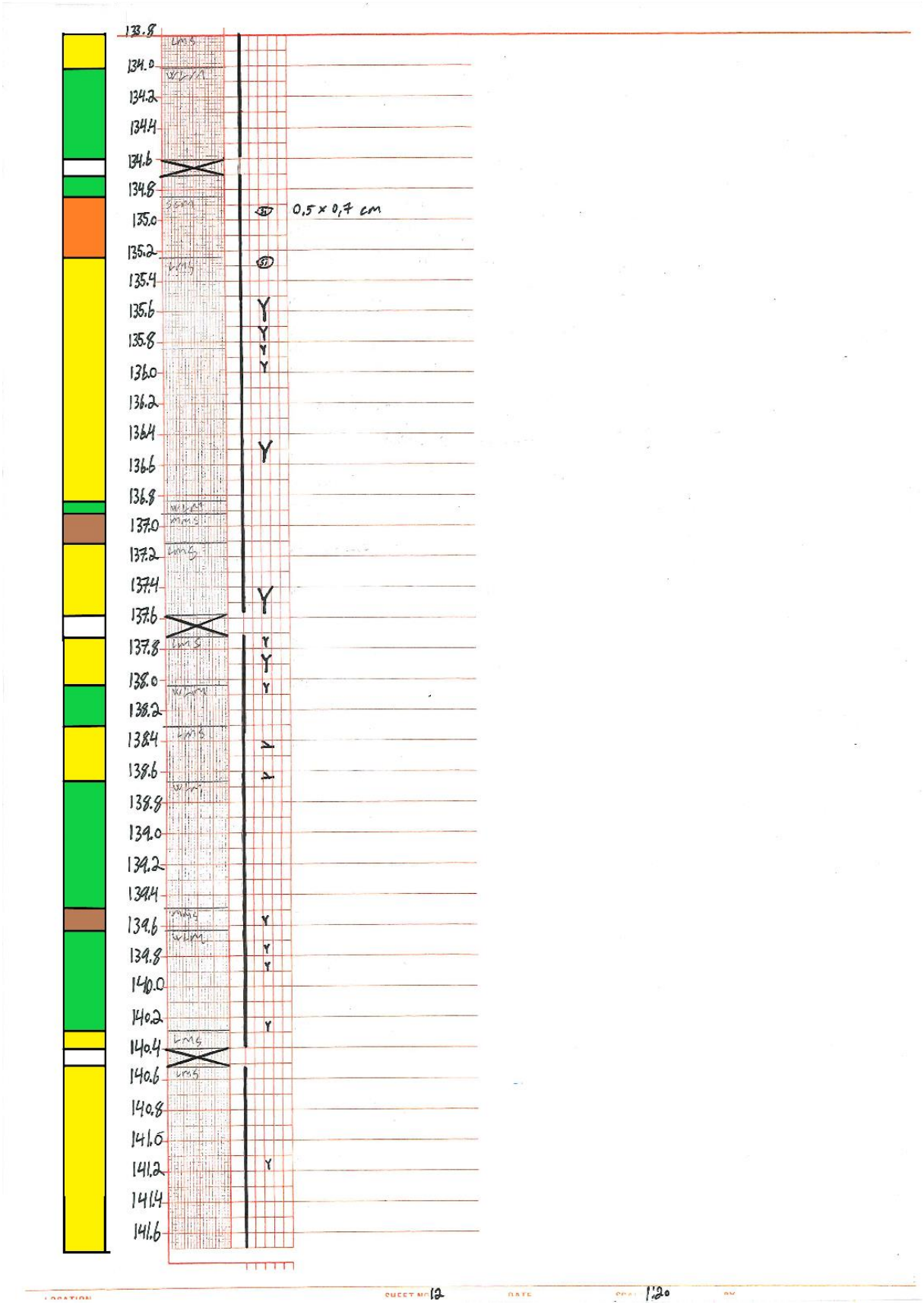
133.8
134.0
134.2
134.4
134.6
134.8
135.0
135.2
135.4
135.6
135.8
136.0
136.2
136.4
136.6
136.8
137.0
137.2
137.4
137.6
137.8
138.0
138.2
138.4
138.6
138.8
139.0
139.2
139.4
139.6
139.8
140.0
140.2
140.4
140.6
140.8
141.0
141.2
141.4
141.6
0,5 x 0,7 cm
SHEET NO 12
1:20

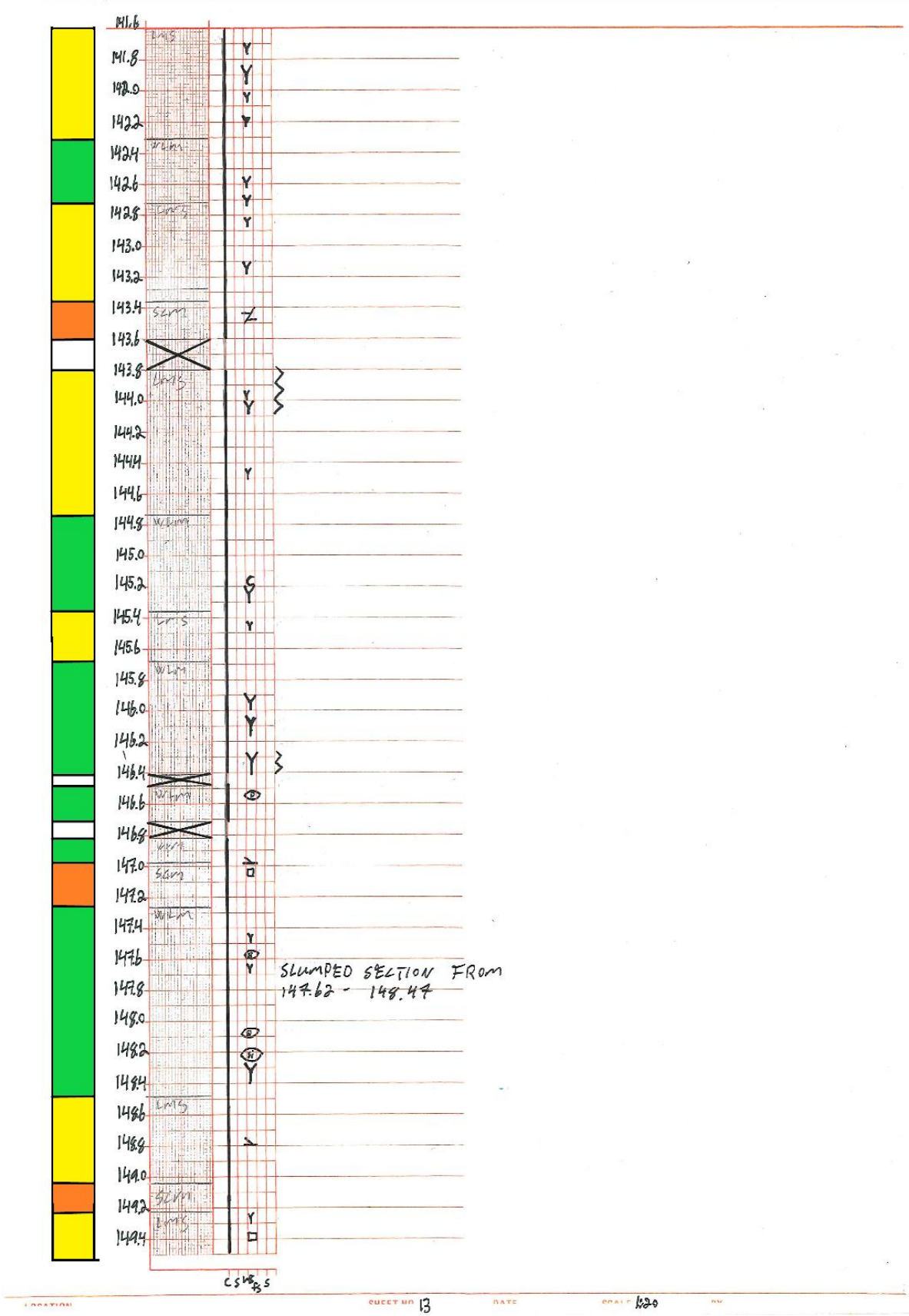
141.6
141.8
142.0
142.2
142.4
142.6
142.8
143.0
143.2
143.4
143.6
143.8
144.0
144.2
144.4
144.6
144.8
145.0
145.2
145.4
145.6
145.8
146.0
146.2
146.4
146.6
146.8
147.0
147.2
147.4
147.6
147.8
148.0
148.2
148.4
148.6
148.8
149.0
149.2
149.4
SLUMPED SECTION FROM
147.62 - 148.44

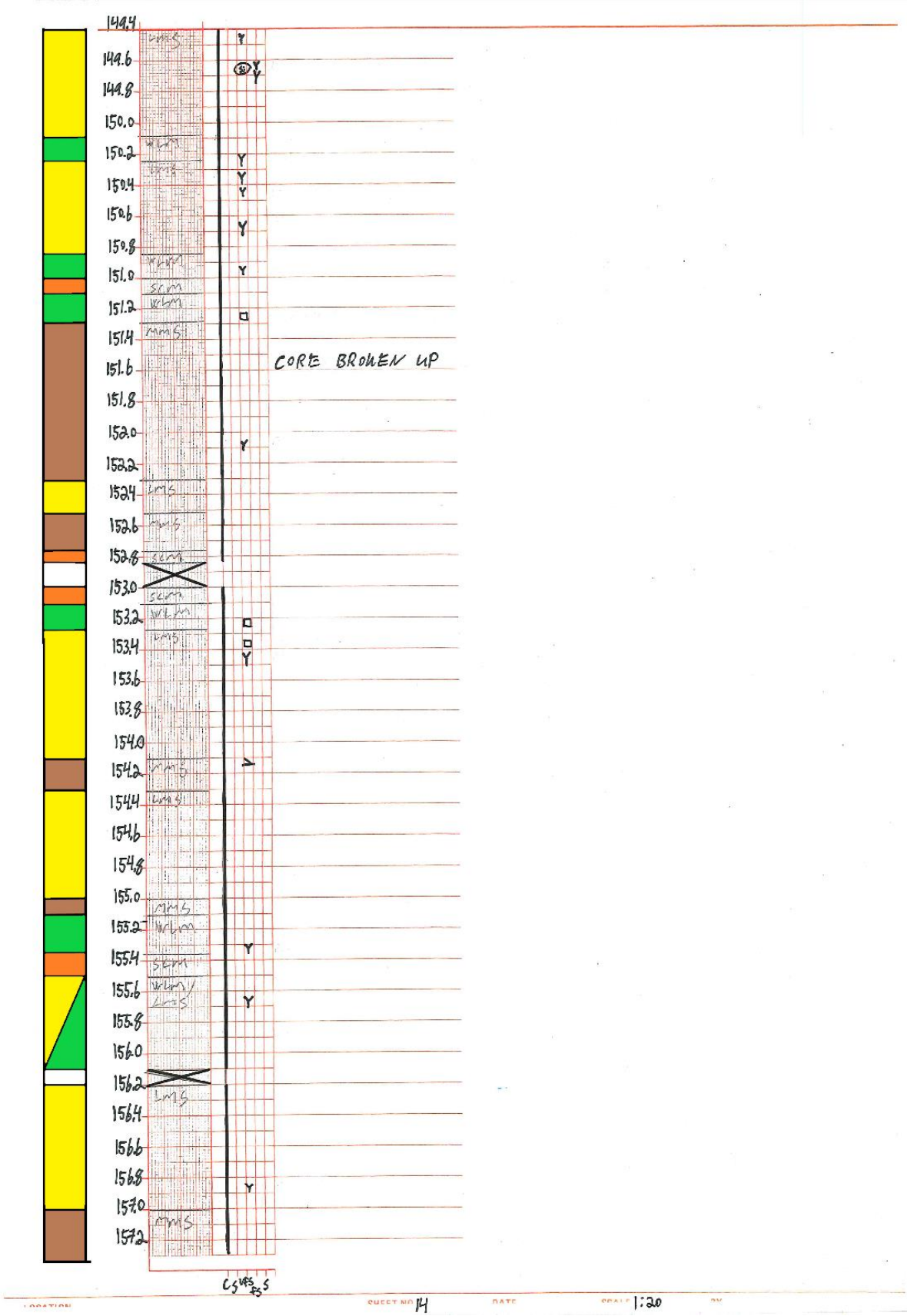
149.4
149.6
149.8
150.0
150.2
150.4
150.6
150.8
151.0
151.2
151.4
151.6
151.8
152.0
152.2
152.4
152.6
152.8
153.0
153.2
153.4
153.6
153.8
154.0
154.2
154.4
154.6
154.8
155.0
155.2
155.4
155.6
155.8
156.0
156.2
156.4
156.6
156.8
157.0
157.2
CORE BROKEN UP
SHEET NO 14
DATE
SCALE 1:20

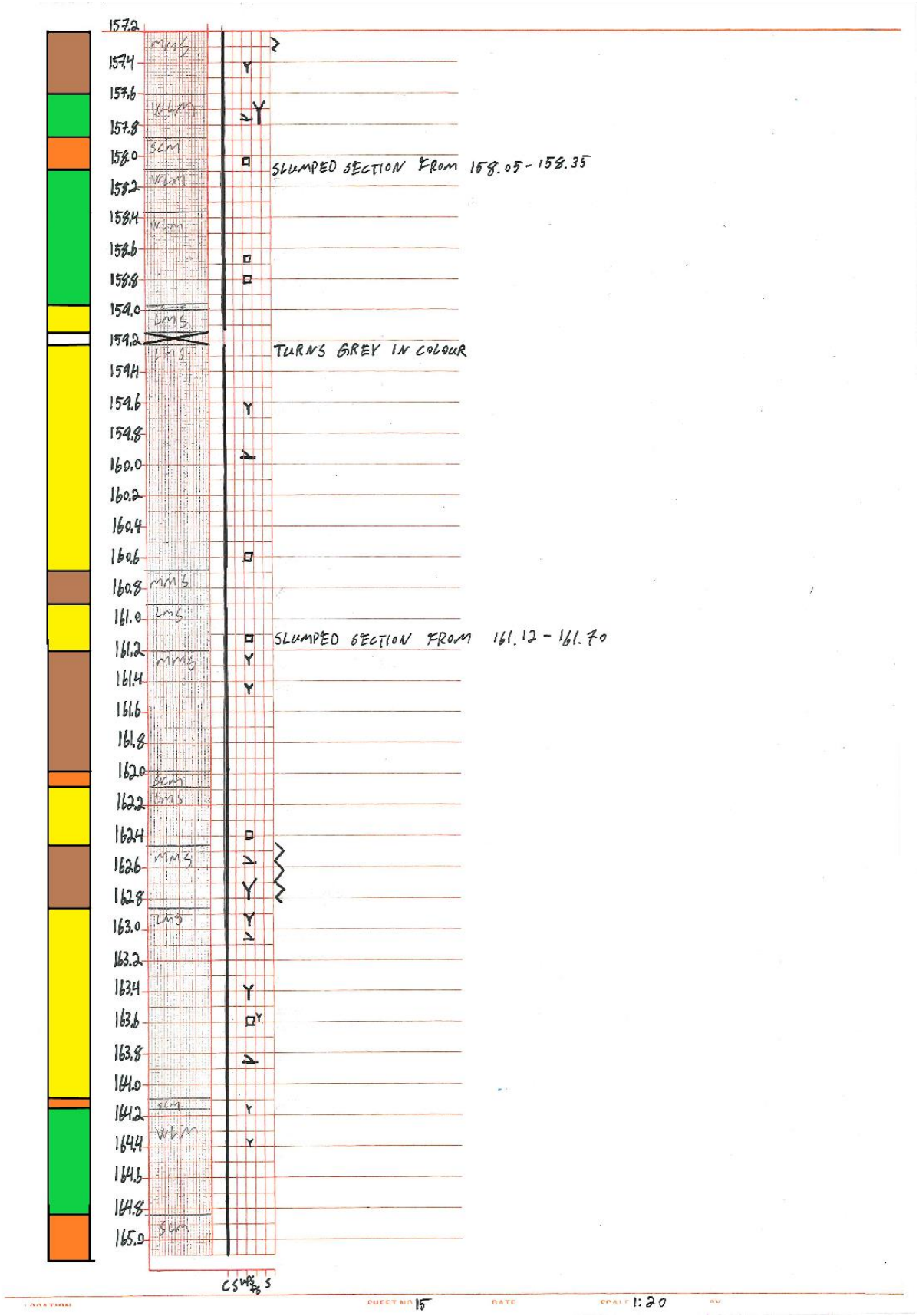
157.2
157.4
157.6
157.8
158.0
158.2
158.4
158.6
158.8
159.0
159.2
159.4
159.6
159.8
160.0
160.2
160.4
160.6
160.8
161.0
161.2
161.4
161.6
161.8
162.0
162.2
162.4
162.6
162.8
163.0
163.2
163.4
163.6
163.8
164.0
164.2
164.4
164.6
164.8
165.0
SLUMPED SECTION FROM 158.05 - 158.35
TURNS GREY IN COLOUR
SLUMPED SECTION FROM 161.12 - 161.70
SHEET NO 15
SCALE 1:20

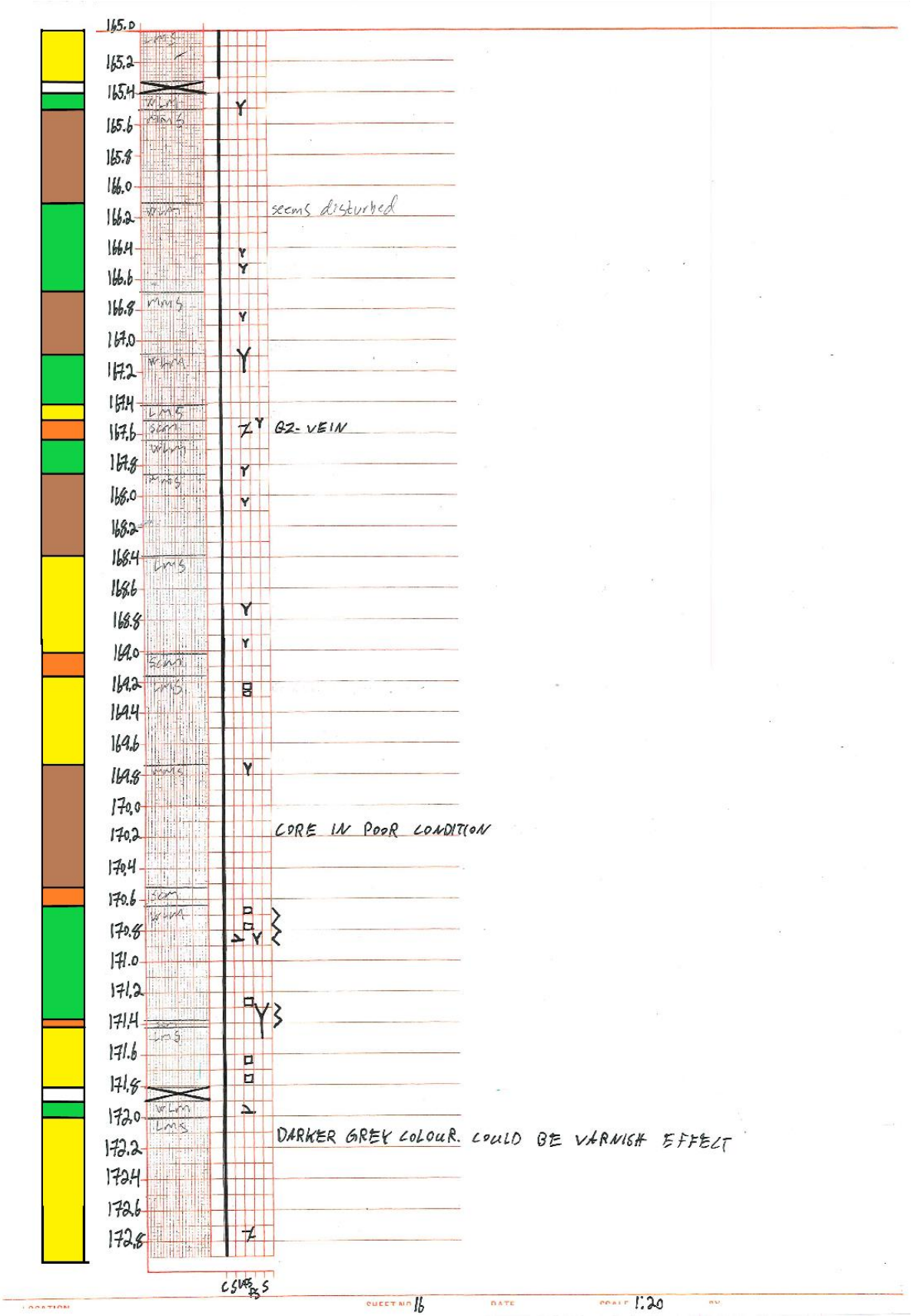
seems disturbed
QZ- VEIN
CORE IN POOR CONDITION
DARKER GREY COLOUR. COULD BE VARNISH EFFECT
SHEET NO 16
SCALE 1:20

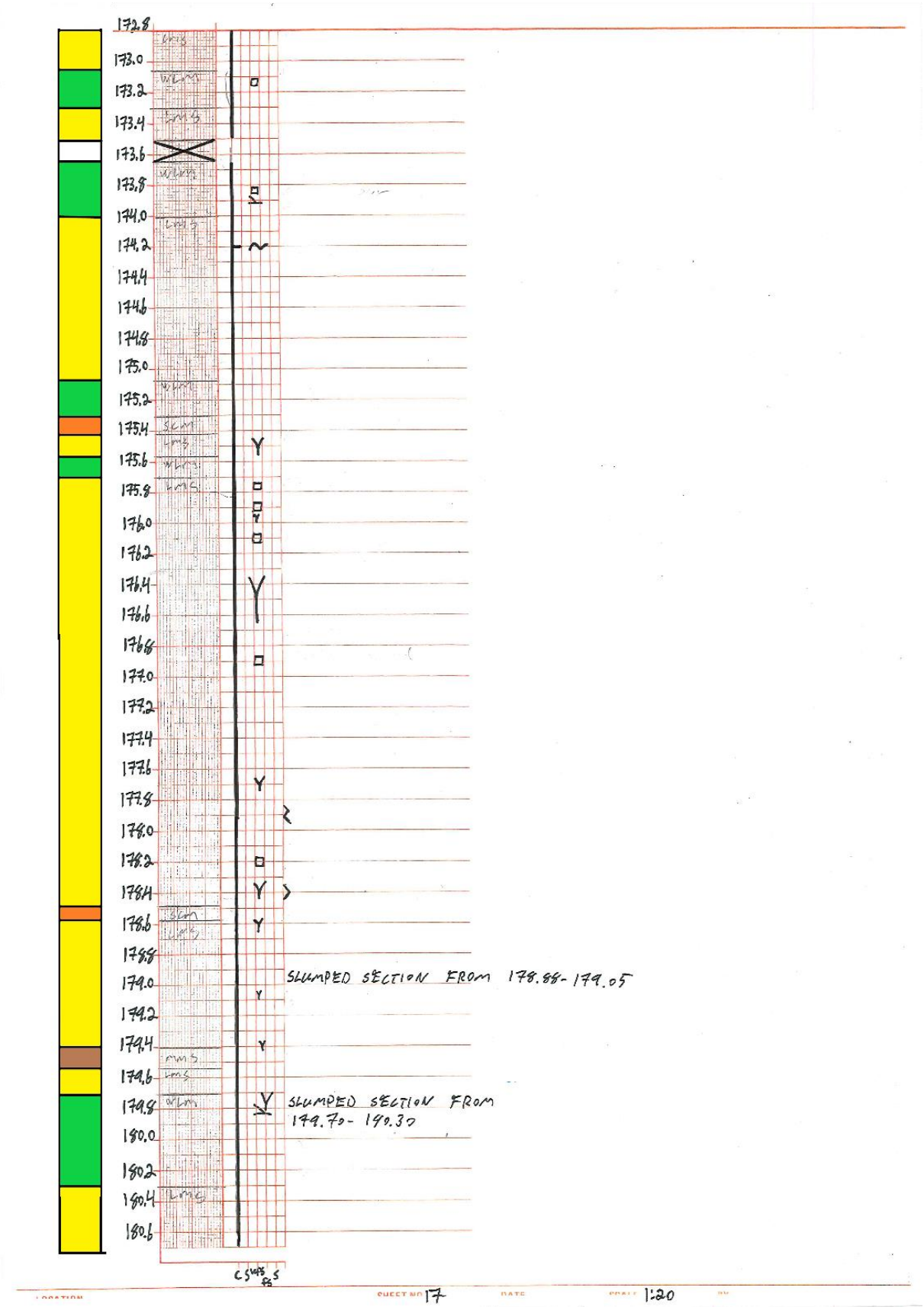
172.8
173.0
173.2
173.4
173.6
173.8
174.0
174.2
174.4
174.6
174.8
175.0
175.2
175.4
175.6
175.8
176.0
176.2
176.4
176.6
176.8
177.0
177.2
177.4
177.6
177.8
178.0
178.2
178.4
178.6
178.88
179.0
179.2
179.4
179.6
179.8
180.0
180.2
180.4
180.6
SLUMPED SECTION FROM 178.88-179.05
SLUMPED SECTION FROM 179.70-180.30
SHEET NO 17
1:20

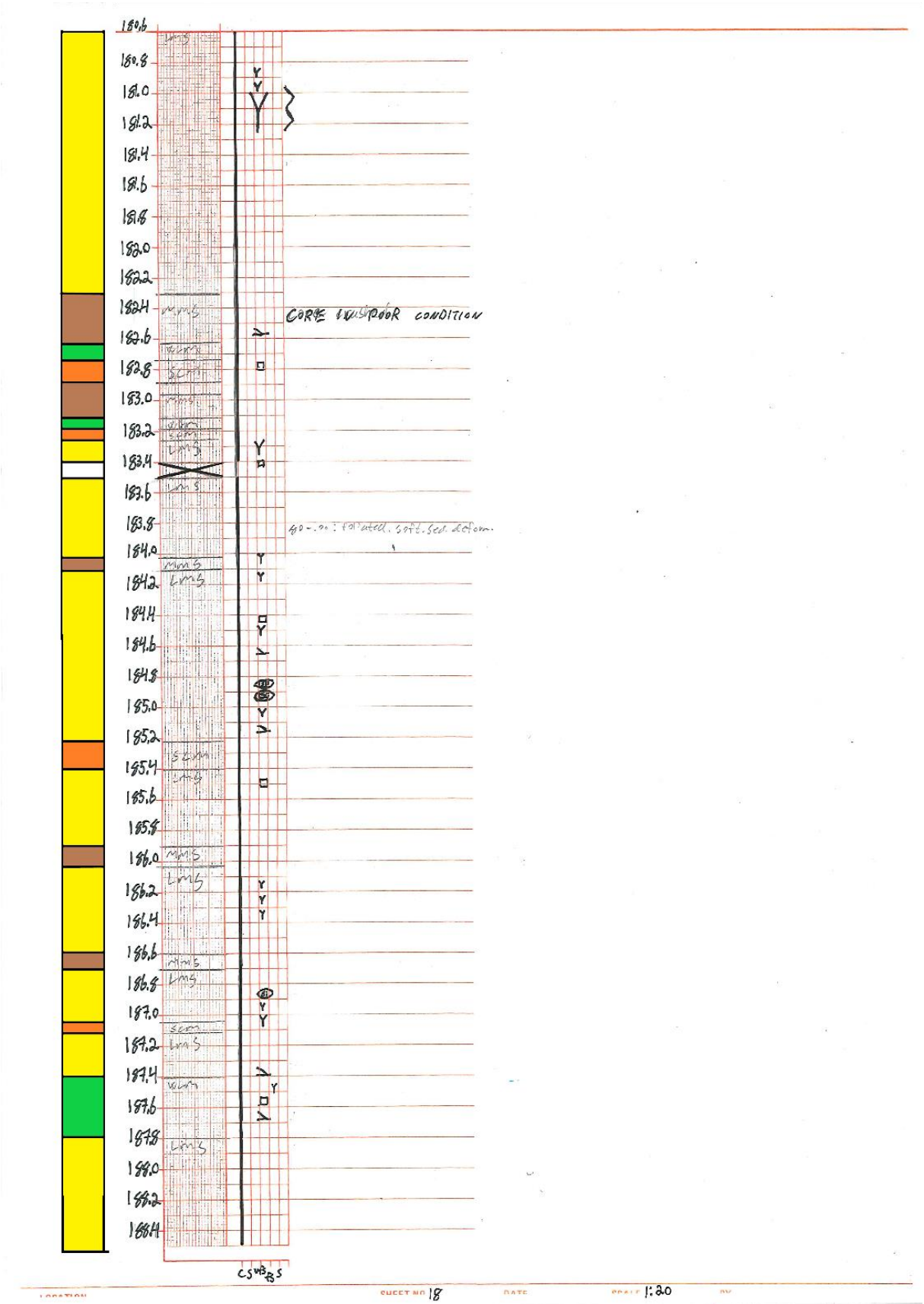
180.6
180.8
181.0
181.2
181.4
181.6
181.8
182.0
182.2
182.4
182.6
182.8
183.0
183.2
183.4
183.6
183.8
184.0
184.2
184.4
184.6
184.8
185.0
185.2
185.4
185.6
185.8
186.0
186.2
186.4
186.6
186.8
187.0
187.2
187.4
187.6
187.8
188.0
188.2
188.4
CORE WASHPOOR CONDITION
CS WB BS
SHEET NO 18
SCALE 1:20

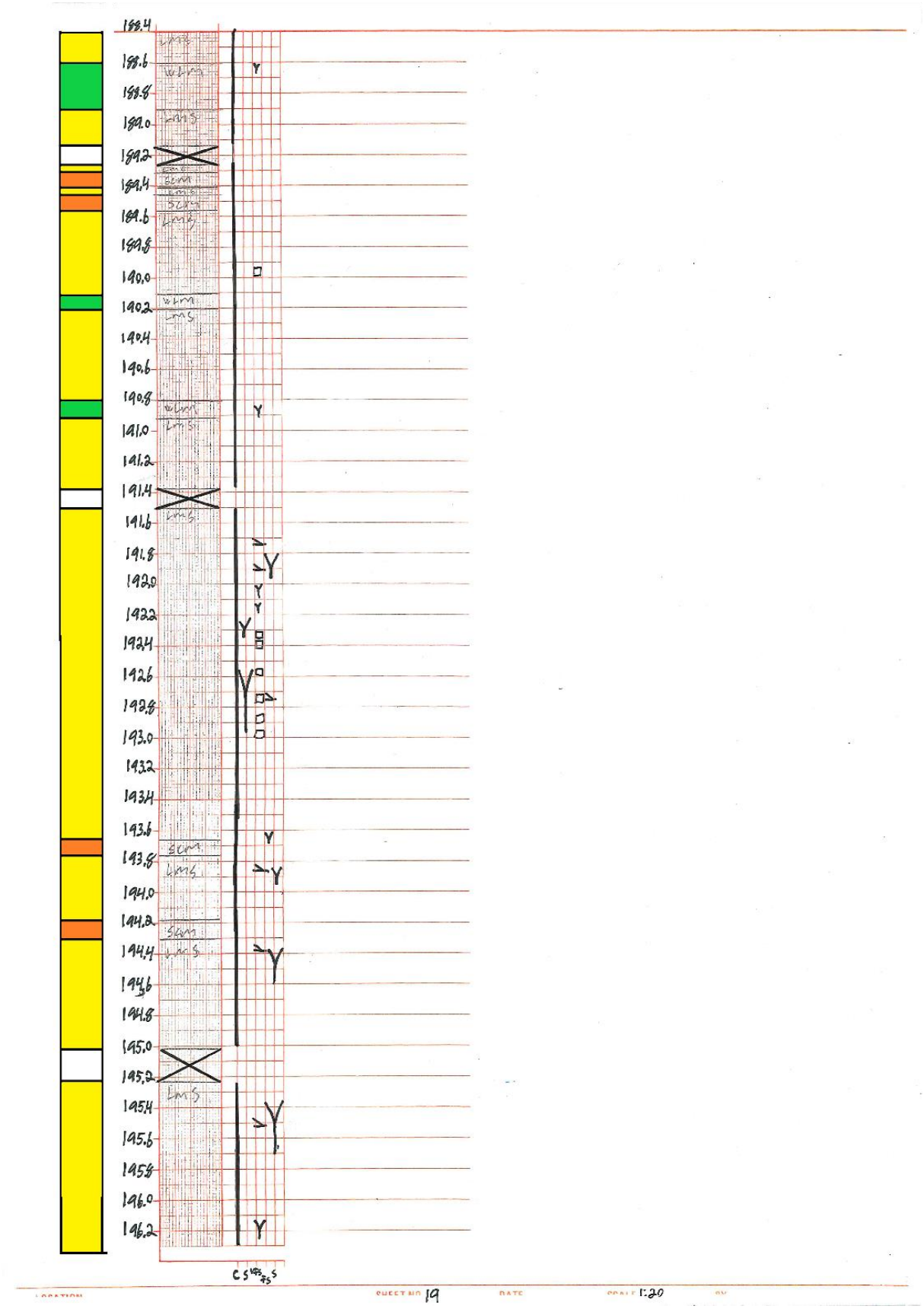
188.4
188.6
188.8
189.0
189.2
189.4
189.6
189.8
190.0
190.2
190.4
190.6
190.8
191.0
191.2
191.4
191.6
191.8
192.0
192.2
192.4
192.6
192.8
193.0
193.2
193.4
193.6
193.8
194.0
194.2
194.4
194.6
194.8
195.0
195.2
195.4
195.6
195.8
196.0
196.2
SHEET NO 19
DATE
SCALE 1:20

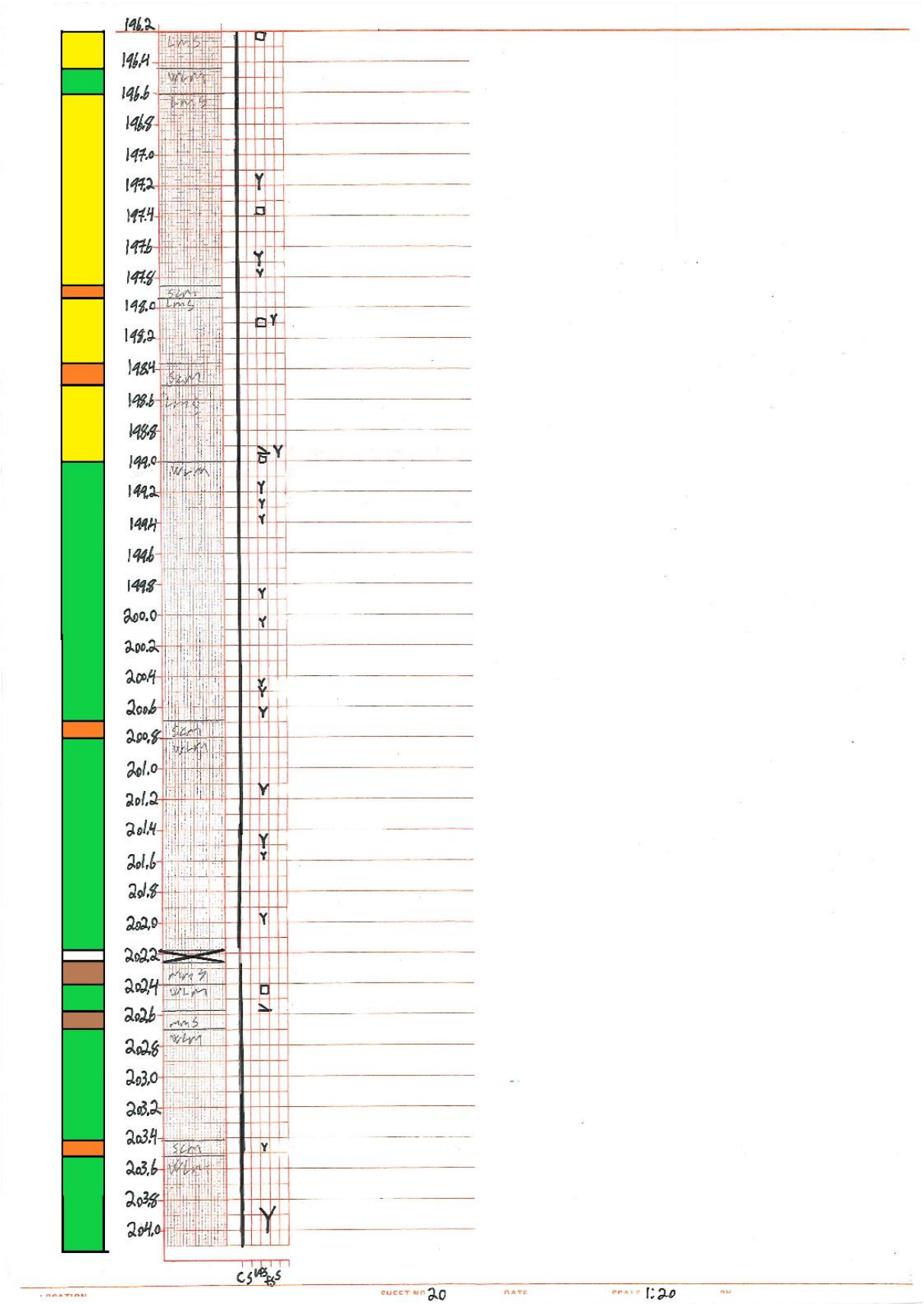
196.2
196.4
196.6
196.8
197.0
197.2
197.4
197.6
197.8
198.0
198.2
198.4
198.6
198.8
199.0
199.2
199.4
199.6
199.8
200.0
200.2
200.4
200.6
200.8
201.0
201.2
201.4
201.6
201.8
202.0
202.2
202.4
202.6
202.8
203.0
203.2
203.4
203.6
203.8
204.0
SHEET NO 20
SCALE 1:20

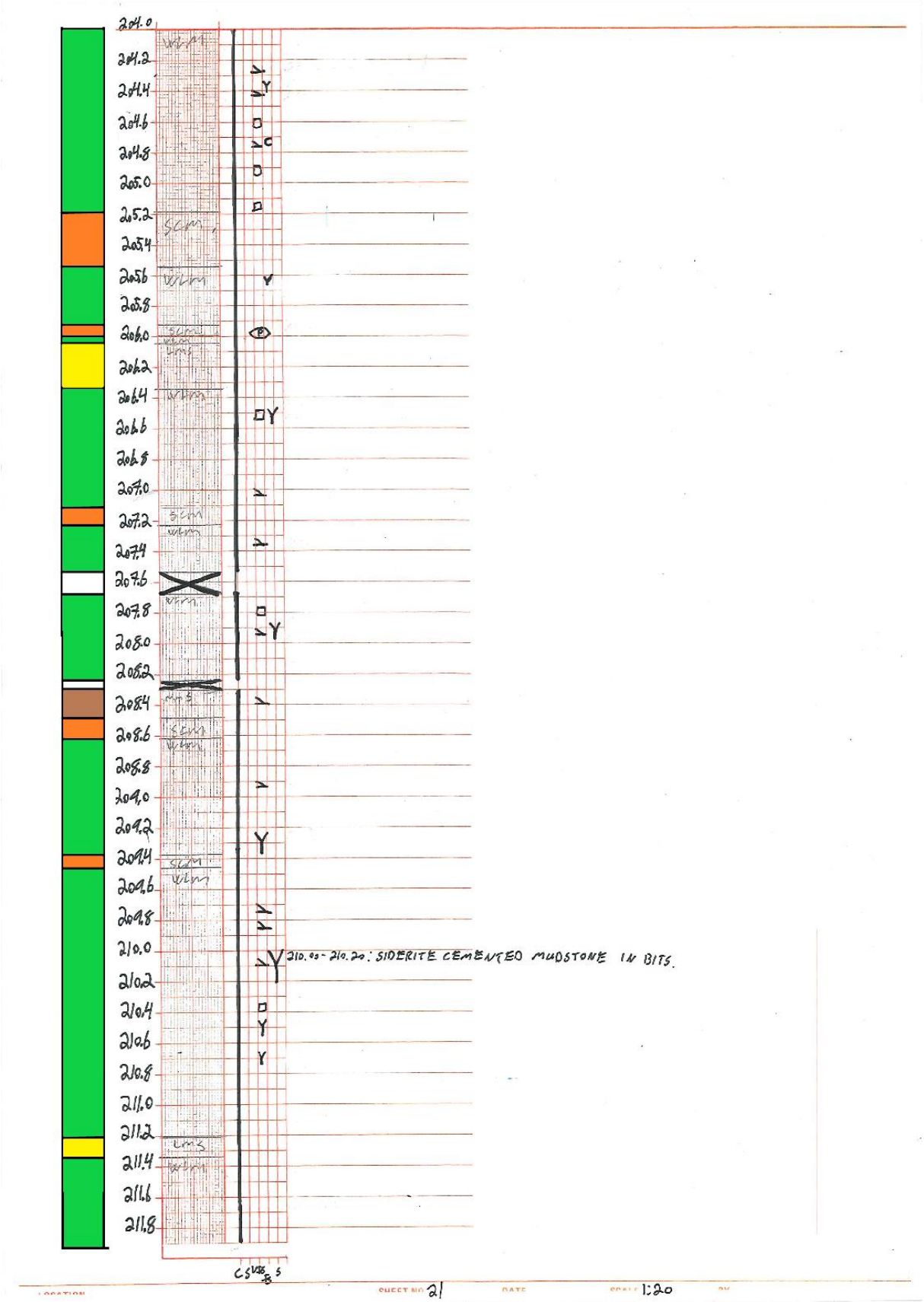
204.0
204.2
204.4
204.6
204.8
205.0
205.2
205.4
205.6
205.8
206.0
206.2
206.4
206.6
206.8
207.0
207.2
207.4
207.6
207.8
208.0
208.2
208.4
208.6
208.8
209.0
209.2
209.4
209.6
209.8
210.0
210.2
210.4
210.6
210.8
211.0
211.2
211.4
211.6
211.8
210.03 - 210.20: SIDERITE CEMENTED MUDSTONE IN BITS.
SHEET NO 21
SCALE 1:20

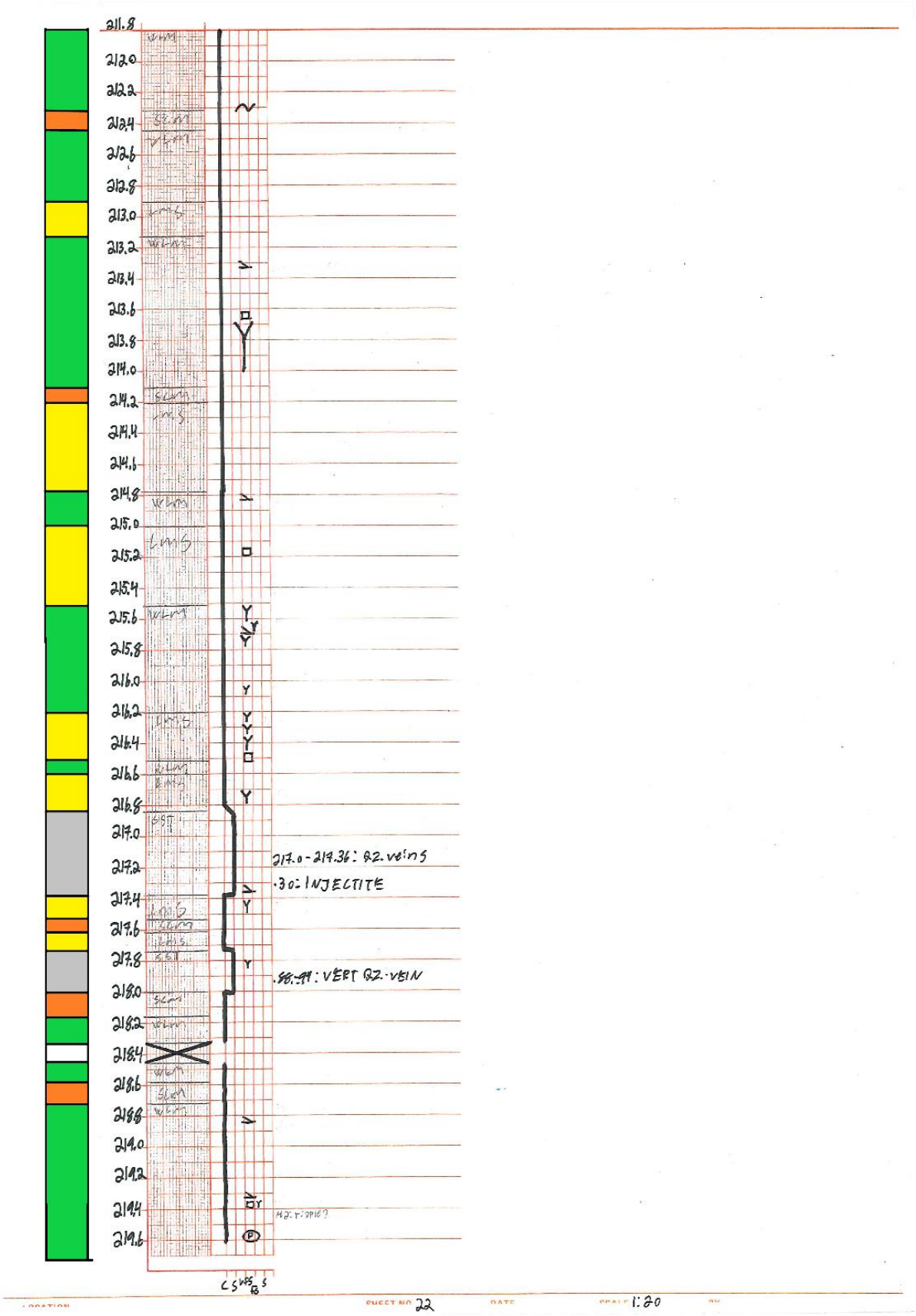
211.8
212.0
212.2
212.4
212.6
212.8
213.0
213.2
213.4
213.6
213.8
214.0
214.2
214.4
214.6
214.8
215.0
215.2
215.4
215.6
215.8
216.0
216.2
216.4
216.6
216.8
217.0
217.2
217.4
217.6
217.8
218.0
218.2
218.4
218.6
218.8
219.0
219.2
219.4
219.6
217.0-217.36: Qz. veins
.30: INJECTITE
.88-.99: VERT QZ. VEIN
SHEET NO 22
SCALE 1:20

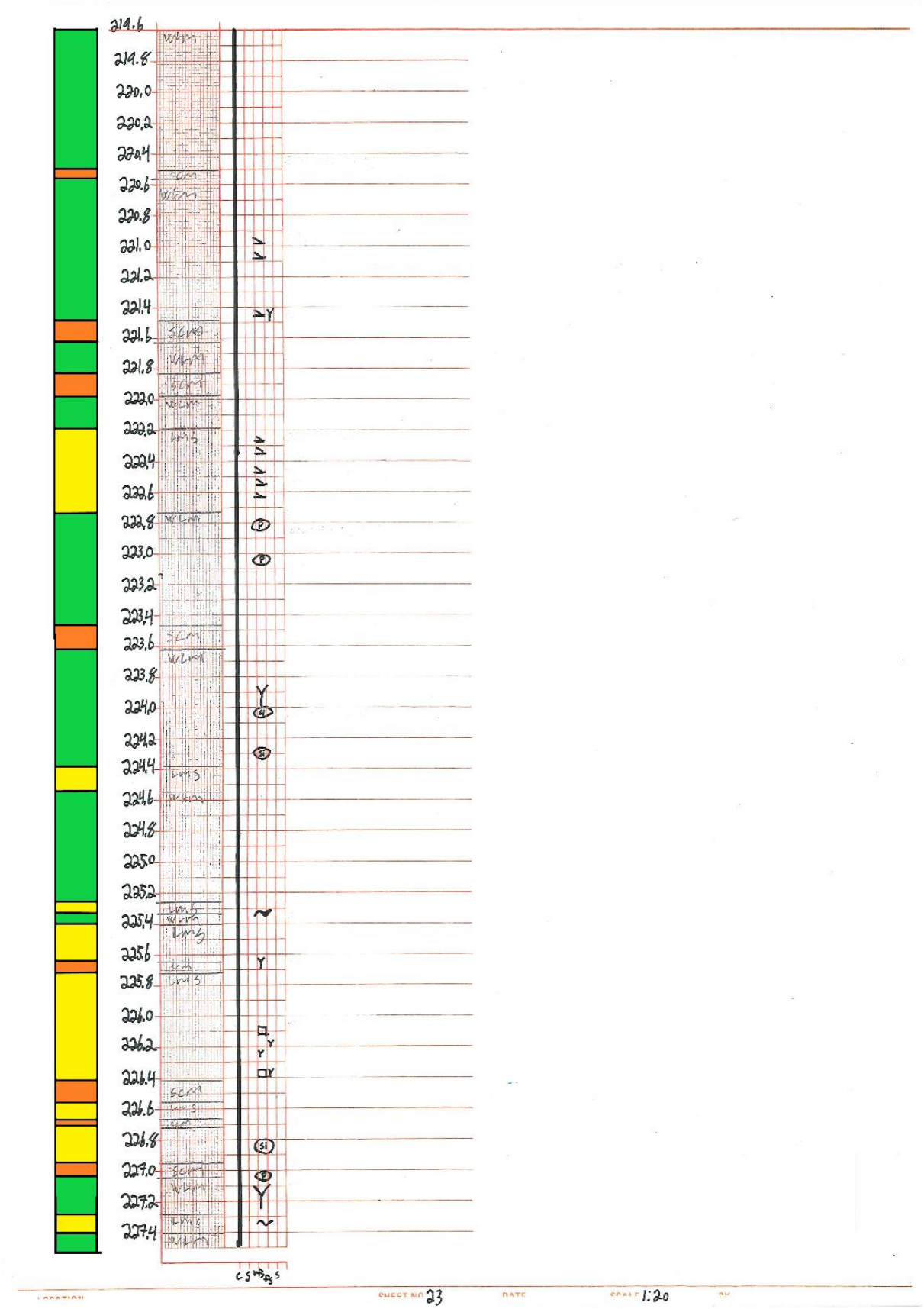
219.6
219.8
220.0
220.2
220.4
220.6
220.8
221.0
221.2
221.4
221.6
221.8
222.0
222.2
222.4
222.6
222.8
223.0
223.2
223.4
223.6
223.8
224.0
224.2
224.4
224.6
224.8
225.0
225.2
225.4
225.6
225.8
226.0
226.2
226.4
226.6
226.8
227.0
227.2
227.4
SHEET NO 23
SCALE 1:20

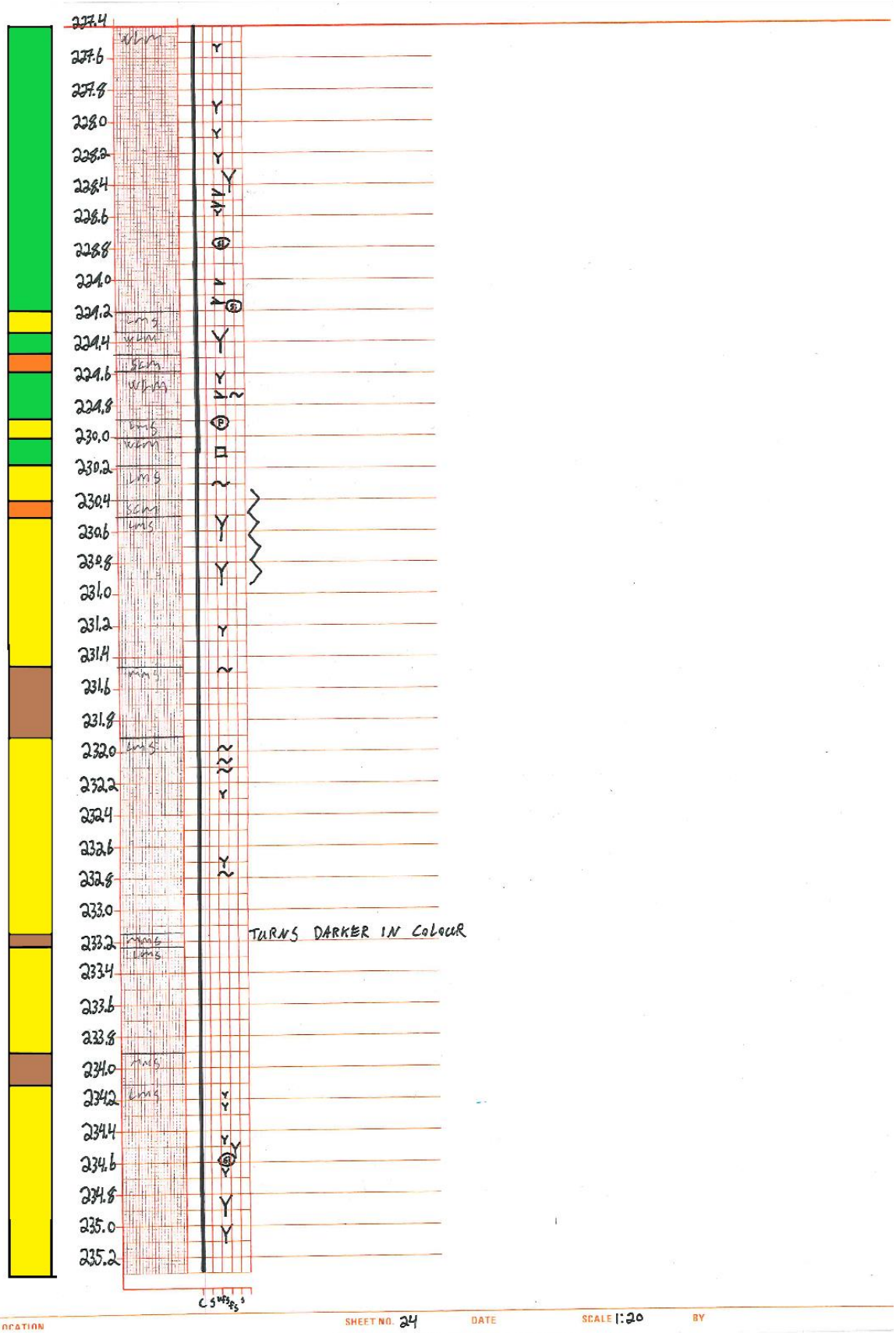
227.4
227.6
227.8
228.0
228.2
228.4
228.6
228.8
229.0
229.2
229.4
229.6
229.8
230.0
230.2
230.4
230.6
230.8
231.0
231.2
231.4
231.6
231.8
232.0
232.2
232.4
232.6
232.8
233.0
233.2
233.4
233.6
233.8
234.0
234.2
234.4
234.6
234.8
235.0
235.2
TURNS DARKER IN COLOUR
LOCATION
SHEET NO. 24
DATE
SCALE 1:20
BY

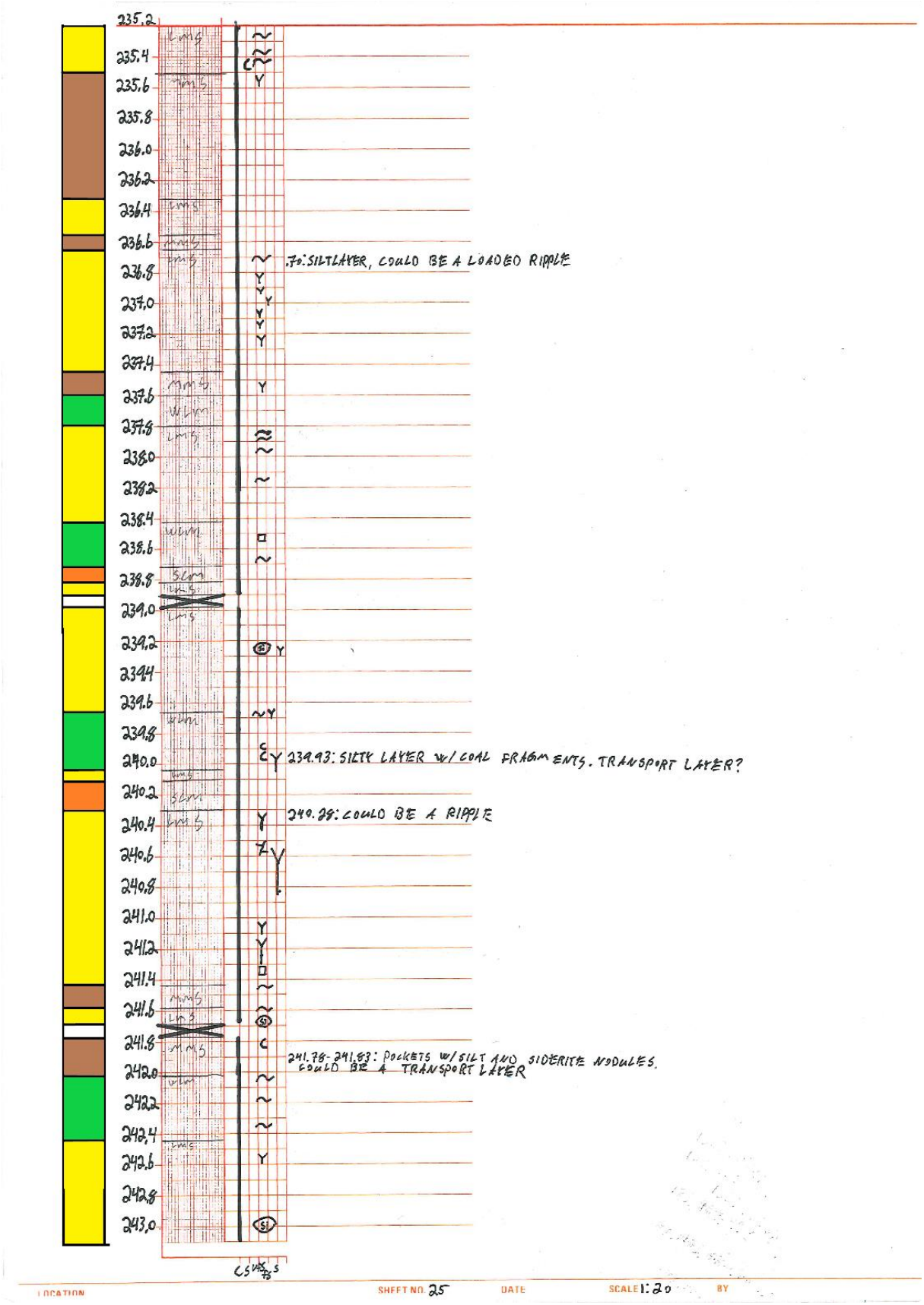
235.2
235.4
235.6
235.8
236.0
236.2
236.4
236.6
236.8
237.0
237.2
237.4
237.6
237.8
238.0
238.2
238.4
238.6
238.8
239.0
239.2
239.4
239.6
239.8
240.0
240.2
240.4
240.6
240.8
241.0
241.2
241.4
241.6
241.8
242.0
242.2
242.4
242.6
242.8
243.0
236: SILTLAYER, COULD BE A LOADED RIPPLE
239.93: SILTY LAYER W/ COAL FRAGMENTS. TRANSPORT LAYER?
240.28: COULD BE A RIPPLE
241.78-241.83: POCKETS W/ SILT AND SIDERITE NODULES. COULD BE A TRANSPORT LAYER
LOCATION
SHEET NO. 25
DATE
SCALE 1:20
BY

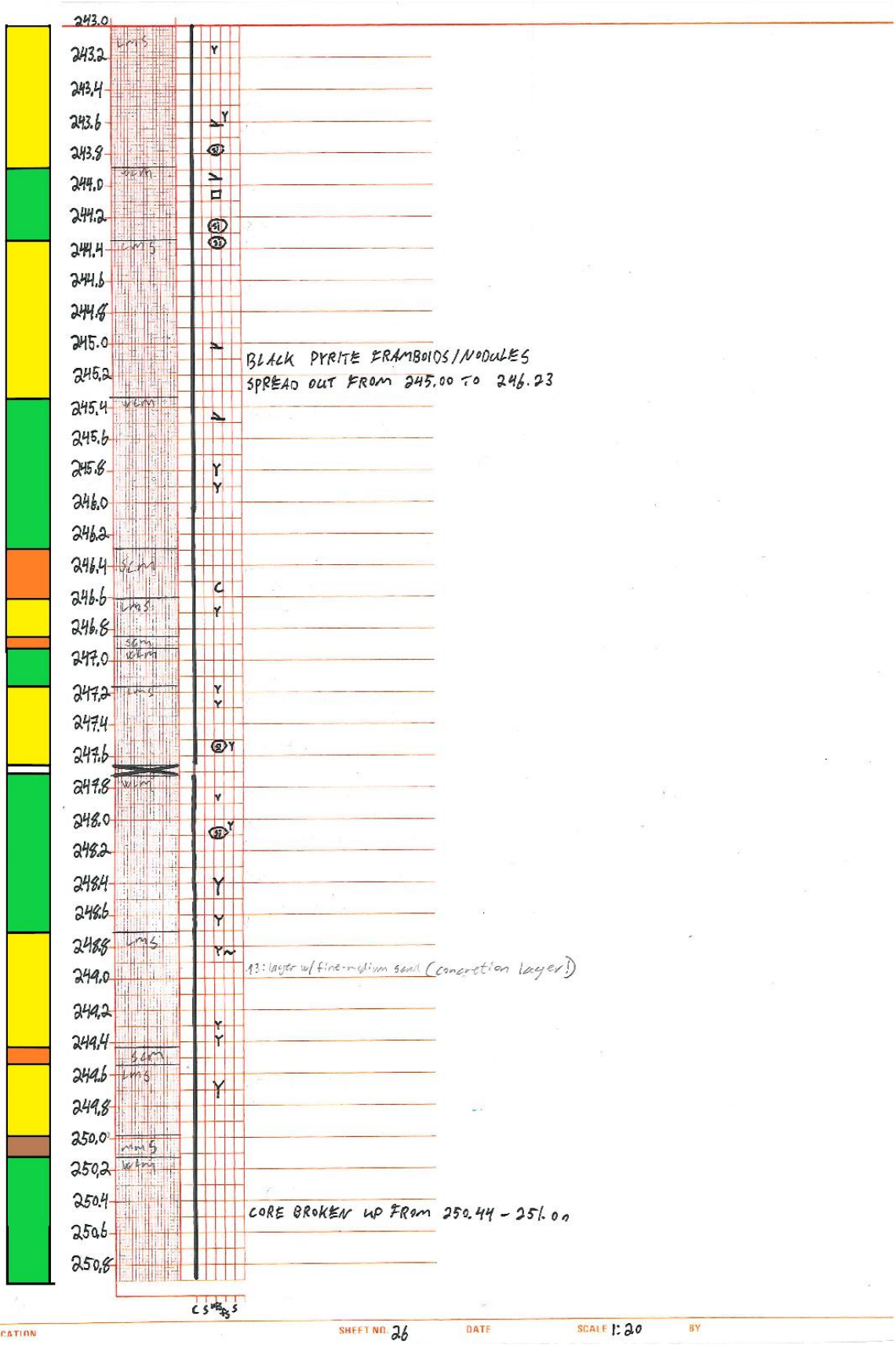
243.0
243.2
243.4
243.6
243.8
244.0
244.2
244.4
244.6
244.8
245.0
245.2
245.4
245.6
245.8
246.0
246.2
246.4
246.6
246.8
247.0
247.2
247.4
247.6
247.8
248.0
248.2
248.4
248.6
248.8
249.0
249.2
249.4
249.6
249.8
250.0
250.2
250.4
250.6
250.8
BLACK PYRITE FRAMBOIDS/NODULES SPREAD OUT FROM 245.00 TO 246.23
93: layer w/ fine-medium sand (concretion layer!)
CORE BROKEN UP FROM 250.44 - 251.00
LOCATION
SHEET NO. 26
DATE
SCALE 1:20
BY

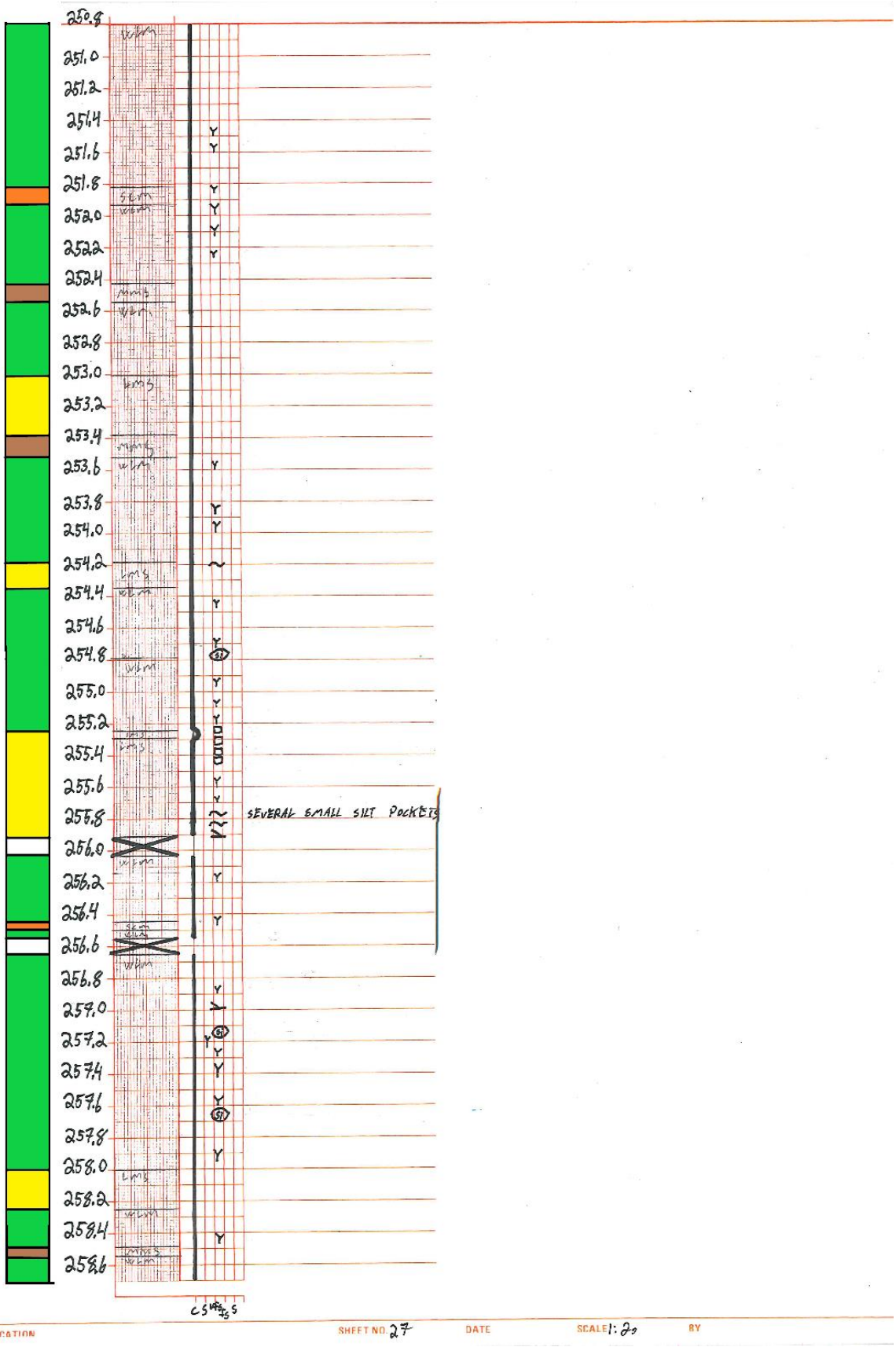
250.8
251.0
251.2
251.4
251.6
251.8
252.0
252.2
252.4
252.6
252.8
253.0
253.2
253.4
253.6
253.8
254.0
254.2
254.4
254.6
254.8
255.0
255.2
255.4
255.6
255.8
256.0
256.2
256.4
256.6
256.8
257.0
257.2
257.4
257.6
257.8
258.0
258.2
258.4
258.6
SEVERAL SMALL SILT POCKETS
LOCATION
SHEET NO. 27
DATE
SCALE 1: 20
BY

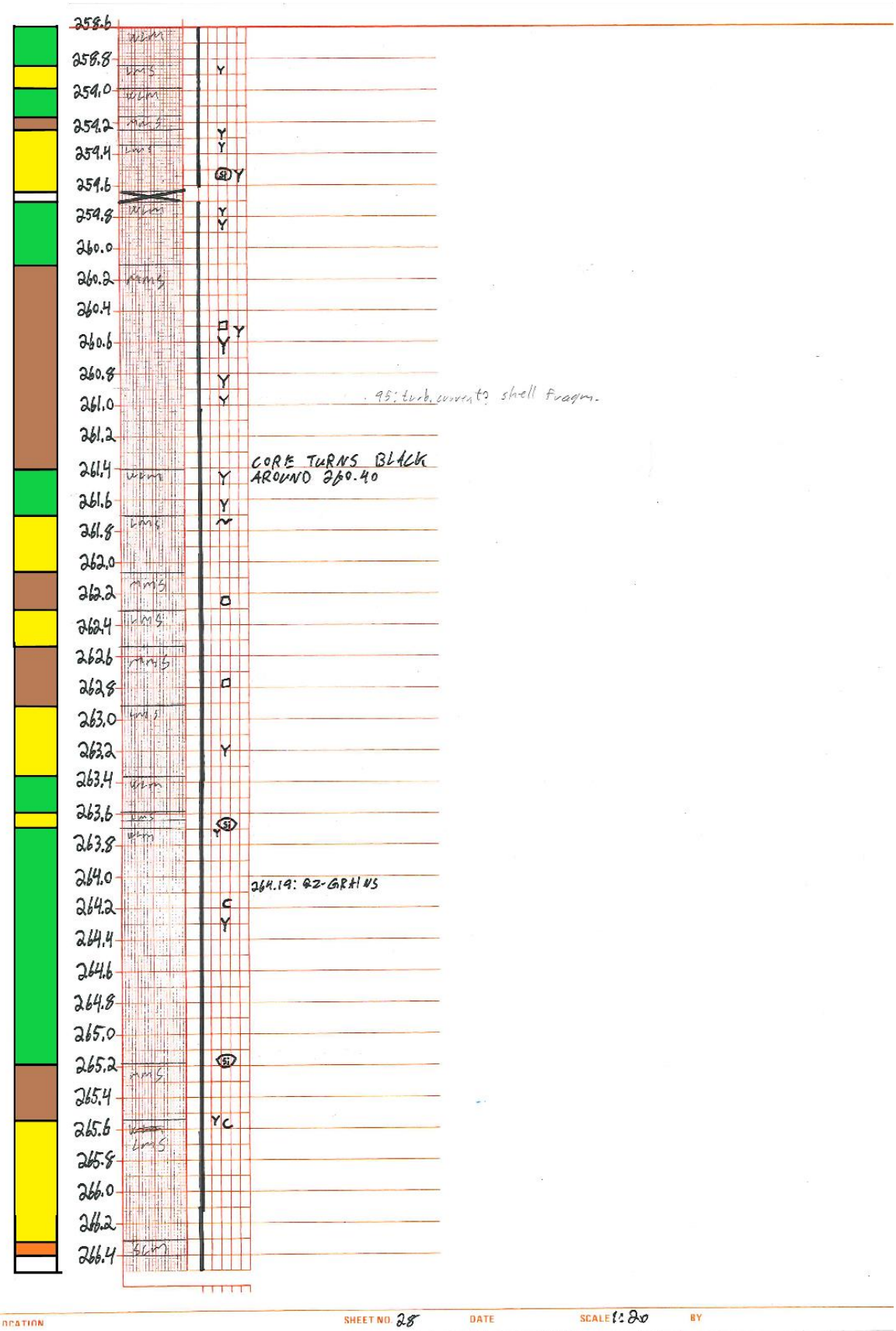

LOCATION SHEET NO. 28 DATE SCALE 1:20 BY

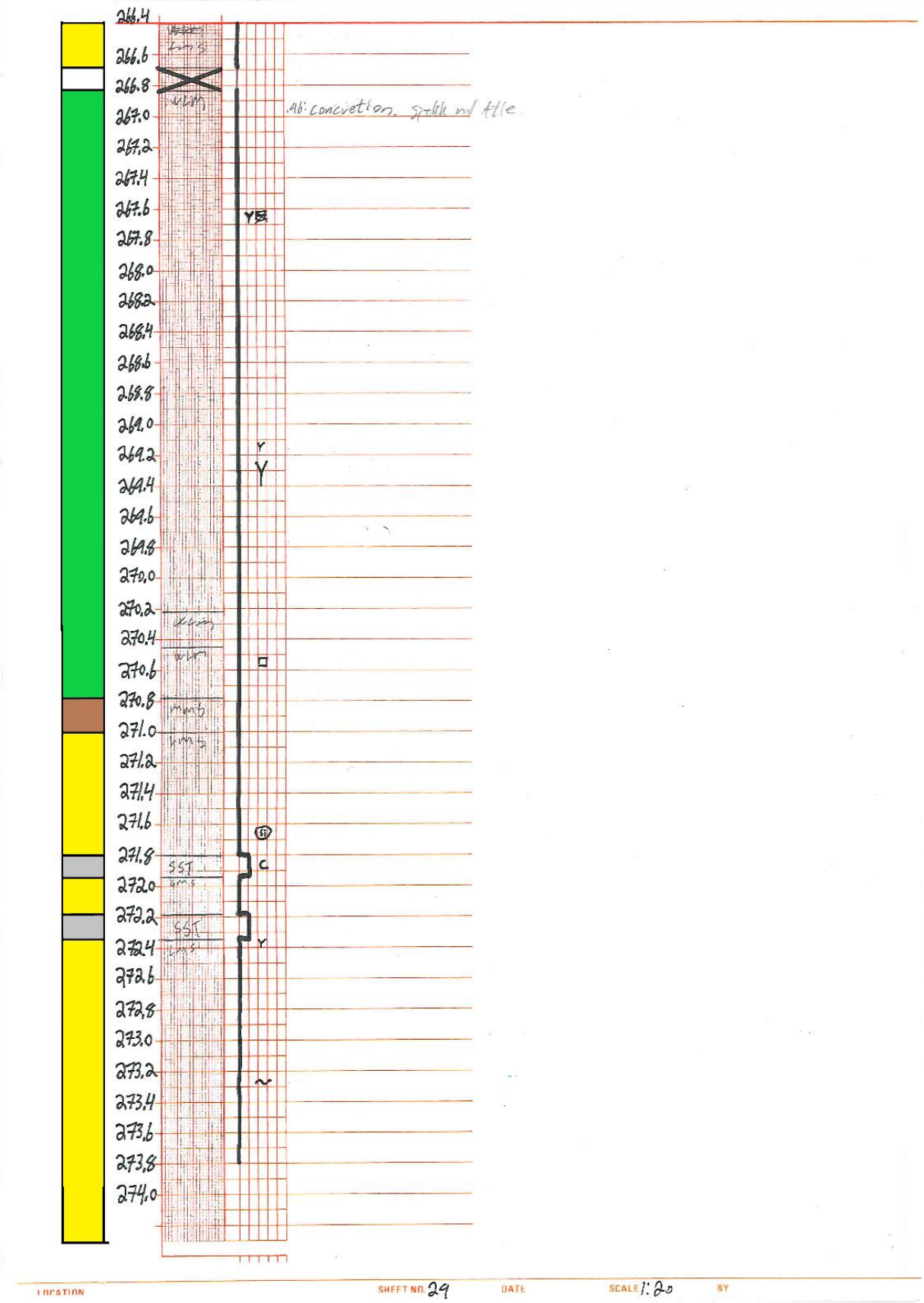
266.4
266.6
266.8
267.0
267.2
267.4
267.6
267.8
268.0
268.2
268.4
268.6
268.8
269.0
269.2
269.4
269.6
269.8
270.0
270.2
270.4
270.6
270.8
271.0
271.2
271.4
271.6
271.8
272.0
272.2
272.4
272.6
272.8
273.0
273.2
273.4
273.6
273.8
274.0
WLM
SST
C
Y
LOCATION
SHEET NO. 29
DATE
SCALE 1:20
BY